RNI No. MAHENG / 2017 / 74063
VOLUME 4 (Issue 2) January - June 2021

ISSN No. 2581-5911
BI-ANNUAL SUBSCRIPTION : Rs. 2000/-

G P GLOBALIZE RESEARCH JOURNAL OF CHEMISTRY

CODEN : GPGRAG

Abstracted in
Chemical Abstracts (CAS), USA

International Scientific Indexing (ISI)
Impact Factor 1.022

International Society for Research Activity Journal
Impact Factor 0.615

International Institute of Organized Research (I2OR)
Impact Factor 1.405

GAURANG PUBLISHING

GAURANG PUBLISHING GLOBALIZE
PRIVATE LIMITED

RNI No. MAHENG/2017/74063

ISSN (Print) No. 2581–5911
CODEN : GPGRAG

Volume 4 Issue 2 ❖ January – June 2021

G P GLOBALIZE RESEARCH JOURNAL OF CHEMISTRY

Abstracted in Chemical Abstracts (CAS), USA
International Scientific Indexing (ISI) Impact Factor 1.022 (2019-2020)
International Institute of Organized Research (I2OR) Impact Factor 1.405
ISRA Journal Impact Factor 0.615

Supported by **ASSOCIATION OF CHEMISTRY TEACHERS**, the National Registered Organisation of Chemistry Educators of India
Registration No. Maharashtra Government, Mumbai, 922, 2010 G.B.B.S.D. dated 08.04.2010.
Website: www.associationofchemistryteachers.org

GAURANG PUBLISHING GLOBALIZE PRIVATE LIMITED, MUMBAI
CIN No. U22130MH2016PTC287238
UAN - MH19D0008178

Published by:
Gaurang Publishing Globalize Private Limited, Mumbai
1, Plot 72, Pandit M.M.M. Marg, Tardeo, Mumbai 400 034.
Email: gpglobalize@gmail.com ❖ www.gpglobalize.in
Tel: +91 9969392245
CIN No. U22130MH2016PTC287238

ISSN (Print) No: 2581-5911
CODEN : GPGRAG

Disclaimer: Please be informed that the author and the published have put in their best efforts in producing this journal. Every care has been taken to ensure the accuracy of the contents. However, we make no warranties for the same and therefore shall not be responsible or liable for any loss or any commercial damages accuring thereof. Neither the publisher nor the author is engaged in providing services of any professional nature and shall therefore not be responsible for any incidental, consequential, special or any other damages. Please do consult a professional where appropriate.

Printed at: Nil Creation, Girgaum, Mumbai - 400 004, India.

GP GLOBALIZE RESEARCH JOURNAL OF CHEMISTRY

An International Peer Reviewed Journal of Chemistry

RNI No: MAHENG/2017/74063 **ISSN (Print) No: 2581-5911**
ISI Impact Factor 1.022 (2019-2020) **CODEN : GPGRAG**

Printed and Published by Gaurang Rajan Pendurkar on behalf of Gaurang Publishing Globalize Private Limited and printed at NIL CREATION, Shop No. 7, 35/55, Bandu Gokhale Path, Mugbhat Cross Lane, Jivanji Maharaj Chawl (Shree Swami Samarth Nagar), Girgaon, Mumbai 400004 and published at Gaurang Publishing Globalize Private Limited 1, Plot 72, P M M M Marg, Tardeo, Mumbai-400034.

Editor-in-Chief Dr. D.V. Prabhu.

Editorial Board

Editorial Board

Editorial Board

Editorial Board

G P GLOBALIZE RESEARCH JOURNAL OF CHEMISTRY

RNI No: MAHENG/2017/74063 **ISSN No. (Print): 2581-5911**
ISI Impact Factor 1.022 (2019-2020) **CODEN : GPGRAG**

GUIDELINES TO AUTHORS

GP Globalize Research Journal of Chemistry is an international peer reviewed journal which publishes full length research papers, short communications, review articles and book reviews covering all areas of Chemistry including Environmental Chemistry. G P Globalize Research Journal of Chemistry is a biannual journal published in English in print and online versions.

(1) Manuscript Preparation

a) Page Layout: A4 (21 cm x 29.7 cm) leaving 2.5 cm margin on all sides of the text. All the text should be in Times New Roman font, double spaced and pages should be numbered consecutively.

b) Use MS word (2003-2007) for text and TIFF, JPEG or Paint for figures.

c) The first page should contain title in bold, 14 point size, name/s of author/s in bold, 12 point size, affiliation/s-address, email id and contact number in 11 point size, abstract-up to 200 words in 11 point size, keywords-between 5 to 10 keywords in 11 point size.

d) Main Text- The paper should be divided into the following sections:

Introduction, Materials and Methods, Results and Discussion, Conclusions, Acknowledgement and References.

Tables and Figures of good resolution (600 dpi) should be numbered consecutively and given in the order of their appearance in the text and should not be given on separate pages.

e) References- References should be cited in the text as superscript numbers in order of appearance.

References at the end of the paper should be listed in serial order to match their order of appearance in the text. Names of journals should be in italics and volume number should be in bold.

Reference to papers e.g. Ganesh R.S., Pravin S. and Rao T.P., 2005, *Talanta,* **66,** 513.

Reference to books e.g. Lee J.D., 1984, A New Course in Inorganic Chemistry, 3rd ed., ELBS and Van Nostrand Reinhold (UK) Co. Ltd., p.268-269.

f) Abbreviations should be explained at first appearance in the text.

g) Nomenclature should be as per **IUPAC** guidelines.

h) SI units should be used throughout.

(2) Manuscript Submission

Manuscripts should be submitted online at dvprabhu48@gmail.com. The paper will be accepted for publication after review. All correspondence should be made to the Editor- in-Chief at dvprabhu48@gmail.com.

(3) Proofs

Galley proofs will be sent online to the corresponding author on request and should be returned to the Editorial office within seven working days.

(4) Plagiarism

GP Globalize Research Journal of Chemistry is committed to avoid plagiarism and ensure that only original research work is published. The journal follows a Zero Tolerance Policy on Plagiarism.

The Editorial Board and panel of reviewers will check and prevent plagiarism in the manuscripts submitted for publication.

(5) Copyright

Publication of a paper in GP Globalize Research Journal of Chemistry automatically transfers copyright to the publisher. Authors can share free eprints of their published papers with fellow researchers.

(6) Circulation and Subscription Rates

The Journal is published twice a year - January and July

Subscription rates are as follows:

Library/Institutional Charges (In India)	Rs. 2000/-
Individual Charges (In India)	Rs. 2000/-
Library/Institutional Charges (Outside India)	US $ 100
Individual Charges (Outside India)	US $ 100

Subscription Charges:
Review of research papers is done free of charge. There is no charge for processing of manuscripts. Subscription to the Journal is welcome.

Mode of Payment:

Demand draft/Multicity cheque payable at Mumbai in favour of **"Gaurang Publishing Globalize Pvt. Ltd. Mumbai"**

For Online Payment:

Name of the Bank	**:**	**Axis Bank**
Branch Name	**:**	**Tardeo, Mumbai (MH)**
Account No.	**:**	**916020066451552**
IFSC Code	**:**	**UTIB0001345**

For further details please contact:

Dr. D.V. Prabhu, Editor-in-Chief,
Email: dvprabhu48@gmail.com
Mobile: 09870 226 899

Mr. Rajan Pendurkar, Managing Editor,
Email: gpglobalize@gmail.com
Mobile: 09969 392 245

A Request to Authors

We thank you for sending your research paper to G P Globalize Research Journal of Chemistry (RNI No. MAHENG/2017/74063 ISSN No. (Print): 2581-5911, CODEN : GPGRAG).

Review and processing of research papers is done free of charge.

You are requested to send a DD/Multicity Cheque for Rs. 2000/- in favour of ***"Gaurang Publishing Globalize Pvt. Ltd., Mumbai"*** *payable at Mumbai,* ***as subscription charges.***

We would appreciate if you help us in our efforts to promote academic excellence.

G P GLOBALIZE RESEARCH JOURNAL OF CHEMISTRY

RNI No: MAHENG/2017/74063 **ISSN No. (Print): 2581-5911**
ISI Impact Factor 1.022 (2019-2020) **CODEN : GPGRAG**

Volume 4 Issue 2 ❄ January - June 2021

CONTENTS

CONTENTS

RNI No. MAHENG/2017/74063
ISSN No. (Print) 2581-5911
ISI Impact Factor 1.022 (2019-2020)

Effect of Predefined Scaling Factors on the Identification of Vibrational Wavenumber and Total Energy Distribution Values Calculated with Scaled Quantum Mechanics

Özgür Alver[1], Cemal Parlak[2] and Ponnadurai Ramasami[3,4*]
[1]Department of Physics, Science Faculty, Eskisehir Technical University, Eskisehir, Turkey
[2]Department of Physics, Science Faculty, Ege University, Izmir, 35100, Turkey
[3]Computational Chemistry Group, Department of Chemistry, Faculty of Science, University of Mauritius, Réduit 80837, Mauritius
[4]Department of Chemistry, College of Science, Engineering and Technology, University of South Africa, South Africa.
Email: p.ramasami@uom.ac.mu

Abstract
The scaled quantum mechanics (SQM) method is widely used for the vibrational assignments and to compute the total energy distribution (TED) values of different types of molecules. In this research, the relation between the pre-defined scaling parameters before the optimization with SQM, the resultant vibrational assignments and TED values were investigated using n-propylamine and density functional theory (DFT) method. The findings indicate that the determination of scaling parameters has an important effect on the results of vibrational frequencies and related TED values. Therefore, before vibrational assignment with SQM, assessment of scaling parameters should be considered carefully and more than one scaling parameters should be taken into account for the best match.

Keywords: *SQM, TED, DFT, Vibrational assignment.*

Introduction

TED calculations are important to make a more quantitative interpretation of the calculated wavenumbers and vibrational analyses. They show the relative percentage contributions of the redundant internal coordinates for each normal vibrational mode of the investigated systems. Therefore, it gives a possibility to describe the character of each vibrational mode numerically[1,2].

In the field of vibrational spectroscopy, TED calculations of vibrational wavenumbers and the assignments of the calculated wavenumbers for a wide range of different types of molecules have been widely carried out using SQM method[3-10]. Non-redundant natural internal coordinates of a given molecule are built for the original SQM procedure and they are grouped depending on common scaling factors calculated by a least-squares fit to experimental vibrational frequencies[11, 12]. SQM takes the advantage of a modified procedure of scaling including the scaling of valence coordinates[2]. The details

of TED matrix for the use of description of the normal modes and the most commonly used scale factors for SQM program are reported[2, 13, 14]. These reported values are commonly used and depending on the molecule being investigated, other scaling strategy can be followed.

In this research, we attempted to find an answer to the question ''what will happen to the results of TED values if anyone use different scaling parameters in SQM?''. This effect is something everybody knows but users of SQM just apply it blindly. The aim of this work was to show how the TED values and vibrational assignments correlate with the pre-assumed scale factors. For this purpose, n-propyl amine (n-pa) was chosen, since vibrational assignments of this molecule are defined and reported[15].

Computational details

The most stable form of n-pa was prepared based on the data reported by Durig et. al.,[15] and then optimized with the B3LYP/6-311++G(d,p) method with the constraint of the C_s point group. After the optimization, no imaginary frequencies were observed. For the scaling procedure with SQM, eight different scaling parameters (S1 to S8) were considered as given in Table 1. Based on the previously reported data, vibrational assignments were done and TED values of these assignments were calculated with SQM method (Tables 2 and 3).

Table 1. Optimized scaling parameters for each scaling list

S1		OSF	S6		OSF
Vibration	**Atoms**		**Vibration**	**Atoms**	
Stretch	X—X	1.0079	Stretch	C—H	0.9050
Stretch	X—H	0.9092	Stretch	N—H	0.9169
Bend	X—X—X	1.0249	Stretch	C—N	1.2576
Bend	X—X—H	0.9159	Stretch	C—C	0.7384
Torsion	X—X—X—X	1.3718	Bend	X—X—X	0.9791
Torsion	H—X—X—X	0.7967	Bend	X—X—H	0.9289
S2			Bend	H—C—H	0.8365
Stretch	X—X	1.0078	Bend	C—N—H	1.0011
Stretch	C—H	0.9050	Bend	C—C—N	1.3980
Stretch	N—H	0.9170	Bend	H—N—H	0.9022
Bend	X—X—X	1.0254	Torsion	X—X—X—X	1.0406
Bend	X—X—H	0.9160	Torsion	H—X—X—X	0.9975
Torsion	X—X—X—X	1.3692	**S7**		
Torsion	H—X—X—X	0.7959	Stretch	C—H	0.9050
S3			Stretch	N—H	0.9170
Stretch	C—H	0.9050	Stretch	C—N	0.9838
Stretch	N—H	0.9170	Stretch	C—C	1.0250
Stretch	C—N	0.9674	Bend	X—X—X	0.9136
Stretch	C—C	1.0339	Bend	X—X—H	1.0191
Bend	X—X—X	1.0230	Bend	H—C—H	0.9431
Bend	X—X—H	0.9156	Bend	C—N—H	0.8448
Torsion	X—X—X—X	1.3696	Bend	C—C—N	1.2402
Torsion	H—X—X—X	0.7954	Bend	H—N—H	1.0227

S4			Torsion	X—X—X—X	1.0800
Stretch	C—H	0.9050	Torsion	H—X—X—H	0.7981
Stretch	N—H	0.9170	Torsion	H—X—X—X	1.1721
Stretch	C—N	0.9672	**S8**		
Stretch	C—C	1.0305	Stretch	C—H	0.9050
Bend	X—X—X	1.0969	Stretch	N—H	0.9170
Bend	X—X—H	0.9495	Stretch	C—N	0.9991
Bend	H—C—H	0.8880	Bend	X—X—X	0.8359
Bend	C—N—H	0.8372	Bend	X—X—H	0.9871
Torsion	X—X—X—X	1.1436	Bend	H—C—H	0.8986
Torsion	H—X—X—X	0.9150	Bend	C—N—H	0.8970
S5			Bend	C—C—N	1.2798
Stretch	C—H	0.9050	Bend	H—N—H	0.9971
Stretch	N—H	0.9170	Torsion	X—X—X—X	1.1020
Stretch	C—N	0.9692	Torsion	H—X—X—H	0.8419
Stretch	C—C	1.0294	Torsion	H—N—C—C	0.9586
Bend	X—X—X	0.9248	Torsion	H—C—C—C	1.3391
Bend	X—X—H	0.9484	OSF: Optimized scaling factors. X: Non Hydrogen atom. Stretch: Stretching vibration. Bend: Bending vibration. Torsion: Torsional vibration.		
Bend	H—C—H	0.8901			
Bend	C—N—H	0.8429			
Bend	C—C—N	1.2253			
Torsion	X—X—X—X	1.1778			
Torsion	H—X—X—X	0.8966			

Table 2. Comparison of the experimental and calculated vibrational wavenumbers for each scaling list.

Mode	Description [15]	Exp.	Cal.	S1	S2	S3	S4	S5	S6	S7	S8
ν_1	NH2 antisymmetric stretch	3415	3570	3404	3419	3419	3419	3419	3419	3419	3419
ν_2	NH2 symmetric stretch	3348	3492	3330	3344	3344	3344	3344	3344	3344	3344
ν_3	CH3 antisymmetric stretch	2948	3086	2942	2935	2935	2935	2935	2935	2935	2935
ν_4	CH2 antisymmetric stretch	2890	3054	2911	2905	2905	2905	2905	2905	2905	2905
ν_5	CH3 symmetric stretch	2879	3020	2880	2873	2873	2873	2873	2873	2874	2874
ν_6	CH2 symmetric stretch	2869	3015	2874	2868	2868	2868	2868	2868	2868	2868
ν_7	CH2 symmetric stretch	2849	3000	2860	2854	2854	2854	2854	2854	2854	2854
ν_8	NH_2 bend	1620	1664	1632	1632	1632	1614	1615	1620	1620	1620
ν_9	CH3 antisymmetric deformation	1460	1509	1485	1485	1485	1471	1468	1460	1460	1461
ν_{10}	CH2 wag	1358	1397	1353	1353	1353	1350	1353	1363	1360	1361
ν_{11}	CH2 twist	1290	1324	1278	1278	1278	1293	1292	1292	1287	1283
ν_{12}	CN stretch (TT)	1076	1082	1081	1081	1075	1074	1075	1074	1076	1078
ν_{13}	NH2 twist	1030	1033	1025	1025	1031	1031	1030	1019	1030	1021
ν_{14}	NH2 wag (TT)	776	810	787	787	786	787	784	782	774	774
ν_{15}	CCN bend (TT)	452	442	441	441	441	442	452	443	452	449
ν_{16}	NH_2 torsion	251	271	263	263	263	270	265	276	266	261
ν_{17}	CH_3 tors	237	220	204	204	204	218	212	225	226	230
ν_{18}	CCC tors	137	129	127	127	127	130	128	132	134	135

Experimental data taken from Ref. 15.
Cal.: Calculated raw data with B3LYP/6-311++G (d.p).
S1 to S8: Scaled wave numbers with SQM.

Table 3. Vibrational assignments and related TED values for each scaling list.

Assignments				
Mode	**S1**	**S2**	**S3**	**S4**
ν_1	νN-H(100)	νN-H(100)	νN-H(100)	νN-H(100)
ν_2	νN-H(100)	νN-H(100)	νN-H(100)	νN-H(100)
ν_3	νC-H(99) (CH_3)	νC-H(99) (CH_3)	νC-H(99) (CH_3)	νC-H(99) (CH_3)
ν_4	νC-H(74) (CH_2)	νC-H(74) (CH_2)	νC-H(74) (CH_2)	νC-H(74) (CH_2)
ν_5	νC-H(71) (CH_3) + νC-H(27) (CH_2)	νC-H(71) (CH_3) + νC-H(27) (CH_2)	νC-H(71) (CH_3) + νC-H(27) (CH_2)	νC-H(71) (CH_3) + νC-H(27) (CH_2)
ν_6	νC-H(65) (CH_2) + νC-H(24) (CH_3)	νC-H(65) (CH_2) + νC-H(24) (CH_3)	νC-H(65) (CH_2) + νC-H(24) (CH_3)	νC-H(65) (CH_2) + νC-H(23) (CH_3)
ν_7	νC-H(92) (CH_2)	νC-H(92) (CH_2)	νC-H(92) (CH_2)	νC-H(92) (CH_2)
ν_8	δH-N-H(53)+ δC-N-	δH-N-H(53) + δC-N-	δH-N-H(53) + δC-N-	δH-N-H(53) + δC-N-H(30)
ν_9	δH-C-H(12) (CH_3) + δH-C-H(12) (CH_2)	δH-C-H(12) (CH_3) + δH-C-H(12) (CH_2)	δH-C-H(12) (CH_3) + δH-C-H(12) (CH_2)	δH-C-H(26) (CH_2)
ν_{10}	-	-	-	δH-C-H(48) (CH_3) + δH-C-C(43) (CH_3)
ν_{11}	δC-C-H(50) (CH_2)	δC-C-H(50) (CH_2)	δC-C-H(50) (CH_2)	δC-C-H(53) (CH_2)
ν_{12}	νC-N(48) + νC-C(36)	νC-N(48) + νC-C(36)	νC-N(51) + νC-C(32)	νC-N(51) + νC-C(40)
ν_{13}	νC-C(73) + νC-N(11)	νC-C(73) + νC-N(11)	νC-C(65) + νC-N(24)	νC-C(62) + νC-N(28)
ν_{14}	δC-N-H(29) + νC-C(11)	δC-N-H(29) + νC-C(11)	δC-N-H(29)	δC-N-H(31)
ν_{15}	δC-C-N(30) + δC-C-C(16) + νC-C(12)	δC-C-N(30) + δC-C-C(16) + νC-C(12)	δC-C-N(30) + δC-C-C(16) + νC-C(11)	δC-C-N(30) + δC-C-C(16) + νC-C(11)
ν_{16}	δC-C-C(41) + δC-C-N(25)	δC-C-C(41) + δC-C-N(25)	δC-C-C(41) + δC-C-N(25)	τH-C-N-H(42) + τC-C-N-H(41)
ν_{17}	τH-C-C-C(56)	τH-C-C-C(56)	τH-C-C-C(56)	τH-C-C-C(55)
ν_{18}	τH-C-C-C(30) + τN-C-C-H(29) + τN-C-C-C(28)	τH-C-C-C(30) + τN-C-C-H(29) + τN-C-C-C(28)	τH-C-C-C(29) + τN-C-C-H(29) + τN-C-C-C(28)	τH-C-C-C(29) + τN-C-C-H(29) + τN-C-C-C(28)
Assignments				
Mode	**S5**	**S6**	**S7**	**S8**
ν_1	νN-H(100)	νN-H(100)	νN-H(100)	νN-H(100)
ν_2	νN-H(100)	νN-H(100)	νN-H(100)	νN-H(100)
ν_3	νC-H(99) (CH_3)	νC-H(99) (CH_3)	νC-H(99) (CH_3)	νC-H(99) (CH_3)
ν_4	νC-H(74) (CH_2)	νC-H(74) (CH_2)	νC-H(74) (CH_2)	νC-H(74) (CH_2)
ν_5	νC-H(71) (CH_3) + νC-H(27) (CH_2)	νC-H(71) (CH_3) + νC-H(27) (CH_2)	νC-H(69) (CH_3) + νC-H(29) (CH_2)	νC-H(70) (CH_3) + νC-H(28) (CH_2)
ν_6	νC-H(65) (CH_2) +	νC-H(65) (CH_2) + νC-	νC-H(63) (CH_2) + νC-	νC-H(64) (CH_2) + νC-
ν_7	νC-H(92) (CH_2)	νC-H(92) (CH_2)	νC-H(92) (CH_2)	νC-H(92) (CH_2)
ν_8	δH-N-H(53) + δC-N-	δH-N-H(53) + δC-N-	δH-N-H(53) + δC-N-	δH-N-H(53) + δC-N-H(34)
ν_9	δH-C-H(33) (CH_2)	δH-C-H(28) (CH_2) + τH-C-N-H(21)	δH-C-H(35) (CH_3) + δC-C-H(10)	δH-C-H(33) (CH_3)

ν_{10}	δH-C-H(49) (CH_3) + δH-C-C(43) (CH_3)	δC-N-H(43) + δN-C-H(28)	δN-C-H(34) + δC-C-H(22) (CH_2)	δN-C-H(34) + δC-N-H(25)
ν_{11}	δC-C-H(54) (CH_2)	δC-C-H(29) (CH_2)	-	-
ν_{12}	νC-N(53) + νC-C(30)	δC-C-H(22) + νC-C(15) + νC-N(11)	νC-N(60) + νC-C(27)	νC-N(62) + νC-C(26)
ν_{13}	νC-C(65) + νC-N(24)	δC-N-H(38)	νC-C(68) + νC-N(18)	νC-C(82)
ν_{14}	δC-N-H(31)	νC-C(33)	δC-N-H(31)	δC-N-H(29)
ν_{15}	δC-C-N(32)+ δC-C-C(12) + νC-C(12)	νC-C(28)	δC-C-N(32) + νC-C(12) + δC-C-C(12)	δC-C-N(34) + νC-C(13) + δC-C-C(11)
ν_{16}	τH-C-N-H(41) + τC-C-N-H(41)	τH-C-N-H(43) + τC-C-N-H(40)	τH-C-N-H(49) + τC-C-N-H(38)	τC-C-N-H(26)
ν_{17}	τH-C-C-C(55)	τH-C-C-C(55)	τH-C-C-C(54)	τH-C-C-C(38) + τC-C-N-H(26)
ν_{18}	τH-C-C-C(29) + τN-C-C-H(29) + τN-C-C-C(29)	τH-C-C-C(29) + τN-C-C-H(28) + τN-C-C-C(28)	τH-C-C-C(29) + τN-C-C-H(28) + τN-C-C-C(27)	τN-C-C-H(30) + τH-C-C-C(29) + τN-C-C-C(27)

-: TED ⩽ 10 was not included.
ν, δ and τ: Stretching, bending and torsional vibrations, respectively.

Results and Discussion

All the optimized scaling factors and scaled wavenumbers are given in Tables 1 and 2, respectively. For the first eight vibrational modes from ν_1 to ν_8, the results are almost the same for all the scaling factors used in this study, except for negligible changes in the TED values of some vibrations such as ν_5 and ν_6 (Tables 2 and 3). In S1, N—H stretching is not defined instead, X—H stretching vibration is defined. X—H stands for C—H and N—H which means that these two vibrations are considered in the same category and scaled with the same number which is 0.9092 as seen in Table 1. The deviations of N—H stretching value with S1 are larger than the others (Table 2). H—N—H bending vibrations match perfectly with the experimentally reported value in S6, S7 and S8 where H—N—H is defined. With the scaling parameters used in S4, S5 and S6, CH_3 deformation vibrations could not be identified. On the other hand, in S1, S2, S3, S7 and S8, CH_3 deformation vibrations were identified. In ν_{10} and ν_{11} modes, TED values of S1, S2, S3 and S7, S8 correspondingly are below 10% which indicates that predefined scaling parameters have considerable effect on determination of the TED values. The results obtained for mode ν_{10} are worth considering for further discussion.

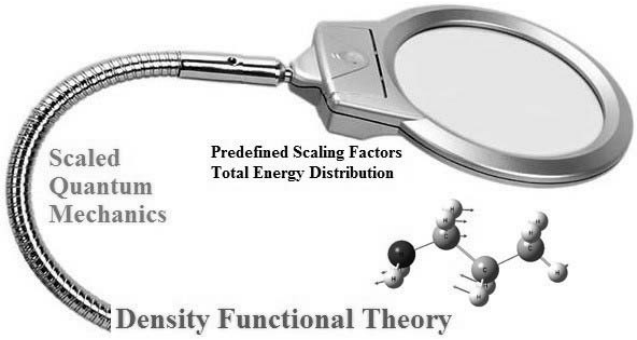

Figure 2 shows the character of CH_2 wagging vibrations. In SQM, wagging vibrations are described in terms of bending vibrations. For example, in S4 and S5 bending vibrations are due to CH_3, in S6 and S8 these are due to NH_2 and CH_2 and in S7 these are only due to CH_2. Pure CH_2 wagging vibrations are available only with the results obtained with S7. Experimental assignment of mode n_{11} is the CH_2 twist[15]. This is found correctly in all scaling files, except for those of S7 and S8. They yielded TED

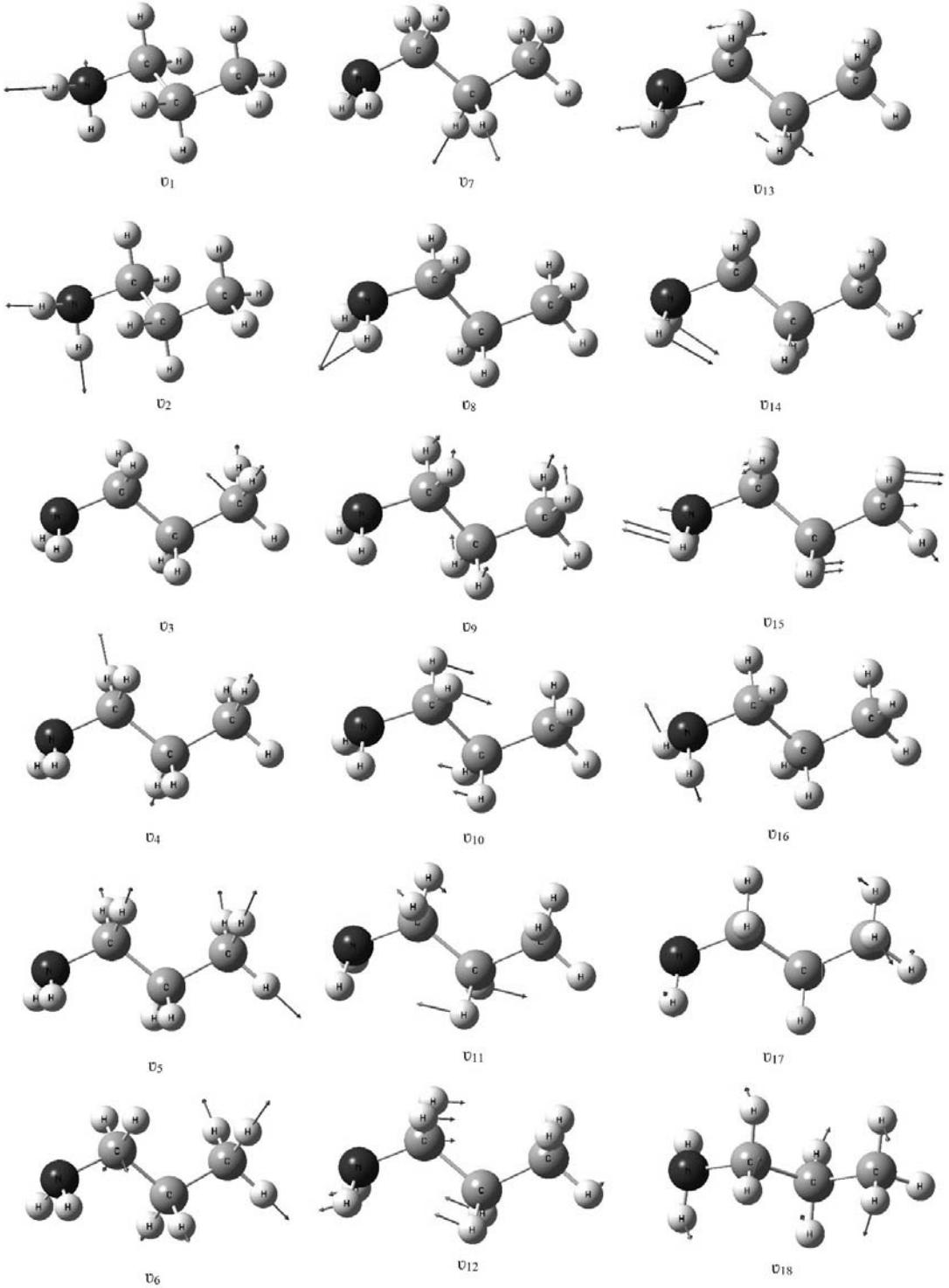

Figure 1. Pictogram of vibrational modes of n-pa.

values lower than 10% so they are disregarded. S7 and S8 include more scaling factors for torsional vibrations than the other scaling files. Upon defining additional torsional scaling parameter H—X—X—H, the TED values of CH_2 decrease below 10%. Therefore, scaling parameters seem to effect each other even though the type of the vibrations are different. It is very interesting that mode ν_{13} can only be correctly predicted by S6. However, the mode ν_{14} can be correctly predicted by all the scaling files except for S6. None of the scaling files show full agreement with the experimentally reported vibrational assignments.

Conclusions

Based on the results obtained in this research, it can be concluded that scaling parameters of SQM method should be carefully defined considering the properties of the investigated compound. Otherwise large deviations and some wrong vibrational assignments are likely to happen. In general, detailed scaling definitions seem to give better results. However, constructing less or more scaling parameters might result lower TED values as observed in this work with S1, S2, S3, S7 and S8. Mean absolute error values were also calculated and found as 11.9, 10.5, 10.0, 8.1, 6.9, 6.9, 4.6 and 5.2 cm^{-1} for S1 to S8, respectively. It can be understood from these results that as the increasing numbers of error values for scaling factors decrease, the calculated values approach those experimentally reported. However, the best results were obtained with S7 instead of S8 for n-pa molecule. As a summary, using different scaling parameters in SQM, we found more than we expected because not only TED values show same alterations but also the nature of the assignment changes. It can be expected that users should give importance to this situation in their upcoming work with SQM.

Acknowledgement

Authors acknowledge Fencluster system and Research Fund of Ege University (Project No: FGA-2019-20390).

References

1. Rauhut, G. and Pulay, P., 1995, *J. Phys. Chem*., **99,** 3093-3100.

2. Baker, J., Jarzecki, A.A. and Pulay, P., 1998, *J. Phys. Chem. A,* **102**, 1412-1422.

3. Coronel, A.C., Zinczuk, J., Fernández, L.E. and Varetti, E.L., 2015, An experimental and theoretical vibrational study of 3,3,6,6-tetramethyl-1,2,4,5-tetrathiane, *Vib. Spectrosc*., **81**, 40-45.

4. Borowski, P., Drzewiecka, A., Fernández-Gómez, M., Fernández-Liencres, M.P. and Ruiz, T.P., 2010, A new, reduced set of scaling factors for both SQM and ESFF calculations, *Vib. Spectrosc*., **52**, 16-21.

5. Fleming, G.D., Koch, R., Perez, J.M. and Cabrera, J.L., 2015, Raman and SERS study of N-acetyl-5-methoxytryptamine, melatonin—The influence of the different molecular fragments on the SERS effect, *Vib. Spectrosc*., **80**, 70-78.

6. Gayathri, R., 2018, *J. Mol. Struct*., **1166**, 63-78.

7. Alphonsa, A.T., Loganathan, C., Anand, S.A.A. and Kabilan, S., 2017, *J. Mol. Struct*., **1130**, 1018-1023.

8. Dikmen, G., 2017, *J. Mol. Struct.,* **1150,** 299-306.

9. Chain, F.E., Romano, E., Leyton, P., Paipa, C., Catalán, C.A.N., Fortuna, M. and Brandán, S.A., 2015, Vibrational and structural study of onopordopicrin based on the FTIR spectrum and DFT calculations, *Spectrochim. Acta*., A., **150**, 381-389.

10. Chain, F.E., Leyton, P., Paipa, C., Fortuna, M. and Brandán, S.A., 2015, FT-IR, FT-Raman, UV–Visible, and NMR spectroscopy and vibrational properties

of the labdane-type diterpene 13-epi-sclareol, *Spectrochim. Acta*., A., **138**, 303-313.

11. Pulay, P., Fogarasi, G., Pang, F. and Boggs, J.E., 1979, *J. Am. Chem. Soc*., **101**, 2550–2560.

12. Baker, J., Kessi, A. and Delley, B., 1996, *J. Chem. Phys.,* **105**, 192-212.

13. Pulay. P., Torok. F., 1965, *Acta Chim. Acad. Sci. Hung. Über die parameterdarstellung der kraftkonstantenmatrix I*., **44**, 287-292.

14. Keresztury, G., Jalsovszky, G., 1971, *J. Mol. Struct*., **10,** 304-305.

15. Durig, J.R., Beshir, W.B., Godbey, S.E. and Hizer, T.J., 1989, *J. Raman Spectrosc*., **20**, 311-333.

RNI No. MAHENG/2017/74063
ISSN No. (Print) 2581-5911
ISI Impact Factor 1.022 (2019-2020)

Heavy Metal Content, Occurrence and Distribution in Soil of Al-Qilt Catchment, Palestine

Hanan Harb[1], Shehdeh Jodeh[1,*], A. Rasem Hasan[2*], Subhi Samhan[3], Bayan Khalaf[1], Ghadir Hanbali[1] and Omar Dagdag[3]

[1]Department of Chemistry, An-Najah National University, P.O. Box 7, Nablus, Palestine.

[1]Laboratory of Industrial Technologies and Services (LITS), Department of Process Engineering, Height School of Technology, Sidi Mohammed Ben Abdallah University, P.O. Box 2427, 30000, Fez, Morocco.

[2]Water and Environmental Studies Institute (WESI) and Civil Engineering Department, An-Najah National University, P.O. Box 7, Nablus, Palestine.

[3] Palestinian Water Authority, Ramallah, Palestine.

***Email: sjodeh@hotmail.com; mallah@najah.edu**

Abstract

Heavy metal pollution in Palestine soils has been ignored for decades; anthropogenic pollution of soils has a negative effect on the environment and on human life. Determination of the elemental background and identifying the anthropogenic pollution in Palestine soils will help in screening the anthropogenic metal-based pollution and lead to the setting of water and soil quality management techniques. Several soil sediment samples were collected from Al-Qilt catchment, in addition to samples from pristine areas along the main wadi of Al-Qilt. All samples were analyzed for heavy and trace metals using inductively coupled plasma (ICP-MS) and after sequential fractional extraction based on Bureau Communautaire de Reference (BCR). Data was analyzed by computing the correlation coefficient of heavy and trace metals versus Al and Fe as reference elements. Fe was chosen as elemental normalizer, based on the higher values of correlation factor (R^2) as compared to Al. Enrichment Factor (EF) was determined for all elements to account for the contribution of anthropogenic sources. Metals Ti, V, Mn, Co, Rb, Ag, Li, B and Be were found to occur as anthropogenic pollutants at most of the Al-Qilt sites. The EF calculation showed that Pb had the highest value of trace metals in most of the studied locations. The heavy metals measured in this study show a high degree of contamination. This should be investigated using other environmental factors. This can be seen as hints for high risk of pollution by these trace metals.

Keywords: *Heavy metals, Sediments, Anthropogenic pollutants, Groundwater, Enrichment factor, Soil*

Introduction

Groundwater is considered to be the main freshwater resource in Palestine. Due to the rapid increase of population which can be referred to natural growth and the increasing number of Israeli settlements, the demand for potable water in West Bank for domestic uses has increased in the last two decades[1].

Environmental pollution continues to grow at an alarming rate due to human activities such as urbanization, technological progress, unsafe agricultural practices and

rapid industrialization, which degrades the environment. Toxic metals released into the environment are persistent and pose a serious threat to organisms exposed to high levels of such pollutants[1,2].

The studies of heavy metal pollution in sediments and soils have increased in recent years[3-8]. Heavy metals are considered as serious pollutants of aquatic ecosystems, due to their environmental persistence[9], toxicity, and ability to combine with food chains[10].

Toxic metal pollution in Palestine soils was ignored for decades; anthropogenic pollution of soil has a negative effect on the environment and human life[11]. Determination of elemental background for anthropogenic pollution in Palestine soils will help in screening the anthropogenic metal-based pollution[12]. Soil samples from pristine areas of Al-Qilt catchments were analyzed for the assessment of heavy and trace metals mainly those considered as anthropogenic sources for pollution in the area. Sources and impact of anthropogenic pollution in Al-Qilt catchment soils are also discussed. Samples along Al-Qilt catchment were collected on a monthly bases.

An environmental survey reveals that there are 363 disposal sites discharging raw waste-water into the environment in the West Bank[13]. Eight of these are at Al-Qilt catchment which starts from Al-Bireh wastewater treatment plant (5000 m^3/d).

This treated wastewater is discharged at Wadi Al-Ein, then mixed downstream with untreated wastewater that is discharged from Qalandiah Camp and Al-Ram (1500 and 1300 m^3/d) respectively. Furthermore, there are Israeli colonies and other Palestinian communities discharging their wastewater into the wadi (Figure 1). Moreover, the problem increases when people evacuate their septic tanks by tanker trucks into Al-Qilt wadi at arbitrary places. All these sources are mixed with the urban runoff and dumping site leachates in the winter season.

In general, soil pollution in urban regions may occur from other pollutants such as non-soil origin pollutants. However, the main soil pollutants are radionuclides, chloro organic compounds, and toxic metals. There are different pollutants sources such as road infrastructures, vehicular traffic, and manufacturing activities[15].

For a long time, the water from the Al-Qilt catchment was used for drinking purposes, irrigation, and washing. Today, more than 65,000 people from Palestinian communities[16] and six Israeli colonies totaling about 15,000 people[14] live in the Al-Qilt catchment. From the wastewater which discharges to the catchment, less than 10 percent is treated efficiently in the West Bank, whereas most of it is discharged untreated into the open environment near the wadis[17].

In our study, the criteria used to define toxic metals have included density, atomic number, atomic weight, or periodic table position[22]. Density criteria range from above 3.5 g/cm^3 to above 7 g/cm^3. The Periodic Table refers to toxic metals as "all the metals in groups 3 to 16 and in periods 4 and greater[23]. There is no widely agreed definition of heavy metal.

The main goal of this research was to study the anthropogenic pollution in Al-Qilt catchment soil and determine the soil elemental background of heavy metals in Al-Qilt catchment. This can be achieved by screening heavy and trace metal content of the Al-Qilt soil as either naturally occurring or resulting from anthropogenic activities using the elemental background for the toxic metals in the pristine area of Al-Qilt soil catchment and studying the occurrence of toxic metals in the pristine area soils of Al-Qilt catchment.

Materials and Methods

Study area

Al-Qilt catchment is located in the West Bank on the western side of the Jordan Valley and covers an area of

about 173 km^2 (Fig.1). It is characterized by a steep relief with elevations in the range of 700 m.a.s.l in the western part to the range of -250 m.b.s.l in the eastern part by the Jordan Valley. At Al-Qilt, there are about 96,935 inhabitants from Palestinian communities and Israeli colonies, and they discharge about 14,000 m^3/d of wastewater. Only about 30% of this wastewater is being treated and then mixed again with raw wastewater. The mean annual rainfall in the Al-Qilt basin is estimated to be about 600 mm in the higher Western part and about 150 mm in the lower Eastern part. The average annual rainfall over the catchment is about 400 mm. The long-term observations of flow mainly for Al-Qilt springs range from 3.0 to 12.0 Mcm/yr, and the continuous base flow for the Ras Al-Qilt spring of around 300 L/s[20].

An environmental survey revealed that there are 363 disposal sites discharging raw wastewater into the environment in the West Bank[19]. Eight of these are in the Al-Qilt catchment which starts from the Al-Bireh wastewater treatment plant (5000 m^3/d). The treated wastewater from Al-Bireh is discharged to Wadi Al-Ein and mixed downstream with untreated wastewater that is discharged from Qalandiya Camp and Al-Ram, 1500 and 1300 m^3/d respectively. Furthermore, there are Israeli colonies and other Palestinian communities discharging their wastewater into the wadi (Fig. 1). Moreover, the problem is exacerbated when people arbitrarily empty the septic tanks of tanker trucks into Al-Qilt wadi at different places. All these sources are mixed with the urban runoff in addition to leachates from dumping sites during the wet winter season[21].

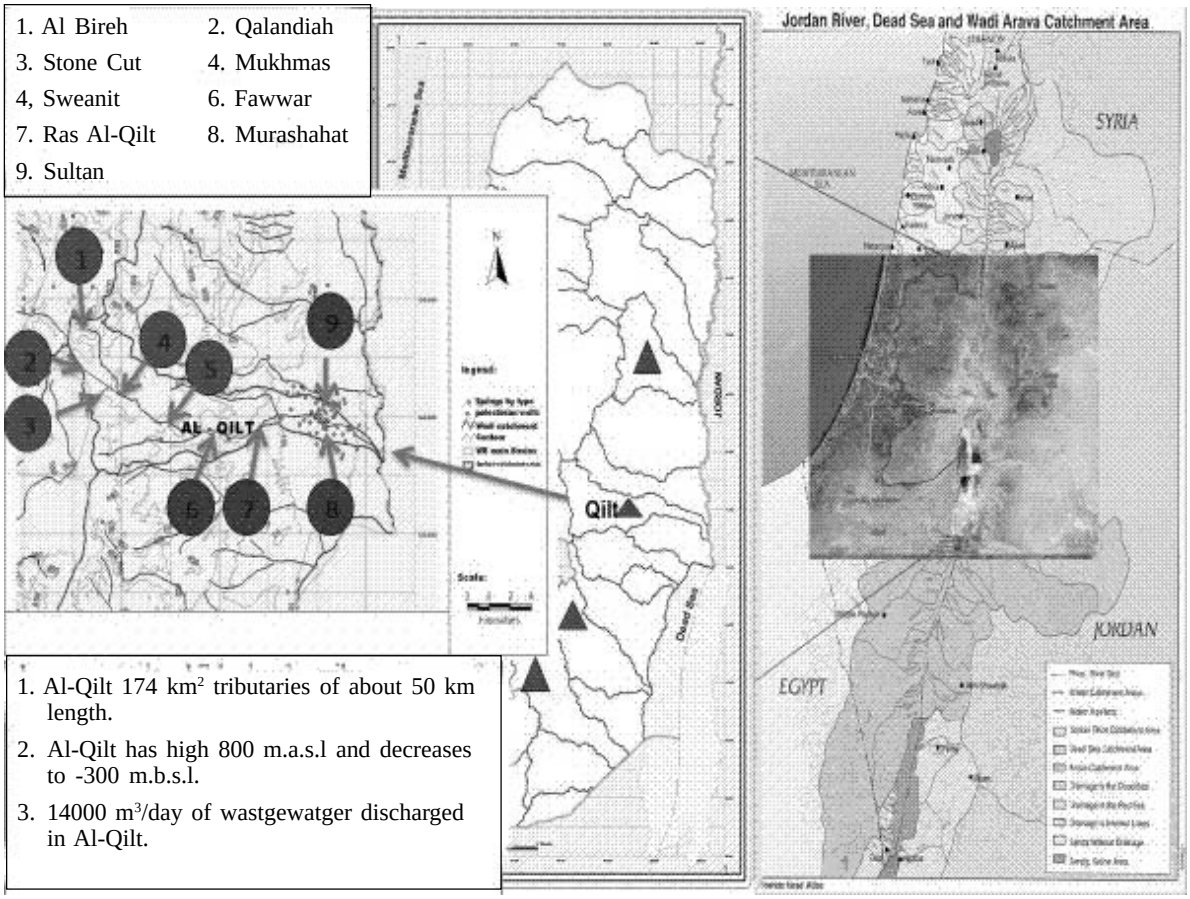

Fig. 1. Location of Al-Qilt catchment

Sampling

Soil sampling can be classified into three major categories: random, systematic and stratified sampling methods. The random sampling is the easiest and can be used for a pilot study with disadvantage is that soil samples may not represent the whole study site. The major objective of random sampling is to determine whether heavy metal concentrations of the soils are above background and/or legislative standards. In heterogeneous sites, stratified and systematic sampling strategies are needed, because they need a more detailed and accurate description of a given site with respect to the spatial and vertical distribution of heavy metals in the soil. In systematic sampling, soil samples are usually collected in a systematic manner, such as at a regular distance from one another across the study area, and at some of the fixed sampling grids., The systematic sampling strategy is often employed in the geochemical mapping of heavy metals, since it enables detailed characterization of the spatial distribution of heavy metals in a large region.

There are several factors that can affect soil sampling include sampling density, sampling depth and the use of composite soil samples. In an ideal situation, the larger the number of soil samples collected, the better the sample population can reflect the conditions of the site.

Like other kinds of environmental assessment, it is important to understand the specific purposes of the investigation. Therefore, at the initiation of the investigation, its primary objectives must be clearly defined and stated, since the objectives will be used as guidelines according to which all subsequent sampling and analytical procedures will be developed. For instance, if the goal of the investigation is to determine whether the soils are contaminated with heavy metals, analysis of the heavy metal concentrations of the soils will be adequate, and sampling of the soils will be relatively simple. However, if knowledge of the spatial distribution of heavy metals in soils is also sought, a systematic sampling approach will be required. In the preparatory stage, site information, such as soil type, parent materials, topography, and surrounding human activities, should also be collected. This information will assist the planning of the sampling strategy and interpretation of analytical results.

Ten soil samples were collected in December 2012 along the Al-Qilt catchment, and from nine locations as shown in Fig. 2: Ramallah, Al Bireh, Mukhmas, Qalandiah, Stone-cut zone, Sweanit, Fawwar, Ras Al-Qilt, Murashahat and Sultan. About 500 g of composite samples were taken below the top surface of the soil by polyvinylchloride-shovel and then placed in 250 mL polyethylene bottles. All samples were refrigerated at 3^0C for further analysis. Samples were analyzed according to the Water and Wastewater Standard Methods[22].

In addition, four samples were taken from Sweanit, Fawwar, Ras Al-Qilt and Murashahat, from a location far away from any human activity and considered as pristine samples.

Sample preparation and analysis

The water samples were collected during December 2012 in one-liter high-density polyethylene bottles (pre-cleaned with 10% nitric acid followed by repeated rinsing with twice distilled water), stabilized with a few drops of ultrapure nitric acid (0.5% HNO3) that were added to prevent additional microbial growth. All water samples were then preserved in a refrigerator at 4^0C and transported to Germany for examination and laboratory analysis purposes.

ICP-MS (Agilent Technologies 7500 Series, Agilent, Santa Clara, CA, USA) was used for analysis of the selected heavy and trace metals.

The analytical technique and operating conditions of ICP-MS were as follows:

Nebulizer gas (argon) flow rate, 0.9 L/min; auxiliary gas (argon) flow rate, 0.3 L/min; plasma (argon) gas flow rate, 15 L/min; reaction gas flow (helium) rate,

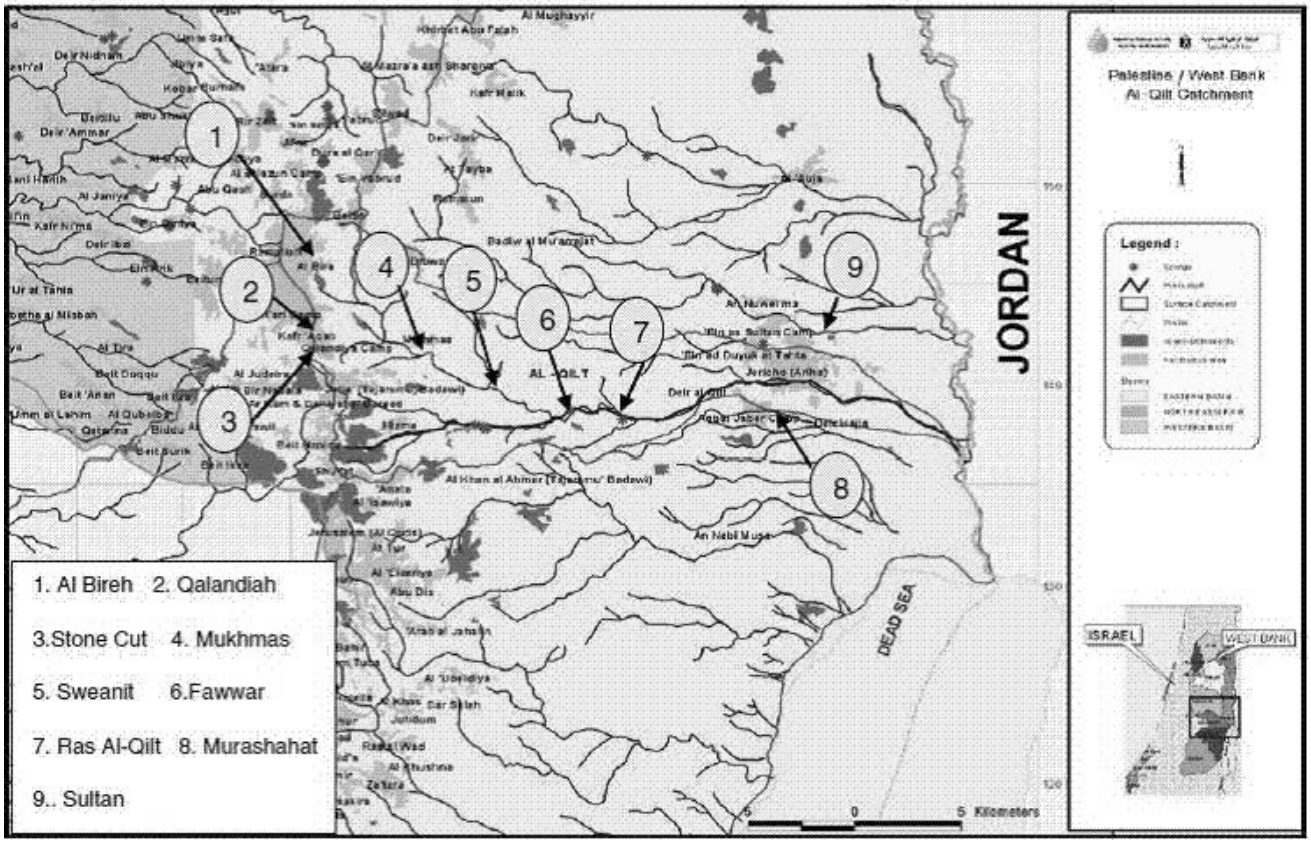

Fig. 2. Sampling location through Al-Qilt catchment

4 mL/min; lens voltage, 7.25 V; and ICP RF power, 1100W.

In terms of quality assurance concepts, an internal standard (Er) and a multi-standard calibration method (29 metal standards with a concentration of matrix 5% HNO3) were used to obtain an accurate quantitative determination for each of the selected toxic metals in water samples. Water samples were prepared by dilution of 1.0 mL of the water samples to 10.0 mL with 0.3% ultrapure nitric acid and they were analyzed by ICP-MS (Agilent, Santa Clara, CA, USA). The descriptive analytical approach has been used to analyze data, as well as to describe the obtained results. For the soil samples:

– About 200-250g of each sample was taken, dried and sieved to <63µm using "Fritsch D-55743" sieving analyzer.
– About 0.25g of each sample and Buffalo Reference Material (8704) as reference standard were weighed accurately in 100 ml Teflon digestion tube for Aqua Regia digestion and then mixed with 6mL of HNO_3 (65%) and 3ml of HCl (37%).
– The samples were digested for two hours using "Microwave MARS 5" digester and then the samples were kept at room temperature
– Samples were centrifuged, and the supernatant transferred to 50mL tube for analysis by doing the proper dilution[21].

Trace metal concentrations of Al, Ti, V, Cr, Mn, Fe, Co, Ni, Cu, Zn, As, Rb, Sr, Mo, Ag, Cd, Sn, Sb, Ba,

Pb, Bi, U, B, Li, and Be were measured by an Inductive Coupled Plasma Mass Spectrometer (ICP-MS) (Agilent 7500).

For BCR fractionation analysis, about one gram of the samples was weighed. All soil samples analyses were conducted in the water research Centre of the Helmholtz-Centre for Environmental Research (UFZ), Magdeburg, Germany.

Bureau Communautaire de Reference (BCR)

BCR sequential fractionation extraction was used as a recommended standard procedure for the characterization of heavy and traces metals in sediment and soil[21]. The BCR method compresses four steps classified in terms of reagents used. 'This method is recommended by the Measurements and Testing Program of the European Commission. The fractions of each method are grouped into four "equivalents" (acid soluble, reducible, oxidable, and residual).

Data Analysis

Statistical analysis

Toxic metals were graphed against Al and Fe as reference elements to facilitate the comparison between Al-Qilt sites. Samples were divided into groups based on comparison with the concentrations of the pristine samples (equal or less than), whereas for Al and Fe concentration was around 17217.5 mg/kg and 15896.25 mg/kg, respectively. Analysis of variance was performed using statistical software package SPSS® to identify the variation among heavy metals in the samples.

Normalization of toxic metals

The normalization was based on the supposition that metal concentrations are very consistent with the concentration of reference elements unless the metals were of anthropogenic origin. Normalization is a way to compensate for the natural variability of trace metals in soils, so that any anthropogenic metal contributed may be detected and quantified by reducing the natural effect of grain size. This assumption allows us to identify the trace metal as a man-made pollutant[23].

The normalization method was based on the following assumptions:

(1) The concentration of metals was regular with respect to the reference elements unless the metals were of anthropogenic origin.
(2) The normalization method is a way to compensate for the natural variability for toxic metals in soil and sediments.
(3) Any anthropogenic metal contribution may be detected and quantified by reducing the natural effect of grain size.

These assumptions allow us to identify the trace metal as a man-made pollutant since many researchers have used Al and Fe as elemental normalizer.

Enrichment Factor (EF)

The first step in the calculation of EF is finding the relation between a metal and a normalizer, and then using this factor to identify anomalous metal concentrations that may have an anthropogenic source. The enriched site can then be specified. The selected normalizer can be divided by the same ratio of anthropogenic to un-impacted geological material (background). This permits the definition of Enrichment Factor (EF) parameters such as (Me/N) sample/(Me/N) background, where (Me/N) sample is metal to normalizer ratio in the soil sample and (Me/N) background is the metal to normalizer ratio in anthropogenic un-impacted geological material[24, 25].

EF = (Me/N) sample/(Me/N) background (1)

Me/N sample is the metal or element to normalizer ratio.

Me/N background is the natural background value of the metal to normalizer ratio.

Enrichment Factor shows the status of environmental contamination where the EF values were interpreted by Acevedo-Figueroa et. al.,[26], where EF < 1 indicates no enrichment; 1-3 is minor; 3-5 is moderate; 5-10 is moderately severe; 10-25 is severe; 25-50 is very severe and Ã 50 is extremely severe.

Elemental background for soil (EBS)

Trace and heavy metal concentrations indicate anthropogenic pollution if they are compared with the elemental background. Samples from the pristine area (places with no known human activities) in Al-Qilt catchment were analyzed to make the elemental background. Average of the four samples from the pristine areas were calculated and used for the calculation of the above EF.

Quality control and assurance

During sampling and lab analysis, care must be taken when storing the samples in bottles and using lab equipment to avoid contamination from the glassware and bottles. Even the chemicals which will be involved should be of analytical grade and of high purity. All metallic devices and containers of metals should be avoided to prevent contamination or leaching of some metals to soil samples. In such cases, stainless steel devices and plastic containers should be used eq. polystyrene plastic bags. Samples should be stored at 4^0C before analysis.

All glass and plastic containers should be rinsed with dilute acid (10% (v/v) nitric acid) and rinsed thoroughly with distilled and deionized water before use, to ensure that there is no contamination from the laboratory accessories.

In order to provide accurate and producible data, a quality control system must be used throughout the analytical process. The quality control is a set of procedures and practices which result in an increase in precision and a decrease in bias. The use of duplicate analysis, spiked samples, standard reference materials, and QC check samples are all mechanisms used to demonstrate the control of quality. In general, to detect contamination and evaluate the reproducibility and effectiveness of the analytical procedures, procedural blanks, duplicates and certified standard reference materials, such as those offered by the National Institute of Standards & Technology (NIST), should be included in the analytical program.

Results and Discussion

The correlation coefficient (R^2)

Toxic concentrations of collected samples from Al-Qilt were graphed as metal vs. reference element such as Al and Fe and the correlation coefficient were calculated.

The correlation factor between the concentration of all measured metals against Fe were higher than Al. Al and Fe were found to be good normalizers due to their high R^2 values. (Table. 1)

Significant variation (α <0.05) were found among the metals V, Mn, Co, Sr and U for normalization with Al. While for normalization with Fe, significant variation (α < 0.05) were found among the metals V, Mn, Co, Rb, Sr, U, and Li. Complete statistical analysis was done for supplementary materials.

Me/Al, Me/Fe normalization for anthropogenic parameters: Normalization procedures were adopted by dividing the concentration of any metal by the concentration of the reference element. In this study, we use the normalization procedure to recover the natural variability of trace metal in soil. In this way, the anthropogenic metal contribution could be detected and quantified. The normalization of metal per Al and Fe were calculated and then the normalization results were visualized as numerical numbers and not fractions; the highest value is considered as an indication of anthropogenic pollutants.

The toxic metals concentrations were graphed as metal vs. reference element and then the correlation coefficients were calculated as shown in Figures 3 to 5.

Table 1. Correlation coefficient values (R^2) for metals with Al, Fe, and EBS. along Al-Qilt catchment

Me	Metal/Al	Metal/Fe	Metal/EBS. *
Ti	0.0469	0.2087	0.8456
V	0.5503	0.7179	0.1000
Cr	0.3837	0.3331	0.8514
Mn	0.4211	0.4222	0.4153
Co	0.6711	0.7253	0.3590
Ni	0.3362	0.3155	0.0939
Cu	0.3602	0.1895	0.4960
Zn	0.3803	0.2362	0.0319
As	0.3942	0.2902	
Rb	0.6297	0.4987	0.0421
Sr	0.5678	0.6026	0.6554
Mo	0.1027	0.1393	0.3333
Ag	0.0068	0.0341	0.3086
Cd		0.0005	0.2727
Sn	0.0762	0.0365	0.1341
Sb	0.2772	0.1698	
Ba	0.1715	0.0194	0.6618
Pb	0.3577	0.2677	0.0884
Bi	0.0003	0.0795	
B	0.0982	0.1277	
Be	0.0727	0.2483	
Li	0.6862	0.7364	
U	0.4127	0.3041	0.0526

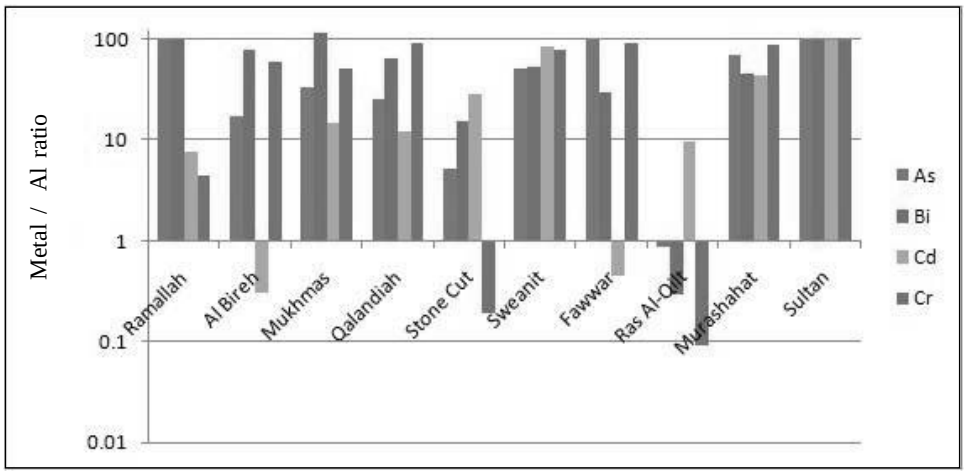

Fig. 3: Metal/Al ratio less than 1 for As, Bi, Cd, and Cr.

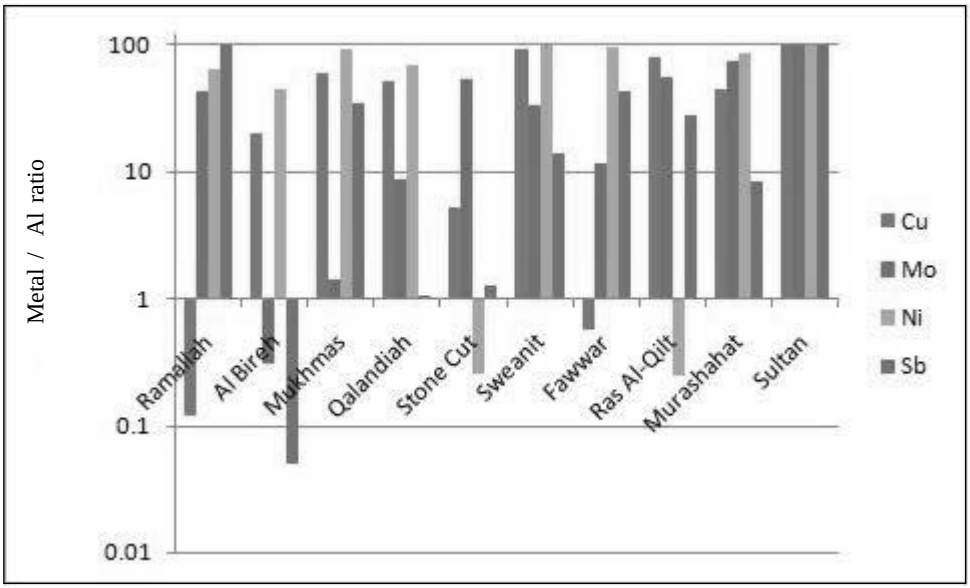

Fig. 4: Metal/Al ratio less than 1 for Cu, Mo, Ni, and Sb.

The results showed that metal/Al was less than 1 for Cr, Ni, Zn, Cu, Sr, Cd, Sb, U, Bi, As and Mo. This indicates that these values of the mentioned parameters are to be considered as background or natural effects. Values of metal/Al greater than one are shown in Figs 6 -8, which indicates anthropogenic pollution.

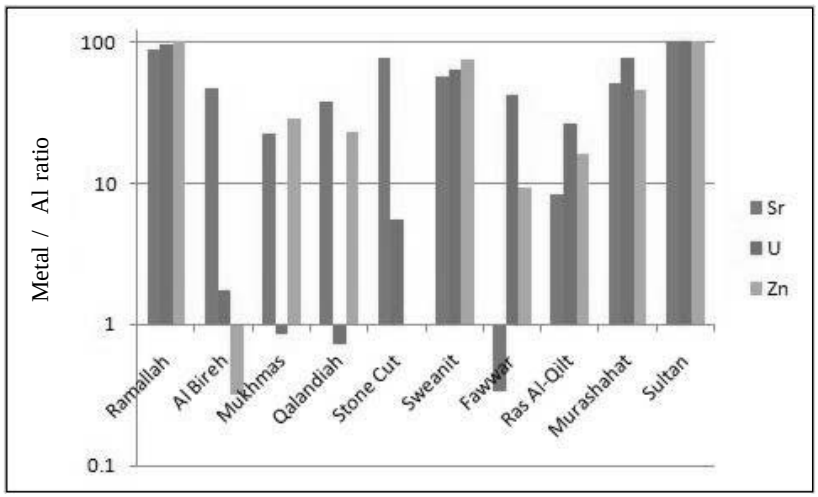

Fig. 5: Metal/Al ratio less than 1for Sr, U, and Zn.

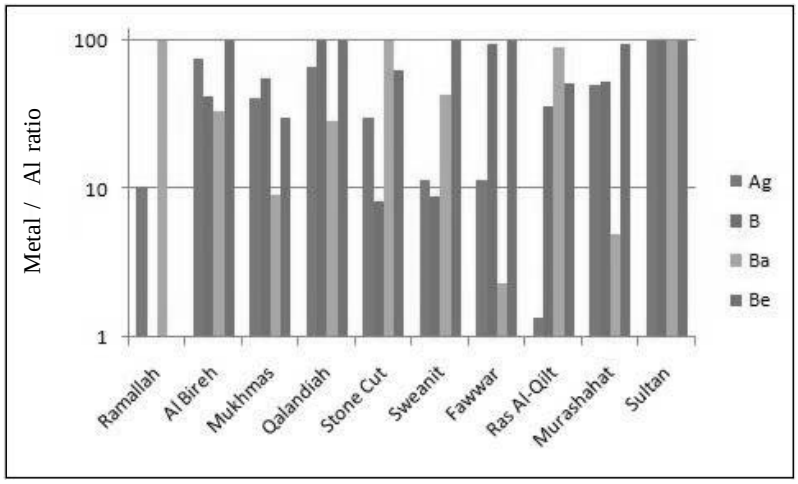

Fig. 6: Metal/Al ratio more than 1for Ag, B, Ba and Be

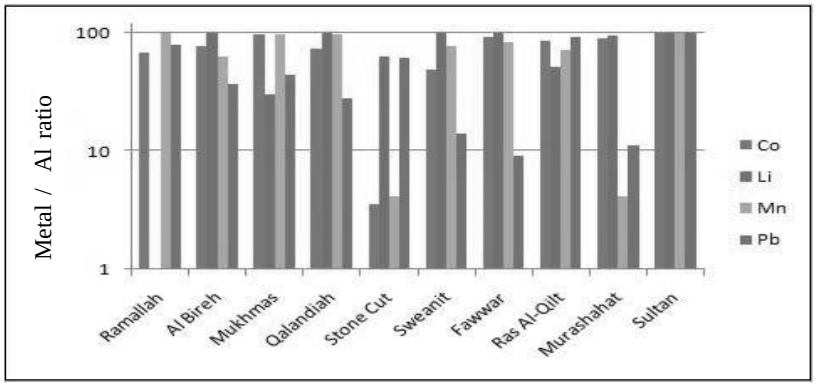

Fig. 7: Metal/Al ratio more 1 for Co, Li, Mn and Pb.

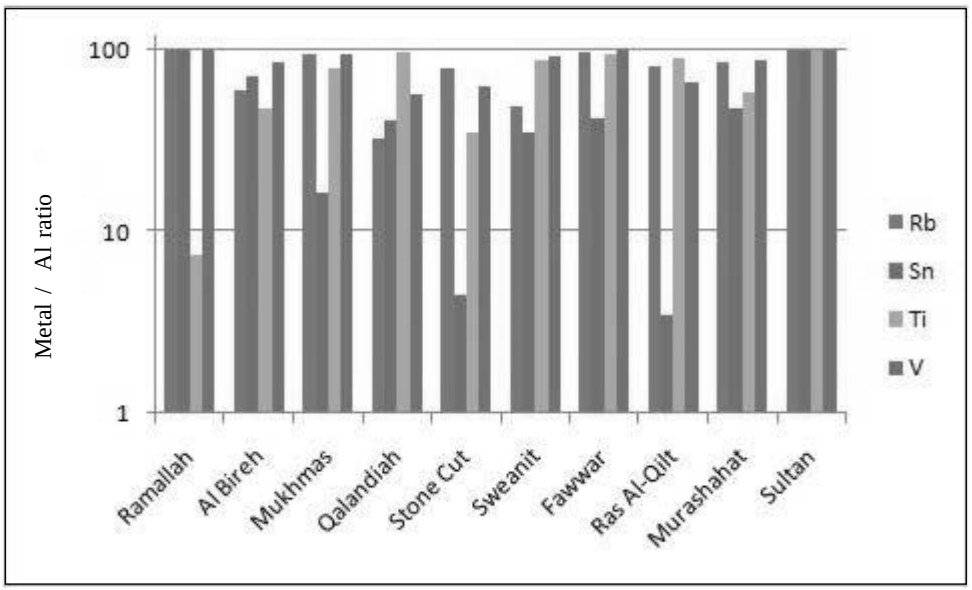

Fig. 8: Metal/Al ratio more 1for Rb, Sn, Ti, and V.

Furthermore, the results showed that metal/Fe ratios for Ni, Zn, Sr, Cd, Sn, Ba, Pb, Bi, and U were less than one, and so these toxic metals are not considered as anthropogenic pollutants at Al-Qilt sampling site as shown in Figs. 9-10.

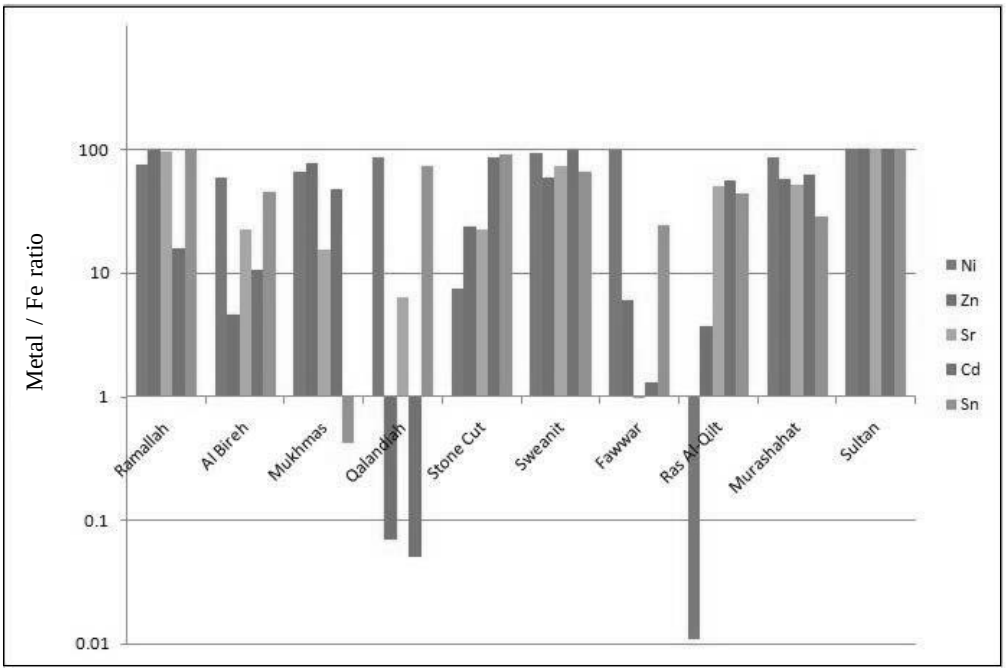

Fig. 9: Metal/Fe ratio less than 1for Ni, Zn, Sr, Cd, and Sn.

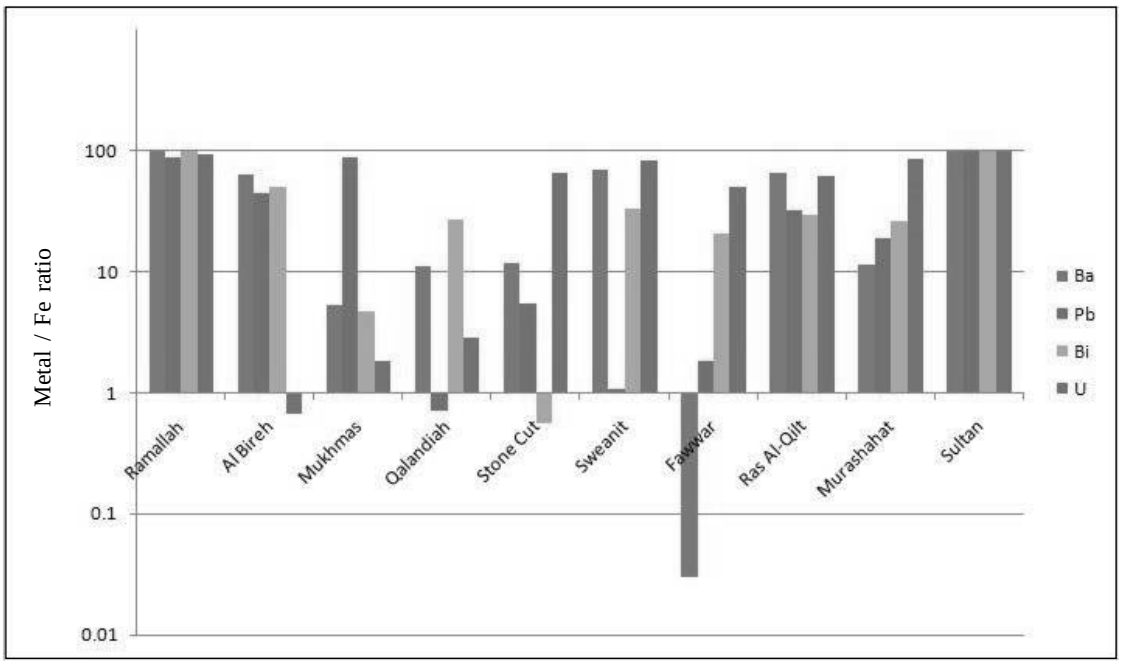

Fig. 10: Metal/Fe ratio less than 1 for Ba, Pb, Bi, and U.

On the other hand, the ratios greater than one, are considered as an anthropogenic indication of pollution and shown in Figs. 11-14.

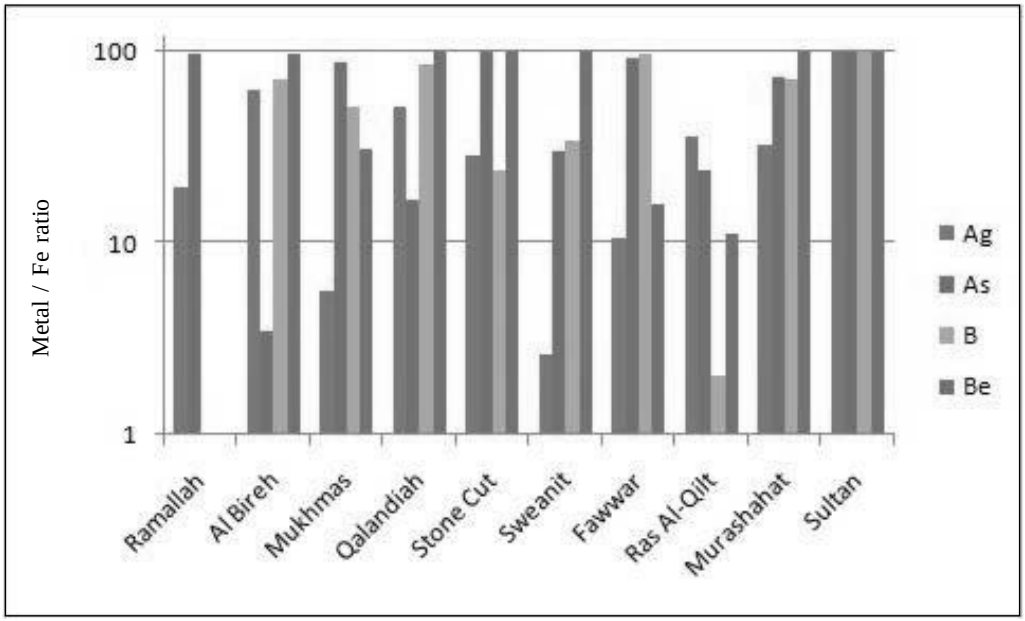

Fig. 11: Metal/Fe ratio more than 1 for Ag, As, B and Be.

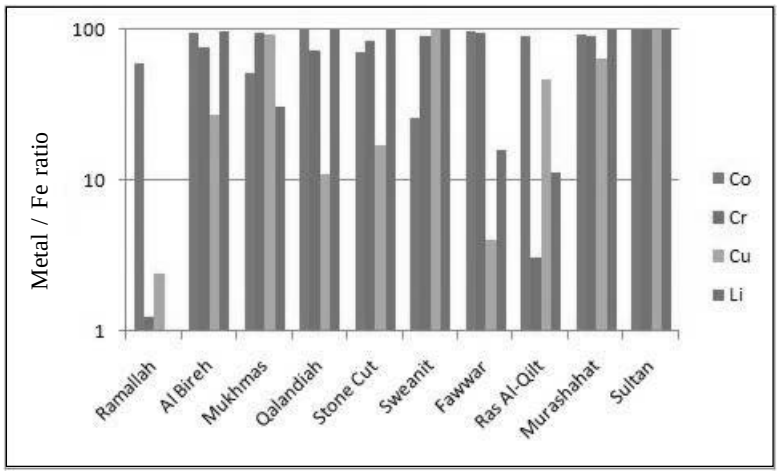

Fig. 12: Metal/Fe ratio more than 1 for Co, Cr, Cu, and Li.

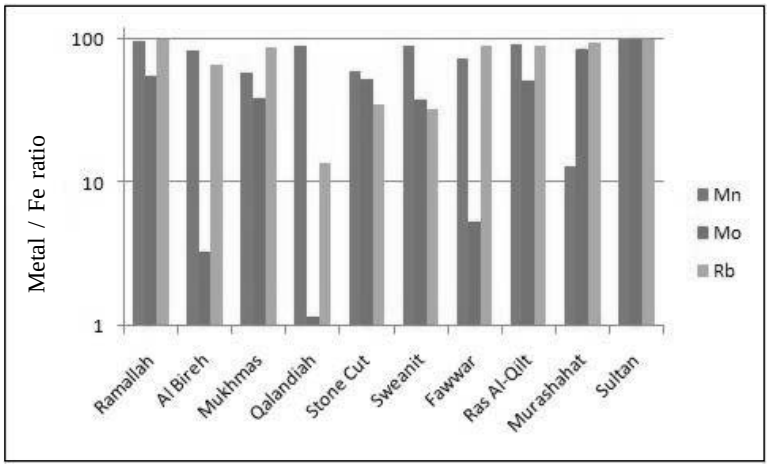

Fig. 13: Metal/Fe ratio more than 1for Mn, Mo, and Rb.

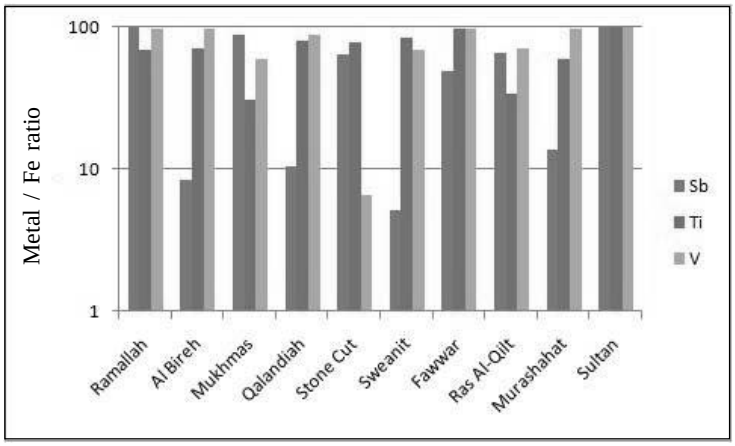

Fig. 14: Metal/Fe ratio more than 1 for Sb, Ti, and V.

The metal/Al and metal/Fe normalization values for Ti, V, Mn, Co, Rb, Ag, Li, B and Be indicated that these metals are anthropogenic pollutants in most of the Al-Qilt sites.

Furthermore, Fe was more suitable for normalization compared to Al for trace and heavy metals, since it has the highest R^2 values compared to Al as shown in Table 1.

According to the normalization method, we can assign them as anthropogenic pollutants. Thus, we can use the results of Fe as background values for the samples to calculate the Enrichment Factor (EF).

Enrichment Factor (EF)

Table 2 summarizes the results of enrichment factors at Al-Qilt catchment for trace metals tested at each site. If the EF values are between 0.5 and 1.5, the metal must be entirely from crustal materials or natural weathering processes. EF value greater than 1.5 suggests that a significant portion of the metal has originated from non-crustal or anthropogenic processes.

Table 2. Enrichment factor along Al-Qilt. For EF<1: no enrichment, EF=1-3: minor, EF=3-5: moderate, EF=5-10: moderately enriched.

Sampling Location	Ti	V	Cr	Mn	Co	Ni	Cu	Zn	As	Rb	Sr
Ramallah	0.15	0.51	0.41	0.52	0.61	0.38	1.05	1.21	1.33	2.18	0.07
Al Bireh	0.66	0.69	0.36	0.74	0.80	0.49	0.41	0.45	0.52	0.98	0.08
Mukhmas	0.96	0.77	0.41	0.80	0.84	0.54	0.47	0.49	0.58	0.90	0.14
Qalandiah	0.94	0.70	0.34	0.79	0.80	0.47	0.48	0.50	0.47	0.93	0.06
Stone Cut	0.84	0.75	0.65	0.75	0.85	0.57	0.71	0.80	0.64	1.00	0.11
Sweanit	0.92	0.96	0.50	0.58	1.14	0.96	0.82	1.40	1.31	1.31	0.57
Fawwar	0.93	0.90	0.74	1.44	1.09	1.01	1.21	0.92	0.87	0.87	0.93
Ras Al-Qilt	1.06	1.21	0.90	0.86	0.85	1.17	0.83	1.04	0.97	0.85	1.46
Murashahat	1.05	0.91	0.66	0.99	0.93	0.83	1.04	0.75	0.93	1.04	0.92
Sultan	2.16	0.90	0.38	0.20	0.98	0.54	0.41	0.32	0.55	0.80	0.13
	Mo	**Ag**	**Cd**	**Sn**	**Sb**	**Ba**	**Pb**	**Bi**	**U**	**B**	**Li**
Ramallah	0.33	0.00	0.64	0.31	1.87	0.63	5.71	0.50	0.21		
Al Bireh	0.25	0.60	0.21	0.12	0.37	0.40	0.81	0.50	0.16	0.55	1.00
Mukhmas	0.42	1.16	0.27	0.40	0.48	0.46	1.10	0.64	0.42	0.46	0.50
Qalandiah	0.22	0.00	0.19	0.22	0.34	0.37	0.93	0.45	0.15	0.29	0.93
Stone Cut	0.44	1.93	0.45	0.36	1.20	0.44	4.09	1.07	0.17	0.45	0.95
Sweanit	1.16	2.10	0.75	3.83	1.31	2.23	1.35	1.75	0.58	0.91	1.12
Fawwar	0.77	0.69	0.49	0.51	0.87	1.24	0.89	1.16	0.77	0.68	0.91
Ras Al-Qilt	1.30	0.78	1.67	0.24	0.97	1.08	1.00	1.30	1.73	1.01	1.02
Murashahat	0.82	0.74	1.06	0.23	0.93	0.65	0.85	0.00	0.82	1.37	0.97
Sultan	0.20	4.07	0.26	0.53	0.46	0.32	0.58	1.85	0.41	0.52	1.10

The EF for heavy and trace metals in soil at Al-Qilt varied with years. From the table we can see that Pb is moderately severe in Ramallah while Pb, Sn and Ag are moderate in stone cut areas (Sweanit and Sultan) respectively.

Values of FE in Table 2 show that there is mostly no enrichment for most of the studied heavy and trace metals. Pb, Sn, and Ag have moderate EFvalues. Pb has the highest value and sometimes showed moderate values like in Ramallah. This value may be due to war and military activities in that region and originates from urban activities such as vehicles, road, and urban runoff prior to phasing out of leaded gasoline.

Conclusions

In this research, Al-Qilt area was found to be with reduced contamination levels in its sediments for heavy and trace metals contents. Such a result is currently a positive factor for the water quality in the region, though, a continuation of discharging untreated wastewater to the main course of Al-Qilt may cause an increase in the contamination levels. When applying the calculation of CF to single steps of the BCR sequential extraction scheme, a more realistic view on the potential impact of the trace metals to the environment is gained. Considering the first two steps of the BCR scheme (exchangeable, reducible) which are the most relevant fractions from which the metals can be released to the environment, Cu, Pb, Zn, Ag, Sb, and Bi exhibit CF values greater than six. The pollution caused by the discharge of wastewater, dumping site leachate, urban runoff, plastic material, and batteries have led to these results. These reveal that there is severe contamination by Ag, Bi, Cd, Zn and Hg at most of the sites. The heavy metals measured in this study show a high degree of contamination and should be investigated. This can be seen as hints for high risk of pollution by these trace metals. For future research, Iron levels are recommended as elemental normalizer. Levels of Pb contamination in Al-Qilt sediments were found to be moderately enriched, and such contamination might decrease with time due to phasing out of leaded gasoline in the country.

Acknowledgment

The authors would like to thank PWA and MEDRC for financial support. Special thanks also go to PADUCO for minor research grants.

References

1. Mahmoud, N., Amarneh, M.N., Zeeman, G., Gijzen, H. and Lettinga, G., 2003, *Environmental Pollution*, **126**,115-122.

2. Ojuederie, O. B., and Babalola, O. O., 2017, *International Journal of Environmental Research and Public Health*, **14**, 1504.

3. Bird, G., Brewer, P. A., Macklin, M. G., Balteanu, D., Driga, B., Serban, M., and Zaharia, S.,2003, *Applied Geochemistry*, **18**, 1583-1595.

4. Veeresh, H., Tripathy, S., Chaudhuri, D., Hart, B.R. and Powell, M.A., 2003, *Applied Geochemistry*, **18**, 1723-1731.

5. Reliæ, D., Đorđeviæ, D., Popoviæ, A., and Blagojeviæ, T.,2005, *Environment International*, **31**, 661-669.

6. Roos, M.., Astroem. M., 2005, *River Research and Applications*, **21**,351–361.

7. Sysalova, J., Szakova. J., 2006**.** *Environmental Research*, **101**, 287–293.

8. Bacon, J., Davidson. C., 2008, *Analyst*, **133**, 25–46.

9. Armitage, P., Bowes, M., Vincent, H., 2008, *River Research and Applications*, **23**, 997–1015.

10. Förstner, U. and Wittmann, G.T., 2012, Metal pollution in the aquatic environment, Springer Science & Business Media.

11. Potapowicz, J., Szumiñska, D., Szopiñska, M. and Polkowska, Z.,2019, *Science of The Total Environment*, **651**, 534-1548.

12. *Mahmoud, S. H., Gan, T,* Y., *2018,* Science of The Total Environment, ***, 633***, 1329-1344

13. Samhan, S., Friese, K., Von Tuempling, W., Poellmann, H., and Ghanem, M., 2011, *International Journal of Environmental Studies*, **68**, 495-507.

14. West, L.J.S., 2018, Palestinian Central Bureau of Statistics (PCBS).

15. Czarnowska, K., Gworek, B., Kozanecka, T., Latuszek, B. and Szafranska. E., 1983**,** *Polish Ecological Studies*, **9**, 63–79.

16. Authority, P.W., 2009. Data Base and GIS units, *West Bank, Ramallah*.

17. ARIJ, A., 2007. Status of the Environment in the Occupied Palestinian Territory, Jerusalem Applied Research Institute (Arij).

18. Saxena, P., Misra, N., 2010, *Soil Heavy Metals*, **19**, 431-477.

19. Hawkes, S.J., 1997, *Journal of Chemical Education*, **74**, 1374.

20. Authority, P.W., 2009. Data Base and GIS units, West Bank, Ramallah.

21. Samhan. S., 2013**,** Doctoral dissertation Halle (Saale), Universitäts-und Landesbibliothek Sachsen-Anhalt, Diss.

22. American Public Health Association, American Water Works Association, Water Pollution Control Federation and Water Environment Federation, 1915, Standard methods for the examination of water and wastewater, **2**.

23. Daskalakis, K. and Conner, T. O., 1995, *Environmental Science and Technology*, **29**, 470–477.

24. Jeong-Yul, S. and Birch, G., 2005, *Water, Air, and Soil Pollution*, **160**, 357-371.

25. Feng, H., Han, X., Zhang, W. and Yu, L., 2004, *Marine Pollutant Bulletin*, **49**, 910–915.

26. Acevedo-Figueroa, D., Jiménez, B.D. and Rodríguez-Sierra, C.J., 2006, *Environmental Pollution*, **141**,336-342.

RNI No. MAHENG/2017/74063
ISSN No. (Print) 2581-5911
ISI Impact Factor 1.022 (2019-2020)

Studies of m-Hydroxybenzaldehyde Derivative of Benzilmonoximethiocarbohydrazide

Deepak Patekar[1], Raj Badekar[2*], Kalpana Patankar-Jain[3] and Rama Lokhande[1]
[1]School of Basic Sciences, Jaipur National University, Jaipur 302 017, India
[2]Riva Industries, Ambernath MIDC - 421 505, Dist. Thane, Maharashtra, India
[3]Department of Chemistry, BNN College, Bhiwandi, Dist. Thane, Maharashtra, India.
Email: badekarrr@gmail.com

Abstract
The synthesis and characterization of α-benzilmonoximethiocarbohydrazide-m-hydroxybenzalidene and its Fe(II), Co(II), Ni(II) and Pd(II) complexes are reported. Elemental analysis, magnetic moments and spectral [UV-Visible, PMR and IR] measurement have been used to characterize the ligand and its complexes. FT(IR) spectra show that the ligand behaves in a bidentate manner.

Keywords: *α-benzilmonoximethiocarbohydrazide, m-hydroxybenzaldehyde, Fe(II), Co(II), Ni(II) and Pd(II)*

Introduction

There has been considerable interest in the Chemistry of Schiff bases containing N, S, and O donor atoms[1-10]. Benzilmonoxime are chelating agents which are frequently used in extractive and analytical chemistry[11-12]. Benzilmonoxime are of specia interest owing to their biological activity and semi-conducting properties.[13-15].

In this paper, we report the preparation and characterization of some new metal complexes derived from benzilmonoximethiocarbohydrazide-m-benzilidene. The synthesized compounds were characterized on the basis of physico-chemical analysis and spectral studies.

Materials and Methods

All chemicals used were of Analytical Grade. Elemental analysis (C, H, N and O) were carried out with a Carlo Erba EA-1108 analyzar. The FT(IR) spectra (400-4000cm^{-1}) were recorded on a Perkin-Elmer Spectrum-100 using KBr discs. The conductivity measurements were carried out on a EQ Laboratory conductivity meter using nitrobenzene as solvent at room temperature. Magnetic susceptibility measurement were determined by Gouy's method using $Hg[Co(SCN)_4]$ and $[Ni(en)_3S_2O_3]$ as calibrates. The PMR spectra were recorded on a Brucker AV300 NMR spectrometer using TMS as internal standard. The electronic absorption spectra (200-1000nm) were recorded in methanol and chloroform with a JASCO V-650 spectrophotometer.

Preparation of HBMTmHB ligand

Benzilmonoximethiocarbohydrazide was prepared by reported method[16]. A mixture of benzilmonoximethiocarbohydrazide (0.10 mol) in 50mL ethanol was added to the ethanolic solution of m-hydroxybenzaldehyde (0.20 mol) and 5mL concentrated HCl. The reaction mixture was refluxed for 11h and allowed to stand overnight at room temperature. The yellow crystals obtained were collected by filtration.

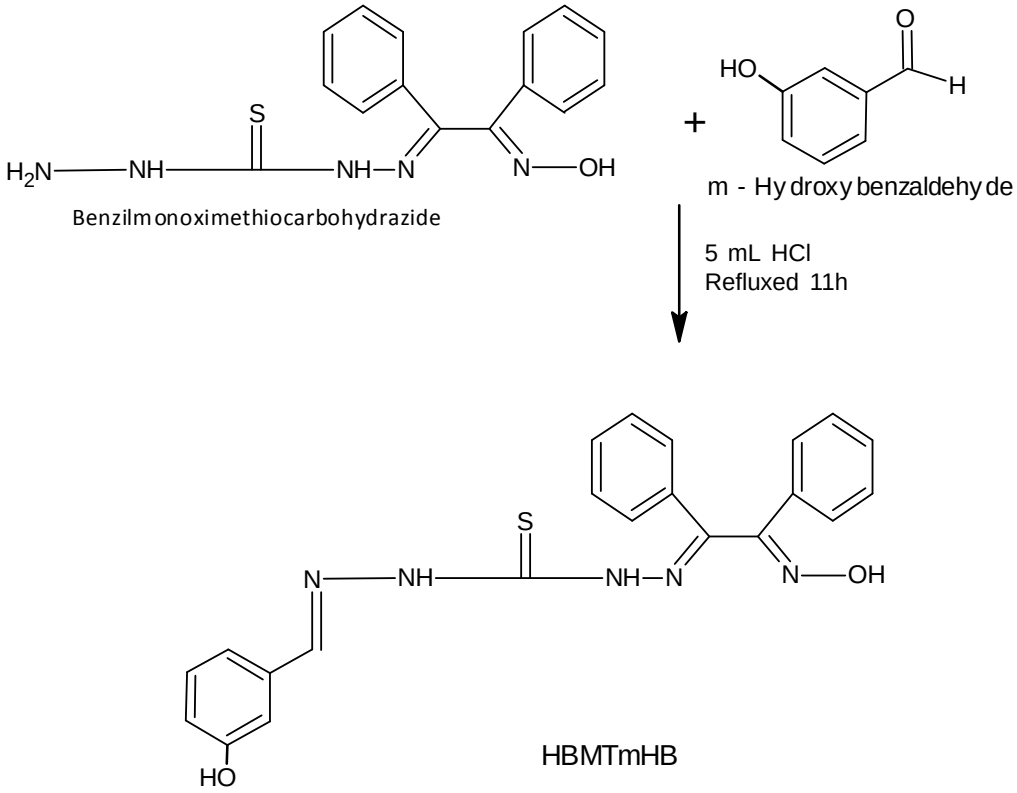

Preparation of metal complexes of HBMTmHB

Bis(α-Benzilmonoximethiocarbohydrazone-m-hydroxybenzaldehyde)Ferrous(II), [Fe(BMTmHB)$_2$]
To a solution of 0.76g ferrous sulfate (5mmol) in 10mL water was added gradually with stirring, a solution of 3.71g (10mmol) of HBOMTH in 20mL ethanol. The pH of the mixture was increased slowly to 5.5 using dilute (0.1 N) NaOH, when an ink blue colored complex separated out. It was filtered, washed with hot water (50mL), dried at 110^{0}C and recrystallized from methanol.

Bis(α-Benzilmonoximethiocarbohydrazone-m-hydroxybenzaldehyde)Cobalt(II), [Co(BMTmHB)$_2$]
To a solution of 0.85g cobalt chloride hexahydrate (5mmol) in 10mL water was added gradually with stirring, a solution of 3.71g (10mmol) of HBMTmHB in 20mL ethanol. The pH of the mixture was increased slowly to 6.5 using dilute (0.1 N) NaOH, when an orange colored complex separated. It was digested for 15 minutes on a hot water bath, filtered, washed with hot water (50 mL), dried at 110^{o}C and recrystallized from methanol.

Bis(α-Benzilmonoximethiocarbohydrazone-m-hydroxybenzaldehyde)Nickel(II), [Ni(BMTmHB)$_2$]

To a solution of 0.85g nickel sulfate hepahydrate (5mmol) in 10mL water was added gradually with stirring, a solution of 3.71g (1mmol) of HBMTmHB in 20mL ethanol. The pH of the mixture was increased slowly to 8.0 using dilute (0.1 N) NaOH, when an light green colored complex separated. It was digested for 15 minutes on a hot water bath, filtered, washed with hot water (50mL), dried at 110^{0}C and recrystallized from methanol.

Bis(α-Benzilmonoximethiocarbohydrazone-m-hydroxybenzaldehyde)Palladium(II), [Pd(BMTmHB)$_2$]

To an acidic solution of 0.50g of palladium chloride (28mmol) was added a solution of 2.08g HBMTmHB (56mmol) in 10mL ethanol. The pH of the solution was increased to 8.0 by adding dilute (0.1 N) NaOH, when a green complex separated. It was digested on a hot water bath for 15 minutes, filtered, washed with hot water (50mL), dried at 110^{0}C and recrystallized from methanol.

Results and Discussion

The analytical and physical data of the HBMTmHB and its complexes is given in Table-1. The molecular weight of the ligand HBMTmHB was found to be 416.90 (expected 471.48) using Rast's method[17]. Considering that its empirical formula is $C_{22}H_{19}N_5O_2S$, it is suggested that the ligand is monomeric in nature. HBMTmHB was obtained in a crystalline form, which melts at 203^{o}C and its metal complexes decomposed at 215-225^{o}C, indicating high thermal stability and stronge metal-ligand bond. Molar conductance analysis shows λ_m value in the range 0.6-16.00W^{-1}cm^2/mol showing that they are non-electrolytes[18].

Table 1: Analytical and Physical data of HBMTmH Ligand and its metal complexes

Compound	Color	% Yield	MP/ DP ^{o}C	Elemental Analysis: Expected (Found)						Molar Conduc-tance	Magnetic Moment
				C	H	N	O	S	M		
HBMTmHB	Yellow	78.90	203	63.29(63.00)	4.59(4.11)	16.78(16.66)	7.66(7.59)	7.68(7.57)	-	-	-
Fe(BMTmHB)$_2$	Green	77.23	215	59.47(59.25)	4.05(3.99)	15.77(15.58)	7.21(7.00)	7.21(7.12)	6.29(6.23)	0.9	5.10
Co(BMTmHB)$_2$	Orange	80.13	217	59.26(59.02)	4.04(4.02)	15.71(15.45)	7.18(7.09)	7.18(7.09)	6.62(6.08)	16.0	5.18
Ni(BMTmHB)$_2$	Light Green	78.38	218	59.28(58.91)	4.04(3.95)	15.72(15.28)	7.19(7.17)	7.19(7.03)	6.59(6.41)	12.3	3.12
Pd(BMTmHB)$_2$	Brown	79.55	225	56.26(56.01)	3.84(3.66)	14.92(14.78)	6.82(6.78)	6.82(6.69)	11.34(11.18)	0.6	Dia

Electronic spectra and magnetic moments

The UV spectrum of the HBMTmHB and that of the Fe(II), Co(II), Ni(II) and Pd(II) complexes are given in Table-2. The electronic spectrum of the free HBMTmHB display three bands at 351nm (ε = 8143dm^3/mol/cm), 300 nm (ε = 5102dm^3/mol/cm) and 225 nm (e = 3194dm^3/mol/cm) corresponding to $\pi\rightarrow\pi^*$ transitions of the >C=NO-, >C=S and >C=NN- groups of the HBMTmHB[19]. In the transition metal complexes of HBMTmHB, these bands are shifted to longer wavelengths with increasing intensities. This shift is attributed to the donation of the loan pair of electron of N and S atoms of the HBMTmHB to the central metal atom (N→M and S→M).

The electronic absorption of Fe(II) complex in chloroform solution displayed broad bands at 658 and 552nm which can be assigned to $^5T_{2g}\rightarrow{}^5E_g$ and $^5E_g\rightarrow{}^5B_{1g}$ transitions which are characteristic of octahedral structure[20]. The μ_{eff} for the Fe(II) complex is 5.10BM which is in accordance with high spin octahedral geometry.

[Co(BMTmHB)$_2$] complex exhibits two bands at 900 and 430nm in the visible region and these can be assigned to $^4T_{2g}(F)\rightarrow{}^4A_{2g}$ and $^4T_{1g}(F)\rightarrow{}^4T_{1g}(P)$ transitions respectively which is in accordance with Co(II) high spin

octahedral geometry[21] which is confirmed by magnetic moment of Co(II) ligand (5.12BM)[22].

The Ni(II) complex of HBMTmHB ligand shows magnetic moment 3.12 BM which suggestes an octahedral environment of HBMTmHB around Ni(II) ion[23]. The Ni(II) complex shows two bands at 980 and 633nm which can be assigned to $^3A_{2g} \rightarrow {}^3T_{2g}$ and $^3A_{2g} \rightarrow {}^3T_{1g}$ transitions respectively[23-27]. The Pd(II) complex is diamagnetic, therefore the square planar arrangement of the HBMTmHB molecules around Pd(II) is assigned to this complex. The electronic spectrum of this complex shows absorption bands at 425 and 353nm due to the metal-ligand charge transfer transition.

Table 2: Electronic Absorption spectra of HBMTmHB ligand and its metal complexes

Compound	Solvent	λ_{nm}	ε	Transition
HBMTmHB	Methanol	351 300 225	8143 5102 3194	Oximino $\pi \rightarrow \pi^*$ >C=S $\pi \rightarrow \pi^*$ Azomethine $\pi \rightarrow \pi^*$
	0.1N NaOH	374 327 233	7440 7580 1557	Oximino $\pi \rightarrow \pi^*$ Azomethine $\pi \rightarrow \pi^*$ Azomethine $\pi \rightarrow \pi^*$
$Fe(BMTmHB)_2$	Chloroform	658 552	192 335	$^5T_{2g} \rightarrow {}^5E_g$ $^5E_g \rightarrow {}^5B_{1g}$
$Co(BMTmHB)_2$	Chloroform	900 430	25 3445	$^4T_{2g}(F) \rightarrow {}^4A_{2g}$ $^4T_{1g}(F) \rightarrow {}^4T_{1g}(P)$
$Ni(BMTmHB)_2$	Chloroform	980 633	69 1499	$^3A_{2g} \rightarrow {}^3T_{2g}$ $^3A_{2g} \rightarrow {}^3T_{1g}$
$Pd(BMTmHB)_2$	Chloroform	425 353	8312 15622	M→L Charge Transfer M→L Charge Transfer

PMR spectra

PMR spectra of HBMTmHB and its Pd(II) complex were recorded in deuteriated DMSO. Two singlets at 11.40 and 10.25 ppm were observed. The oximino group is not expected to release the proton more easily than the phenolic proton, since the desheilding effect is more on the proton of the phenolic group. Therefore the singlet at 11.25ppm is ascribed to phenolic –OH in the HBMTmHB and the singlet at 11.40ppm to oximino proton (>C=NOH). This proton disappeared in the PMR spectrum spectrum of Pd(II) complex indicating deprotonation of oximino proton during complexation. The singlets at 8.50 and 8.40ppm in ligand and Pd(II) complex respectively, can then be ascribed to either the –SH or –NH moiety. This assignment is favored by the thione=thiol tautomerism possible HBMTmHB. A broad multiplet between 7.30-8.10ppm has its origin in the phenyl rings proton of the HBMTmHB.

Table 3: ^{1}H NMR α-Benzilmonoximethiocarbohydrazide-m-hydroxybenzelidene and its Pd(II) metal ion complex in ppm (δ)

Compounds	-OH	Phenolic -OH	>C=N-NH-	-SH/-NH	-CH=	Phenyl rings
HBMTmHB	11.40	10.25	8.40	8.50	9.00	7.30-7.8
$Pd(BMTmHB)_2$	-	10.30	8.30	8.40	9.10	7.50-8.10

FT(IR) Spectra

In the FT(IR) spectra of HBMTmHB, the observed band at 3326cm^{-1}of oximino (>C=NOH), disappeared in its metal complex showing the participation of the N→M group in coordination after decomposition. The HBMTmHB show strong bands at 2853, 1617 and 1571cm^{-1} due to >C=S, >C=NN- and >C=NO- groups respectively. These bands are shifted to lower frequencies in the complexes, indicationg the coordination through these groups. It is found from the FTIR of the complexes that there are wide and strong bands at 505-533cm^{-1} for M-N, M→N and M→S which are assigned to metal stretching vibrations.

Table 4: FT(IR) spectral bands of the HBMHmHB and its metal complexes (cm^{-1})

Compounds	-OH	Phe OH	ν(C-S-H)	ν(C=NO)	ν(C=NN)	ν(N-H)	ν(N-O)	ν(N-N)	Benz ring	M-N
HBMTmHB	3326	2853	2853	1571	1617	1505	1007	1089	747	--
[Fe(BMTmHB)$_2$]	-	3196	2862	1537	1597	1467	1009	1112	754	525,504
[Co(BMTmHB)$_2$]	-	3181	2862	1505	1603	1473	1008	1152	754	533, 505
[Ni(BMTmHB)$_2$]	-	3348	2864	1529	1596	1472	1008	1100	748	522, 504

Conclusions

The results of this investigation support the structures suggested for HBMTmHB and its metal complexes. A square planar structure was suggested for Pd(II) complex and octahedral geometry for Fe(II), Co(II) and Ni(II) complexes. On the basis of spectral studies the tentatively assigned structures are:

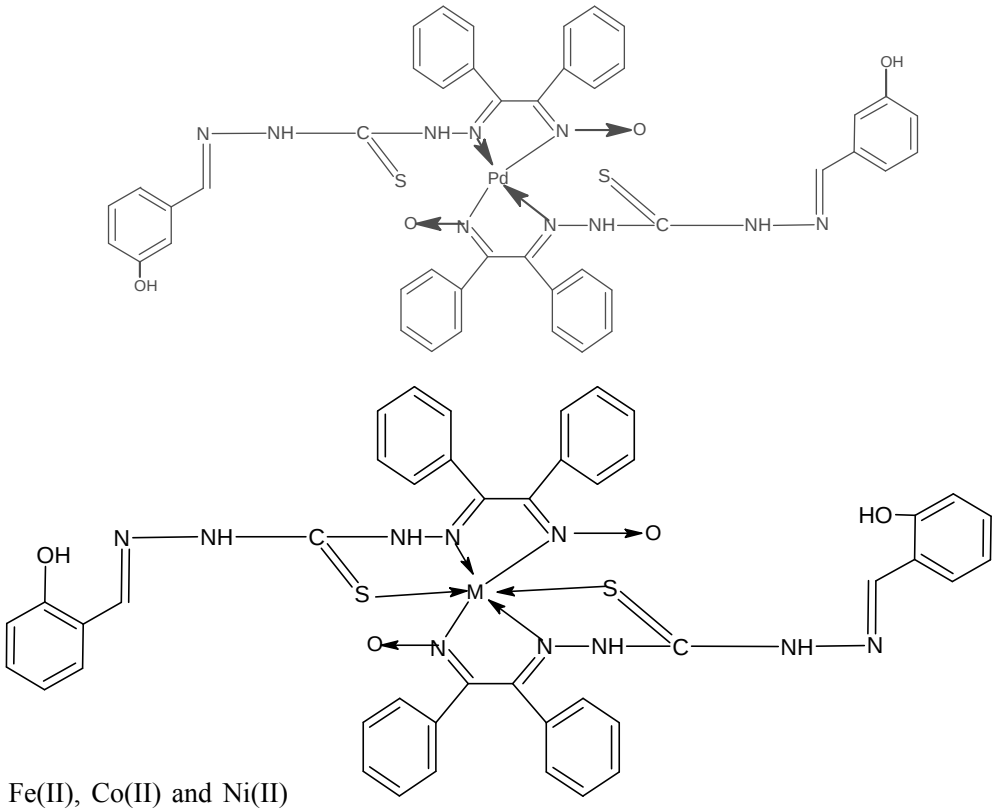

where M = Fe(II), Co(II) and Ni(II)

References

1. Ali, M. and Livingston, S; 1974, *Coord Chem Rev.,* **13**, 101.
2. Williams D; 1972, *Chem. Rev.,* **72**, 203.
3. Clearke, M., 1974, *Coord Chem Rev*; **12(4)**, 349.
4. Das. M. and Livingstone, S., 1976, *Inorg. Chim. Acta*., **19(1)**, 5.
5. Ali, M. and Tarafdar, J., *J. Inorg. Nucl., Chem*., **39**, 1785.
6. Ali, M. and Bose, R., 1977, *J. Inorg. Nucl. Chem*., 1977, **30**, 265.
7. Ali, M. and Bose, R., 1984, *Polyhedron;* **3**, 517.
8. Elsmy, A. and Al-Ansi, T., 1989, *Synth. React. Inorg. Met-Org. Chem.,* **19(4)**, 309.
9. Abdu, G., et. Al., 1990, *Synth React Inorg Met-Org Chem*; **20(7)**, 887.
10. A. Braibanti, A., 1968, *Inorg. Chem*., **7**, 1730.
11. Eskandari, H., Ghaziaskar, H.S. and Ensafi, A.A; 2001, *Anal. Sci*; **17**, 327.
12. Gup, R. and Beduk, A.D., 2002, *Synth. React. Inorg. Metal-Org. Chem*., **32**, 1043.
13. Ocak, U., Alp, H., Gok, C.P. and Ocak, M., 2006, *Separ. Sci. Techn*., **41**, 391.
14. Karapýnar, E. and Kabay, N., 2007, *Transition Met. Chem., (Dordrecht, Neth.)*, **32**, 784.
15. Dede, B., Karipcin, F. and Cengiz, M., 2009, *J. Chem. Sci*., **121**, 163.
16. Kulkarni, S., Badekar, R., Gore, G. and Shimpi, P., 2019. *JETIR,* **6(2)**.
17. Vogel, A.I., 1996, "Vogel Textbook of Quantitative chemical analysis"- 5th Ed. Revised Longman Publications.
18. Singh, D.P., Vidhi Grover., Krishan Kumar and Kiran Jain., 2010, *Acta Chim Slov*; **57**, 775–780.
19. EI-Ajaily M.M., EI-Ferjani R.M. and Maihub A.A., 2007, *Jordan. J. Chem*., **2(3)**, 287-296.
20. Raman, N., Pichaikaniraja and Kulandaisamy., 2001, *Proc. Indian Acad. Sci., Chem Sci*., **113(3)**, 183-189.
21. Lever ABP., 1968, *Inorganic Electronic Spectroscop;* Elsevier Amsterdam., **294**
22. Sawant, D.C., 2006, M.Sc. Thesis, Univ. of Mumbai.
23. Lever, A.B.P., 1984, Inorganic Electronic Spectroscopy (second edition), Amsterdam, Elsevier.
24. Patil, R.B., 1981, *J. Indian Chem. Soc.,* **58**, 944 and 1983, **60**, 79.
25. Atre, V. Reddy., G.V. Sharada L. N. and Ganorker M.C., 1982, *Indian J. Chem*., **21A**, 935.
26. Rajib Lal De and Mahuya Mandal, 2008, Lovely Roy and Jaydeep Mukherjee; *Indian J. of Chem.,* **47A**, 207-213.
27. Abdu El-Reash, G.M., Taha, F.I. and Badr, G.E., 1990, *Bull. Soc. Chim. Fr.,* **127**, 387.
28. Konig, E., 1971, The nephelauxetic effect- structure and bonding, Springer, New York.

RNI No. MAHENG/2017/74063
ISSN No. (Print) 2581-5911
ISI Impact Factor 1.022 (2019-2020)

Synthesis and Spectral Characterization of Ni(II) and Pd(II) Complexes of Benzilmonoximethiocarbhydrazide-p-dimethylaminobenzaldehyde

Priya Belavale[1], Raj Badekar[2*], Rama Lokhande[1] and Vijay Ghodvinde
[1]School of Basic Sciences, Jaipur National University, Jaipur, India
[2*]Riva Industries, Ambernath MIDC, Dist. Thane, Maharashtra, India
[3]Department of Chemistry, S.V. Jr. College Vasind, Dist. Thane, Maharashtra, India
Email: badekarrr@gmail.com

Abstract
The Schiff base ligand HBMTDAB was prepared by condensation of Benzilmonoximethiocarbohydrazide with p-dimethylaminobenzaldehyde. The present study has been undertaken to prepare the Ni (II) and Pd (II) complexes of the ligand. The complexes are soluble in common organic solvents such as methanol DMF, DMSO etc. The synthesized complexes were investigated by elemental analysis, molar conductivity and magnetic susceptibility data, FTIR, electronic and ESR Spectra.

Keywords: *Benzilmonoximethiocarbohydrazide, p-dimethylaminobenzaldehyde, N, N-dimethylaminobenzaldehyde, 4-dimethylaminobenzaldehyde, condensation, spectral analysis.*

Introduction

Schiff bases and their transition metal complexes continue to be of interest due to their antibacterical[2-3] antioxidant[4]antimalarial[5], antiviral[6], anticancer[7-8], antifungal[9-10] and antinflammatory properties[11-15]. Metal complexes of Schiff bases play an essential role in agriculture, pharmaceutical, industrial and chemical sectors. In this paper we report the synthesis of HBMTDAB complexes with Ni(II) and Pd (II).

Materials and Methods

All chemicals and solvents used were Analytical grade. All metal salts used were in chloride form. The elemental analyses were carried by standard methods. The molar conductance measurements of the complexes in DMF were done using an EQ-660 conductivitimeter. FTIR spectra were recorded on FTIR-1615 Perkin-Elmer Spectrometer using KBr pellets. The effective magnetic moments were calculated after diamagnetic correction for ligand component using Pascal's constant[21]. The UV-Visible Spectrum was recorded on Shimadzu UV-190 Spectrometer and Magnetic susceptibility measurements were carried out by using Gouy's balance.

Synthesis of Ligand

The title ligand was prepared by reported method[22].

Preparation of metal complexes of HBMTDAB

A) Ni(BMTDAB)

The Ni(II) metal complex of HBMTDAB was prepared by dissolving 4.45g of HBMTDAB in minimum quantity of ethanol and adding aqueous solution containing 1.278g of nickel chloride. The final mixture was neutralized with 0.1 N Sodium hydroxide. On cooling, the precipitate formed was filtered, washed with hot water and dried at 110^0C. The complex obtained was brown in colour.

B) Pd(BMTDAB)

To 4.45g HBMTDAB, 0.0885g palladium chloride was added. This mixture was neutralized with 0.1 N sodium hydroxide. The precipitated complex was washed with hot water, recrystallized from chloroform and dried at 110^0C.

Results and Discussion

The ligand and its metal complexes were soluble in water and organic solvents such as DMF, DMSO, ethanol, ACN, Chloroform, nitrobenzene etc. All metal complexes have high thermal stability and strong metal-ligand bonds. The synthesized complexes are insoluble in dilute alkali solution, suggesting the absence of oximino proton in the complexes due to deprotonation during complex formation. The conductivity of the complexes in nitrobenzene solvent indicates that they are non-electrolyte in nature[23].The metal complexes were characterized on the basis of elemental analysis, FTIR, magnetic susceptibility measurements, electronic spectra and EPR data.The physical properties and elemental analysis data of the synthesized metal complexes are summarized in **Table 1**.

Table 1: Analytical and physical data for HBMTDAB and its divalent metal complexes

Compounds	Color	% Yield	DP in ^{0}C	% of the expected (observed)						Magnetic Moments in BM	Conductance in Ω^{-1}
				M	C	H	N	O	S		
HBMTDAB	Yellow	86.94	204	---	64.84 (63.39)	5.44 (5.21)	18.90 (18.80)	3.60 (3.59)	7.21 (7.03)	--	---
$Ni(BMTDAB)_2$	Brown	81.61	291	6.55 (6.19)	60.90 (61.00)	4.86 (5.09)	17.76 (17.60)	3.38 (3.33)	6.77 (6.72)	3.15	0.32
$Pd(BMTDAB)_2$	Green	80.68	308	10.67 (11.06)	57.98 (57.70)	4.63 (4.58)	16.91 (16.69)	3.22 (3.21)	6.44 (6.40)	--	1.80

Magnetic moment

The brown colored Ni(II) complex shows magnetic moment of 3.15BM at room temperature. The observed magnetic moment for Ni(II) complex is in the range expected for octahedral Ni(II) complexes. The green colored Pd(II) complex is diamagnetic and has square planar geometry[21].

Electronic Absorption Spectra

The bands observed at 913 and 625nm in the Ni(II) complex electronic spectrum are assigned to $^3A_{2g}\rightarrow{}^3T_{2g}(\upsilon_1)$ and $^3A_{2g}\rightarrow{}^3T_{2g}(F)$ (υ_2) transitions respectively on the basis of idealized octahedral geometry[24]. The ratio υ_2/υ_1 is found to be 1.46, which falls in the range reported for the other octahedral complexes of Ni(II)[25]. From the observed position of υ_1 and υ_2 transitions, the frequency of the third transition $^3A_{2g}\rightarrow{}^3T_{1g}(P)$ (υ_3) and B values have been calculated[26].

The third band is not observed in the spectrum of the complex probably because it is masked by the tail-end of the strong charge transfer band around 408nm. The value of the Racah interelectronic repulsion parameter B is 7420cm^{-1}, the covalency factor is found to be 8216cm^{-1} and is in close agreement with octahedral Ni(II) complexes[27].

The electronic spectra Pd(II) complex in chloroform solution exhibits absorption bands at 370 nm and 263nm with high molar extinction coefficient (Table-2) which can be assigned to $\pi \rightarrow \pi^*$ intra ligand charge transfer transitions. These absorption bands have high intensity since they obey the Lapport selection rule[28].

Table 2: Electronic spectral data for divalent metal complexes of HBMTDAB

Sr. No.	Compound	Solvent	Band position in nm	Intensity ϵ	Assignment
1	$Ni(BMTDAB)_2$	Methanol	249	2910	Charge transfer M→Ltransition
			250	18190	Charge transfer M→Ltransition
		Chloroform	913	20	$^3A_2g \rightarrow {}^3T_1g$transition
			625	108	$^3A_2g \rightarrow {}^3T_1g(F)$transition
			408	14000	Charge transfer M→Ltransition
2	$Pd(BMTDAB)_2$	Methanol	384	1799	Charge transfer M→Ltransition
		Chloroform	370	189	Charge transfer M→ Ltransition
			263	13803	Charge transfer M→ Ltransition

Infrared spectra

The infrared spectral bands of ligand and their metal complexes are listed in Table 3. In the ligand, the medium absorption band observed at 3385cm^{-1} is due to oximino proton, but in its metal complexes this band is absent due to deprotonation during complex formation. This observation is supported by the fact that both complexes are insoluble in dilute alkali solution.

The broad and medium band observed in the region 1505-1550cm^{-1} in the FTIR spectra of complexes is assigned to stretching vibration of >C=N-N (Azomethine group) and another medium intensity absorption band observed in the region 1473-1519 cm^{-1} is assigned to >C=N-O stretching vibration of oximino group. Both azomethine and oximino groups are shifted to higher frequencies as compared to HBMTDAB ligand, which suggests that they are involved in complex formation. υ(C-S-H) band of the title ligand reported at 2329cm^{-1} is also shifted to the higher side (2362-2375cm^{-1}) suggesting that the thiophene group participates in complex formation.

Table 3: FTIR spectral data for divalent metal complexes of HBMTDAB

Compound	-OH	Ar(c-c)	-CH=	νC-S-H	-NH	>C=N-N	>C=N-O	Phenyl Rings	M-N, M→N
HBMDAB	3385	3155	2926	2359	1606	1508	1504	722	-
Ni(BMTDAB)	-	3241	2909	2375	1599	1550	1519	742	563, 517
Pd (BMTDAB)	-	3181	2926	2362	1603	1505	1473	721	523, 505

Conclusions

Ni(II) and Pd(II) complexes have high thermal stability and are non-electrolytic in nature. The spectral and magnetic data suggests that Ni(II) complex is high spin octahedral and Pd(II) complex is square planar. FTIR spectral data suggests that complexes coordinate with the metal ion through nitrogen and sulfur atoms. On the basis of magnetic and spectral data, structures of Ni(II) and Pd(II) complexes are tentatively assigned as:

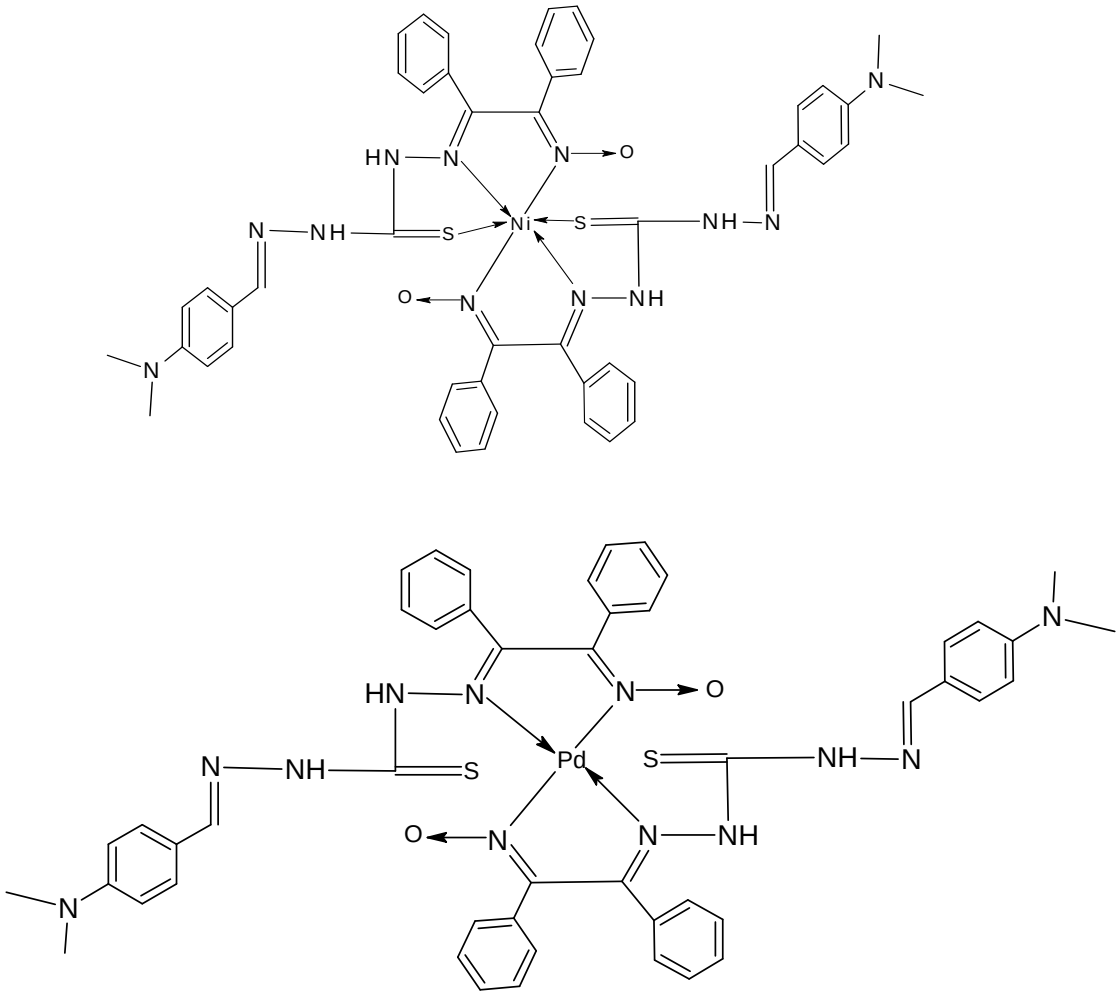

Acknowledgment

The authors are thankful to Dr. Santosh Kulkarni, Agrawal College, Kalyan (West), Dist. Thane, Maharashtra, India for providing instrumentation facilities and moral support.

References

1. Mayers, D.L., 2009, Antimicrobial Drug Resistance C., Springer Dordrecht Heidelberg, London., p.681-1347.

2. Guschin A; 2015, *BMC Infect. Dis*., **15**, 1-7.

3. Cacic, M., Molnar, M., Sarkani, B., Hutschon, E. and Rajkovic, V., 2007, *Molecules*, **13**, 6793-680.
4. Dave, S. and Bansal, S., 2013, *International Journal of Pharmaceutical Research*, **51**, 6-7.
5. Thangudurai, T. and Ihm, S., 2003, *J. Ind. Eng. Chem.,* **9,** 563.
6. Mladenova, R., Ignatova, M., Manolova, N., Petrova, T. and Rashkov I., 2002, *Eur-Polym. J.,* **38**, 989.
7. Walsh, O.M. and Meejan, M.J., 1996, Prendergast R. M. and Makib T.A., 1996, *Eur. J. Med. Chem.,* **31**, 989.
8. Singh, K., Barwa, M.S. and Tyagi, P., 2006, *Eur. J. Med. Chem.,* **41**, 1.
9. Pannerselvam, P., Nair, R.R., Vijayalakshmi, G., Subramanion, E.H. and Sridhar, S.K., 2005, *Eur. J. Med. Chem.,* **40**, 225.
10. Bawa, S. and Kumar, S., 2009, *Indian Journal as Chemistry,* **48B**, 142.
11. Lavecchia, G., Berteina-Robin, S. and Guillaumet, G., 2005, *Tetrahedron Lett.,* **46**, 5851-5855.
12. Cottam, H.B., Petrie, C.R., McKernan, P.A., Goebel, R.J., Dalley, N.K., Davidson, R.B., Robins, R.K. and Revankar, G.R., 1984, *J. Med. Chem*., **27**, 1119-1227.
13. Griengl, H. and Günzl, F., 1984, *J. Heterocycl. Chem.,* **21**, 505-508.
14. Petrie III, C.R., Cottam, H.B., McKernan, P.A., Robins, R.K. and Revankar, G.R., 1985, *J. Med. Chem.,* **28**, 1010-1016.
15. Ugarkar, B.G., Cottam, H.B., McKernan, P.A., Robins, R.K. and Revankar, G.R., 1984, *J. Med. Chem.,* **27**, 1026-1030.
16. Hussen, A.I., *J. Coord. Chem*., **59**, 157.
17. Karthikeyan, S., Prasad, M.J., Poojary, D. and Bhat, B.S., 2006, *Bioorg. Med. Chem*., **14**, 7482.
18. Cacic, M, Molnar, M., Sarkani, B., Hutschon, E. and Rajkovic, V., 2000, *Molecules*, **13**, 6793-680.
19. Dave, S. and Bansal, 2013, *International Journal of Pharmaceutical Research,* **5C1**, 6-7.
20. Jeffery, G.H. and Bassett, J., 1996, Vogel's Textbook of Quantititive Chemical Analyses., 5th edition, Longman Publication.
21. Datta, R.L. and A. Syamal., 1982, Elements of Magnetochemistry, S. Chand and Company Ltd., Ramnagar, New Delhi.
22. Belavale, P., Badekar, R., Kulkarni, S. and Lokhande, R., 2019, *International Journal of Advance and Innovative Research*, **6(2)**, 9.
23. Geary, W.J., 1971, *Coord. Chem. Rev.,* **7**, 81.
24. Low, W., 1960, Paramanetic Resonance in Solid, Acad Press, N.Y. p.76.
25. Lever A.B.P., 1968, Inorganic Electronic Spetroscopy, Elsevier, Amsterdam, p.168.
26. Drago, R.S., 1965, Physical Methods in Inorg. Chem., EWP, New Delhi, p.135-181.
27. Koing, E., 1971, Structure and Bonding, p.9, R175**.**
28. Wulfsberg, G., 2000, Inorganic Chemistry, University Science Books, p.680.

RNI No. MAHENG/2017/74063
ISSN No. (Print) 2581-5911
ISI Impact Factor 1.022 (2019-2020)

Removal of Organic Dye Pollutants using Advanced Ultra-Oxidation System (Mn / H_2O_2)

Rafia Azmat*, Muhammad Hasan, Noshab Qamar and Ailyan Saleem
Department of Chemistry, University of Karachi, 75270, Karachi, Pakistan.
Email: rafiasaeed200@yahoo.com

Abstract
Recent investigations provide a new advanced oxidation process whose efficiency, design, laboratory and pilot plant testing demonstrate an integrated dye wastewater treatment process in an alkaline medium. The study describes a laboratory analysis of the use of permanganate oxidation to decolorize Reactive Black 5 by studing various operational parameters like the effects of concentration of dye, oxidant, urea, anions, cations, temperature, and hydrogen peroxide dosage spectrophotometrically at wavelength 597.5 nm. The use of urea in dye industry for hydrolyzing the dye molecule is a common practice. The new advanced oxidation process (AOP) through permanganate oxidation shows that urea is effective along with H_2O_2 in the decoloration of the dye. The new Mn/ H_2O_2 system emphasizes the reduction of manganate with the H_2O_2 couple with the generation of two dominant oxidizing species, oxygen and urea- H_2O_2 complex, which degraded 80% of the dye in the initial ten minutes with complete mineralization in 1 h. The strong nitrogen bond and ring structure associated with RB5 successfully degraded the dye through generation of two powerful oxidizing species, (urea- H_2O_2 complex) and nascent [O] leading to complete mineralization of the dye. The dye decolorization took place through potassium permanganate with sludge formation which disappeared on the addition of H_2O_2 in the presence of urea. This new advanced oxidation process of dye wastewater treatment appears to be the most promising among the existing advanced oxidation processes and may be used in dye treatment plants.

Keywords: *Reactive Dyes, Permanganate, Urea, H_2O_2 Complex, Nascent Oxygen*

Introduction

Textile industries produce more than 7×10^5 tons of synthetic dyes annually. Reactive dyes, have a strong nitrogen bond with a ring structure are universally employed in dye fabrication. Textile wastewater is characterized by high content of dyestuff, salts, high chemical oxygen demand (COD) derived from additives, suspended solids (SS) and fluctuating pH.[1] Generally, the dye fabricating processes require a large quantity of water for dyeing purposes and discharge 2.8×10^5 tons of wastewater[2] which is generated from the different steps of dyeing and finishing processes. In general, the majority of these dyes, or their degraded products (like aromatic amines) may be lethal or mutagenic. Therefore, treatment of wastewater containing such dyes is required to avoid damage to the ecology.[3] Initially, Advanced Oxidation Processes (AOPs) were employed for treatment of drinking water in the early eighties which is now extended to wastewater management via generation of hydroxyl radicals ($OH\cdot$, 2.8 V)[4]. The hydroxyl radical generation processes use various reactions in which Fenton reaction is commonly employed for dye waste-

water treatment and expected to convert wastewater pollutants into less and even non-toxic products, thereby providing an ultimate solution for wastewater treatment.[5] Furthermore, the coloring of different kinds of fabrics, leather, and other coloring processes demands continuous research to find an eco-friendly solution for the treatment of dye wastewater. Black dye requires suitable dyeing temperature and pH for coloring the fabrics.[6] The action of the alkaline medium on Methylene blue (C.I. Basic Blue 9) and other thiazine dyes is examined by UV/visible spectroscopy, thin layer chromatography, mass and NMR spectrometry and computational methods. In 0.1 M aqueous alkali solution highly colored and lipophilic species was formed.[7]

The aim of the present research is to find a rapid, green advanced oxidation system for reducing color and harmful impact of colorant material on the ecosystem. The article highlights the efficiency of the current advanced oxidation process for laboratory prepared dye water as well as dye wastewater collected from the small dye shop.

Materials and Methods

Chemical, materials, instruments and removal methods

Reactive Black 5 was purchased from the local dyeing market and used without further purification. The structural formula of RB 5 dye shown in Fig. 1.

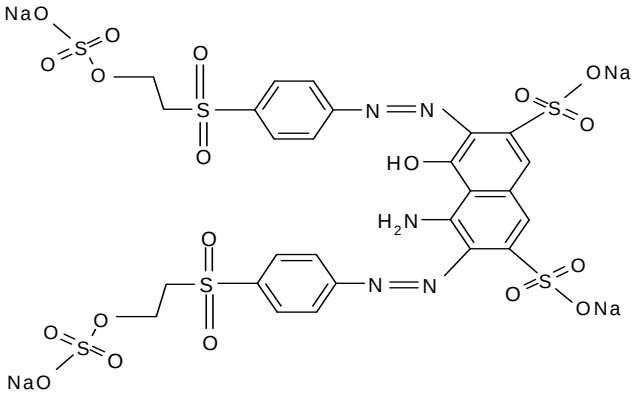

Fig. 1 Chemical Structure of Reactive Black 5 dye

A stock solution of 1×10^{-4} mg/L of RB 5 dye was prepared using double distilled water and diluted to the desired concentration. Usual standard methods were employed for the preparation of other aqueous solutions including acid, base, potassium permanganate, various metal ions and urea, and diluted at the time of the experiment. The dye concentrations were determined in aqueous solution by comparison with standard solutions in the visible range using UV–VIS spectrophotometer (1800 A UV–VIS) Spectrophotometer. λ_{max} for RB 5 dye was determined as 597.5 nm.

The % color removal rate of RB 5 dye was determined by using Equation 1:

$$\text{Color removal efficiency \%} = \frac{A_o - A_t}{A_o} \times 100 \quad (1)$$

Analysis

The mineralization of Reactive Black 5 was evaluated by the decrease in the chemical oxygen demand (COD) which was determined according to the procedure stated in APHA (2005) using COD analyzer APHA 5220-C. The COD was calculated for both untreated and treated RB 5 dye solutions at a concentration of 500 mg/L. The degraded product was identified by IR technique and the peaks compared with that of dye and $KMnO_4$ before and after oxidation.

Toxicity test

Toxicity test of sludge and filterate was performed on seeds and fishes. The seeds were cultivated in normal greenhouse conditions in regular water (control plants) and in treated filtrate (experimental plants grown in soil mixed with sludge). The toxicity test on fishes was performed in a fish aquarium with recycled water in comparison to fish in ordinary water.

Results and Discussion

The kinetics of oxidation was studied using different parameters to optimize the dye degradation process. The

change in concentration of dye RB 5 was monitored at λ_{max} 597.5 nm and 298 K keeping one parameter as a variable and others constant to optimize the oxidation reaction. Initially, the reaction between the dye and urea (as an additive in dye fixing processes on fabrics) was studied at five different initial concentrations of alkali [0.1M – 0.5M] in aqueous medium. The time-based resolution of UV/ Visible spectrum showed that the dye remains persistent and unaffected in the presence of urea in alkaline medium with irrelevant color change (Fig.2a). The insignificant effect of temperature in the presence of urea showed that urea helps in the solubilization and fixing of the dye on fabric without any de-coloration (7.4%, Fig 2b). The pattern was persistent in the presence of various anions (I^{-1}, CH_3COO^{-1}, NO_3^{-1}, $CO_3^{-2,}$ and $C_2O_4^{-2}$) and cations (Na^{+1}, Mg^{+2}, Ba^{+2}, Al^{+3}) in alkaline medium. It shows that the dye remains persistent in the presence of dye additive. The dye wastewater is of complex nature due to the presence of these dye pollutants in addition to coloring material. Hence, this

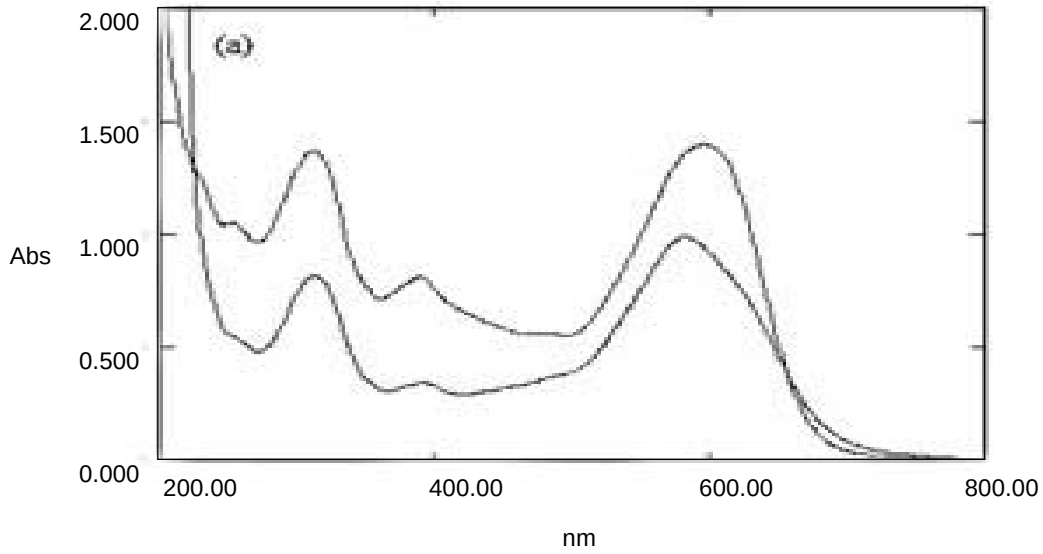

Fig. 2(a) Spectral changes of dye and urea solution in alkali medium

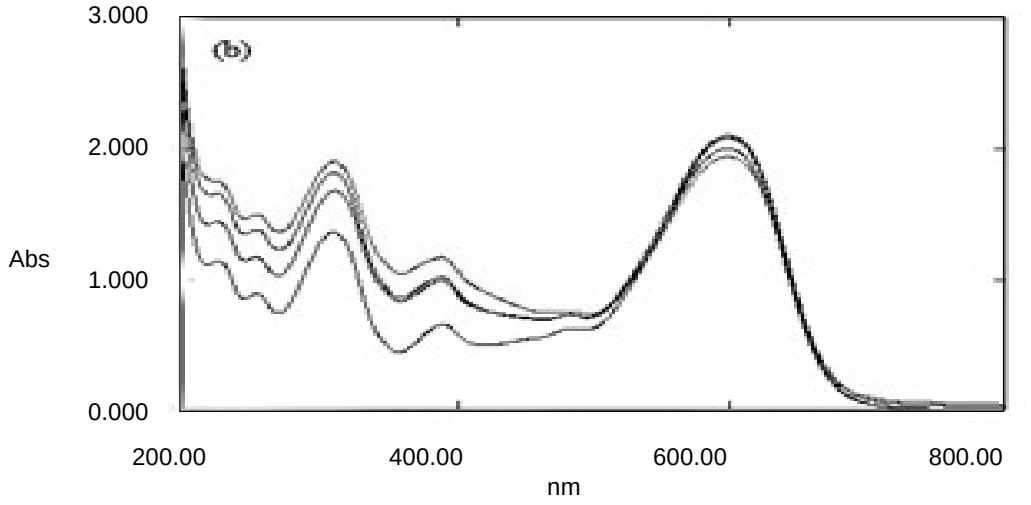

Fig.2(b) Spectral changes of dye urea reaction at various elevated temperatures in alkaline medium

study was planned to develop a cost-effective and eco-friendly process using potassium permanganate and H_2O_2 for the treatment of dye wastewater containing all dye additives employed during the dye fabrication process. The initial conditions were studied to optimize the dye oxidation using the newly developed advanced oxidation processes in the presence of alkali. For this purpose, the oxidizing capability of potassium manganate in the presence of alkaline medium was accelerated using hydrogen peroxide (H_2O_2) to achieve the complete mineralization of dye having all additives. The additives included urea and some inorganic anions and cations used for fixing dye on fabrics. The kinetics of oxidation were studied using different parameters to optimize the dye degradation process.

Effect of dye dose

The influence of the concentration of RB 5 dye on oxidation kinetics were monitored at several initial cocnetrations viz. $5x10^{-6}$ M – $5x10^{-5}$ M , keeping constant the concentration of $KMnO_4$ ($2.5x10^{-4}$M), urea (0.075M), and NaOH (0.005M). The order of reaction was determined by plotting the variation in concentration of dye with respect to time. The plot of ln A vs. time was a straight line with negative slope, and the value of R^2 showed the dependence of depletion of change in optical density with respect to time (Fig. 2c). The plot showed that initially, the reaction was rapid which later on proceeds slowly to achieve a complete decoloration within 60 min. The results as tabulated in Table 1 showed that an increase in the concentration of dye increases the rate of reaction (Fig. 2c) in alkaline medium. The % decoloration of dye at $5x10^{-5}$M was 74.37% in alkaline medium with sludge formation which disappeared with the addition of H_2O_2. The spectral change with respect to time presented in Fig. 2d showed that dye decoloration takes place due to the complex formation with $KMnO_4$ in alkaline medium. These complexes have different λ_{max} values indicating that they are slowly degradated into smaller compounds leading to dye degradation / mineralization. Oxidation of the dye leading to mineralization was related to the oxidizing capability of potassium permanganate in alkaline medium and urea hydrogen peroxide complex.

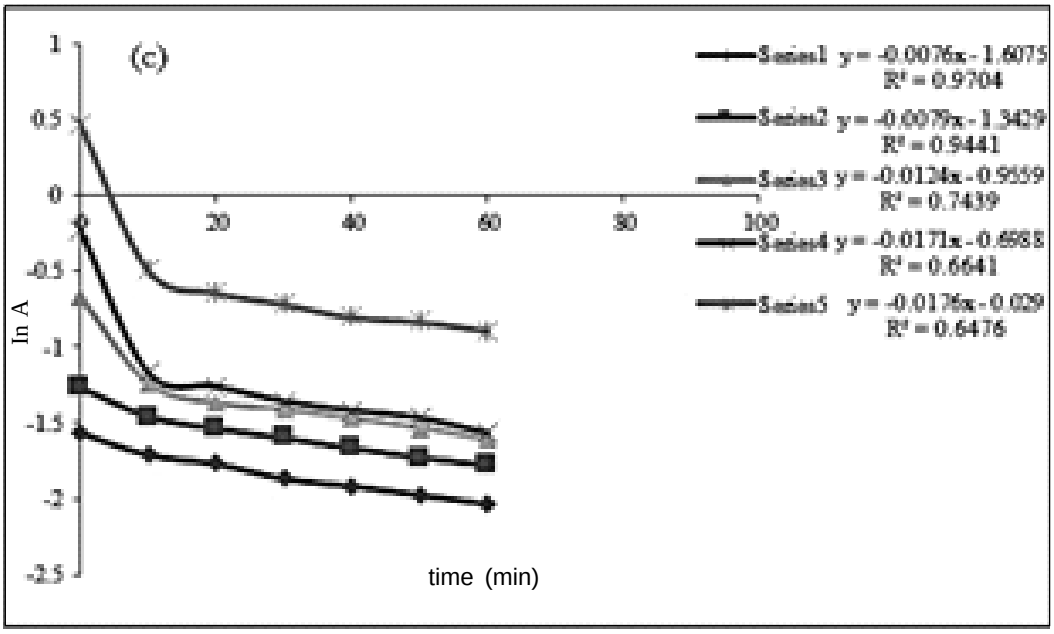

Fig. 2(c) A plot of ln A versus time of RB5 ($KMnO_4$ in basic medium)

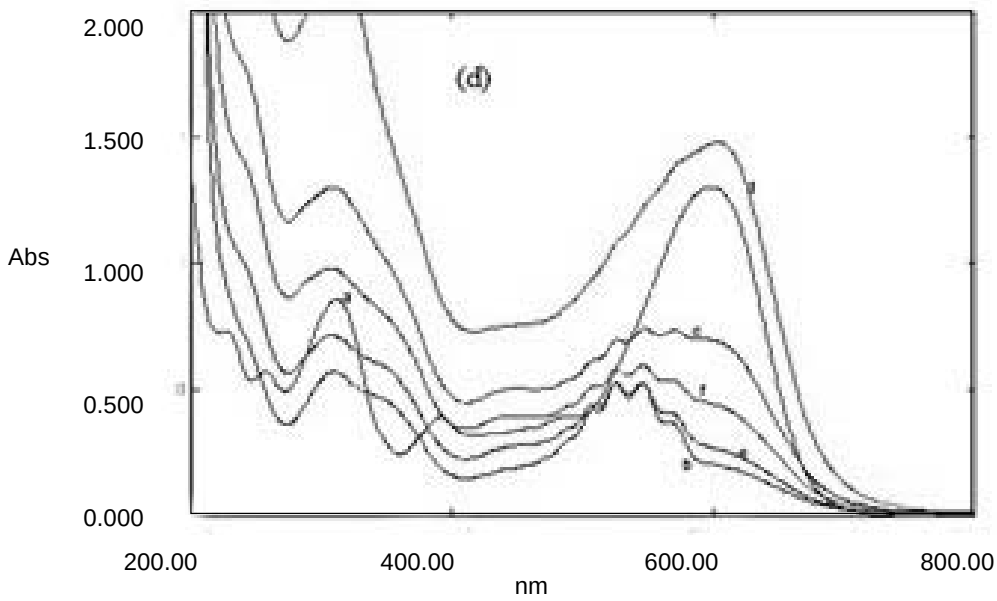

Fig. 2(d) Spectral change at elevated concentrations of RB5 with a constant concentration of $KMnO_4$ after 5 min in alkaline medium (a=Dye, b=5x10^{-6} M dye, c= 2.5x10^{-5} M dye, d=5.0x10^{-5} M dye, e=1.0 x10^{-5} M dye, f=2.0x10^{-5} M dye)

Effect of $KMnO_4$ dose

The impact of varying concentrations of $KMnO_4$ [1.5x10^{-4} M – 3.43x10^{-4} M] on the rate of oxidation of RB 5 in the presence of urea (0.075M) was observed at a constant concentration of Reactive Black 5 (5x10^{-5} M) and constant temperature in alkaline medium. The results are tabulated in Table 1 which showed that an increase in the concentration of $KMnO_4$, increases the rate of reaction up to a certain extent after which the rate was inversely related to the concentration of $KMnO_4$. The

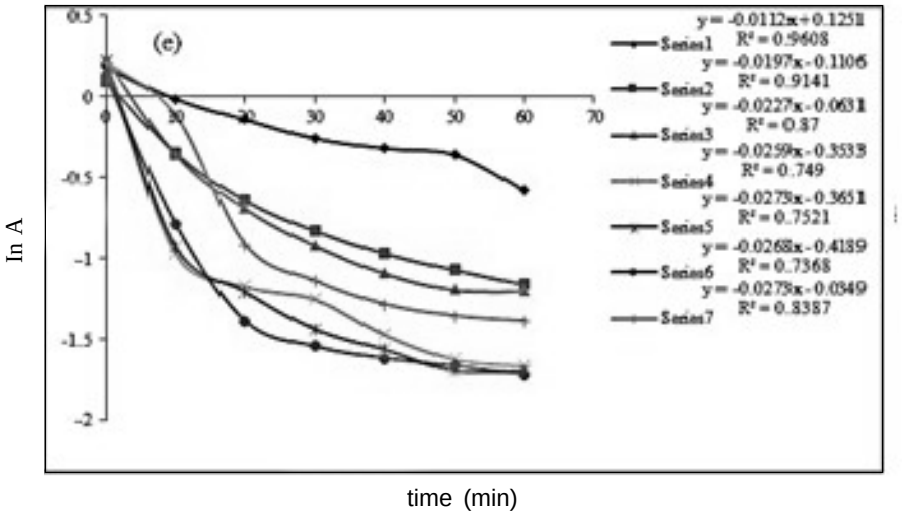

Fig.2(e) A plot of ln A versus time (various concentrations of $KMnO_4$ in basic medium)

order of reaction was determined by the plots of ln A vs. time, (Fig. 2e) and the value of R^2 showed the dependence of depletion of change in optical density with respect to time. A first-order kinetics was established which showed that the rate of reaction depends upon the concentration of $KMnO_4$ in alkaline medium. The % decoloration (84.8%) reaches the maximum extent at a concentration of $KMnO_4$ ($2.5x10^{-4}$ M) and decreases with further incremental concentration. The percent decoloration accelerated in the presence of H_2O_2 upto 97.12%. The time-based resolution of UV/Visible spectra showed the decoloration of RB5 was followed by complex formation which degraded into smaller components (Fig. 2f).

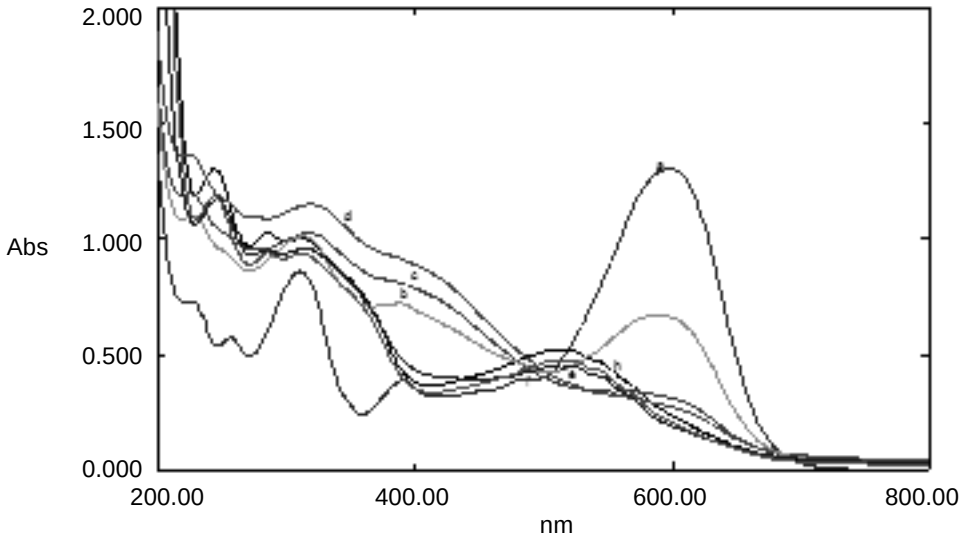

Fig.2(f) Spectral change at elevated concentrations of $KMnO_4$ with a constant concentration of RB5 after 5 min in alkaline medium

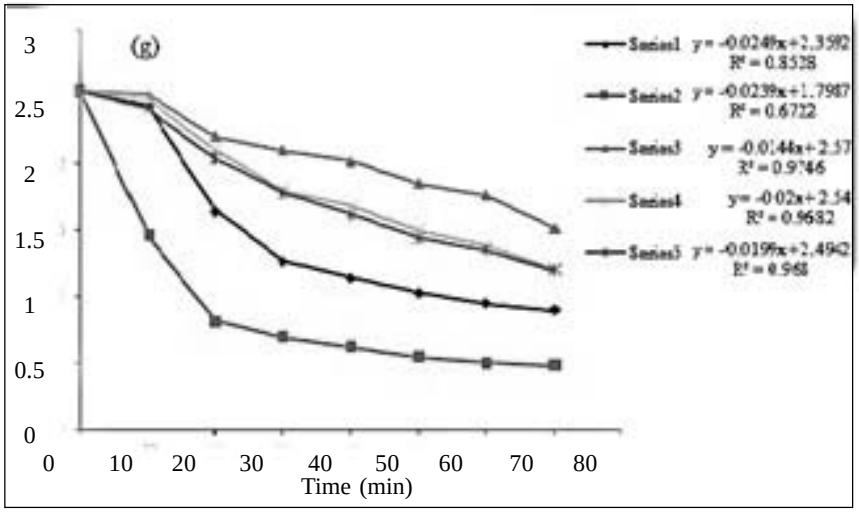

Fig.2(g) A plot of Abs versus time (various concentrations of H_2O_2 with $KMnO_4$ and RB5 in alkaline medium)

Effect of dosage of H_2O_2 in alkaline medium

The kinetics of decoloration of RB5 were accelerated by the addition of different dosages of H_2O_2 [$3.75x10^{-4}$M - $18.75x10^{-4}$M] at a constant concentration of $KMnO_4$, dye, and urea at 298K respectively. The results are tabulated in Table 1 which showed that an increase in the concentration of H_2O_2 showed no effect on the rate of reaction. It indicated that the rate of reaction is independent of the concentration of H_2O_2 and showed zero order kinetics in alkaline medium (Fig. 2g). The % de-coloration (97.12%) reaches to the maximum extent at a concen-tration of H_2O_2 ($7.5x10^{-4}$ M) and decreases with further increase in the concentration of H_2O_2. Spectral analysis (Fig. 2h) showed that certain complexes were formed initially, which degraded into smaller compounds immediately.

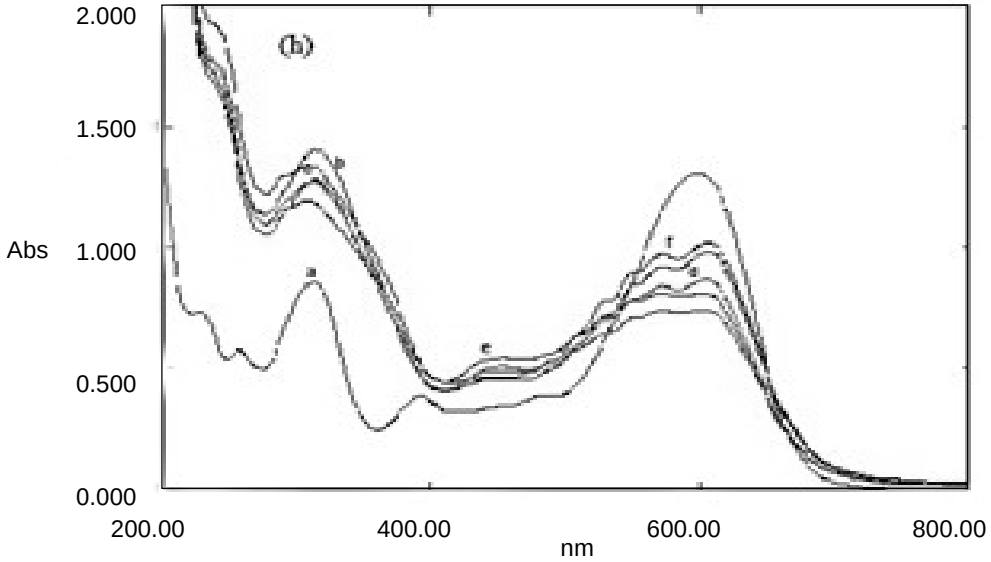

Fig.2(h) Spectral changes at elevated concentrations of H_2O_2 at a constant concentration of RB5 after 5 min in alkaline medium

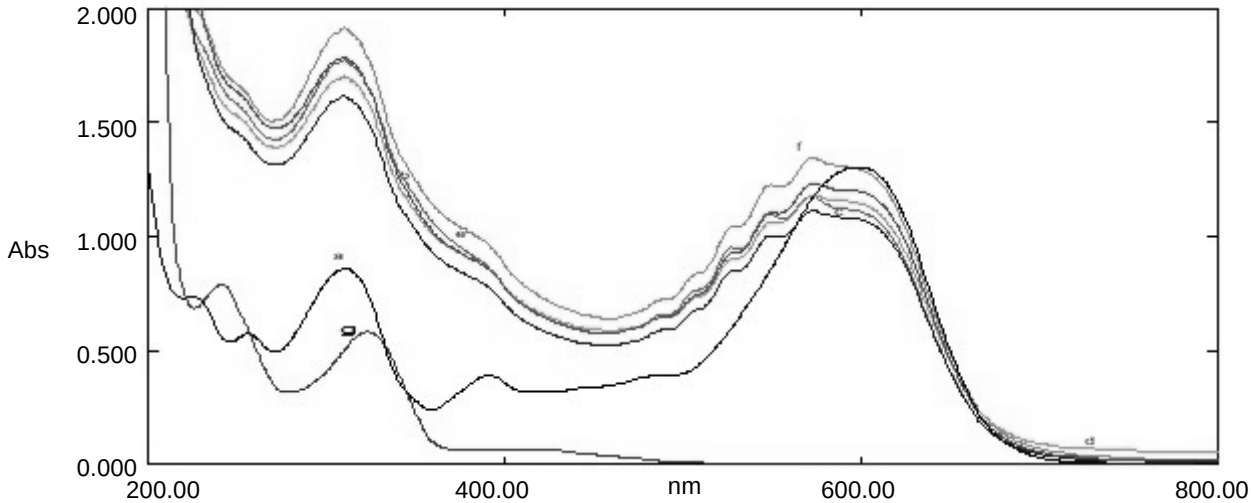

Fig. 2(i) Spectral change at elevated concentrations of urea with constant concentrations of $KMnO_4$ and dye after 5 min in alkaline medium

Effect of urea dosage

The influence of the various concentrations of urea [0.025M - 0.375M] on decoloration of dye was monitored, keeping all variables constant at 298K (Table 1). No significant effect of change in concentration of urea on the rate of oxidation was observed indicating that urea was required in a very small quantity which was enough for acceleration of oxidation reaction. Spectral analysis (Fig. 2i) showed that the complex was formed at all concentrations of urea in alkaline medium which later on decomposed into smaller fragments showing maximum absorbance in the UV-region.

Table 1 Effect of Dye, $KMnO_4$, H_2O_2, and Urea on de-coloration of dye

[Dye] 10^5 mol dm^{-3}	**dx/dt 10^3 mol dm^{-3} min^{-1}**	**k_{obs} 10^3 min^{-1}**	**% De-coloration**
0.5	1.2	7.6	38.09
1.0	1.7	7.9	40.35
2.0	3.9	12.4	60.90
2.5	7.0	17.1	73.8
5.0	14.3	17.6	74.37
[$KMnO_4$] 10^4 mol dm^{-3}			
1.5	9.4	1.12	53.33
1.87	11.5	1.97	71.45
2.18	13.7	2.27	76.11
2.5	13.9	2.59	84.8
2.8	13.0	2.73	84.00
3.1	12.4	2.68	84.2
3.43	15.6	2.73	79.83
[H_2O_2]10^4 mol dm^{-3}			
3.75	2.49	1.61	64.67
7.5	2.39	2.17	97.12
11.25	1.44	0.71	40.34
15.0	2.00	1.10	52.51
18.75	1.99	1.11	52.90
[Urea]mol dm^{-3}			
0.375	10.3	23.8	89.5
0.25	13.9	26.8	88.23
0.125	13.2	25.7	97.52
0.075	12.8	27.9	98.15
0.025	14.9	25.4	89.39

Effect of Alkali dose

The decoloration of dye was studied at various concentrations of NaOH (0.005M – 0.025M) (Table 2). It was found that a significant increase in the concentration of alkali had a negligible effect on the rate of reaction i.e. the rate was favored in the lower alkaline range. This showed that OH^{-1} ions are not effective for the oxidation of dye or that oxidation is independent of OH^{-1} ions indicating zero-order kinetics. The addition of H_2O_2 increases the efficiency of oxidation as percent decoloration was 97.12% as compared to 84.7% in absence of H_2O_2. Spectral analysis showed

that complexes are formed between dye and $KMnO_4$ at all concentrations of NaOH and later decomposed into new compounds having λ_{max} values different from that of the dye. The spectral analysis with respect to time showed that there was a hypsochromic shift from visible region to UV region with no peak due to dye (Fig. 3a). Figure 3a shows complete degradation of dye into low molecular weight components as reported earlier.[8] It was observed that in the absence of H_2O_2, sludge was formed at various concentration of alkali which disappeared in the presence of H_2O_2.

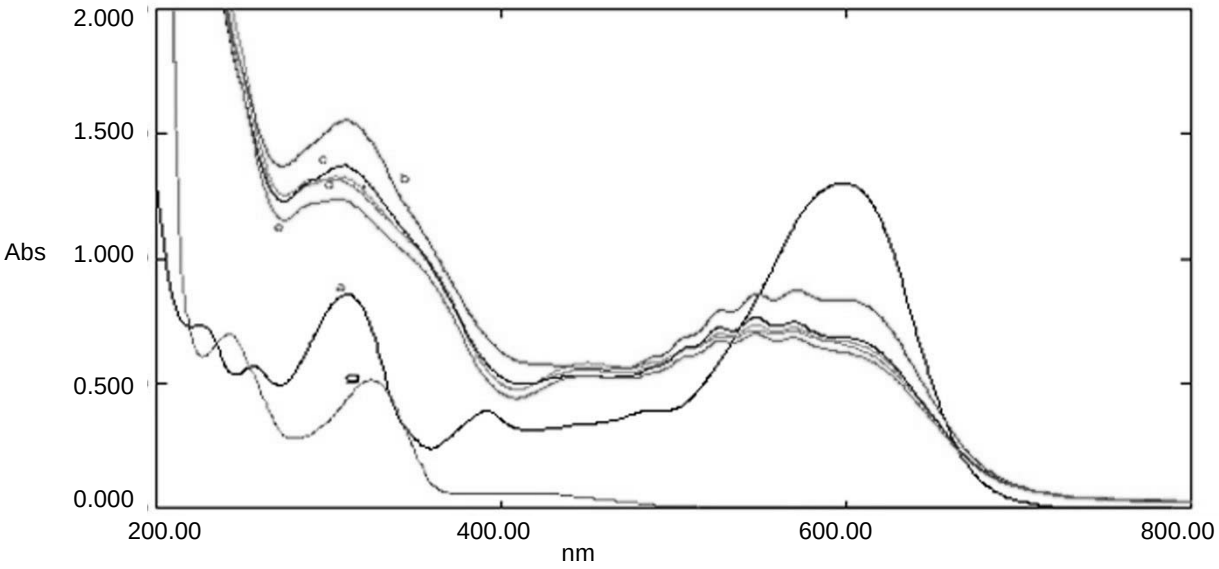

Fig.3(a) Spectral change at increasing concentrations of NaOH with constant concentration of H_2O_2, Urea, $KMnO_4$ and dye after 5 min

Table 2: Effect of NaOH on de-coloration of dye

[RB5] = $5x10^{-5}$M [Oxidant] = [$KMnO_4$] Temperature=298K [Urea] = 0.075M

[NaOH] mol.dm^{-3}	dx/dt 10^3 mol dm^{-3}. min^{-1}	k_{obs}. 10^3 min^{-1}	k_{sp}. 10^3 min^{-1}	log [NaOH]	log k_{obs}	1/k_{obs}	1/ [NaOH]	log dx/dt	% De-coloration
0.005	15.0	13.0	11.85	-2.30	-1.88	-41.49	200	-1.82	84.4
0.01	14.8	6.4	7.82	-2	-2.19	-41.49	100	-1.83	84.7
0.015	13.6	4.6	7.29	-1.82	-2.33	-49.75	66.67	-1.87	82.96
0.02	12.7	4.2	8.98	-1.7	-2.37	-56.82	50	-1.9	80.24
0.025	12.3	4.6	6.81	-1.60	-2.33	-217.39	40	-1.91	81.28

Effect of various ions as dye additives

The influence of several anions and cations on oxidation kinetics of RB5 was monitored at 597.5 nm and 298K. The impact of these anions and cations on the rate constant of oxidation of Reactive Black 5was studied at a constant concentration of $KMnO_4$, RB 5, urea and H_2O_2 (Table 3). It was observed that the rate of the oxidation was independent of the concentration of anions and cations in alkaline medium. Results reported in Table 3 show that the presence of I^- slows down the rate of

reaction as compared to other anions. The % decoloration with I^- was 76.89%, which was less as compared to other anions while in the presence of Na^{+1} and Al^{+3} ions, the rate of reaction was rapid as compared to other cations. The % decoloration was 87.88% and 92.55% respecti-vely. Spectral analysis showed that no complex formation was observed in the presence of anions in basic medium (Fig.3b) while the degradation of dye in the presence of cations takes place through complex formation (Fig.3c).

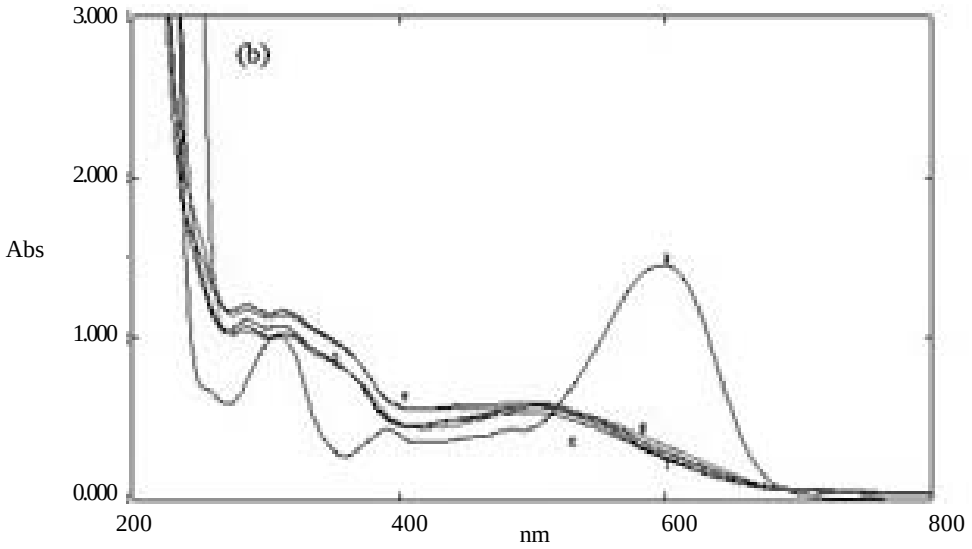

Fig. 3(b) Spectral changes of oxidation of RB5 in the presence of anions in alkaline medium at the start of the reaction

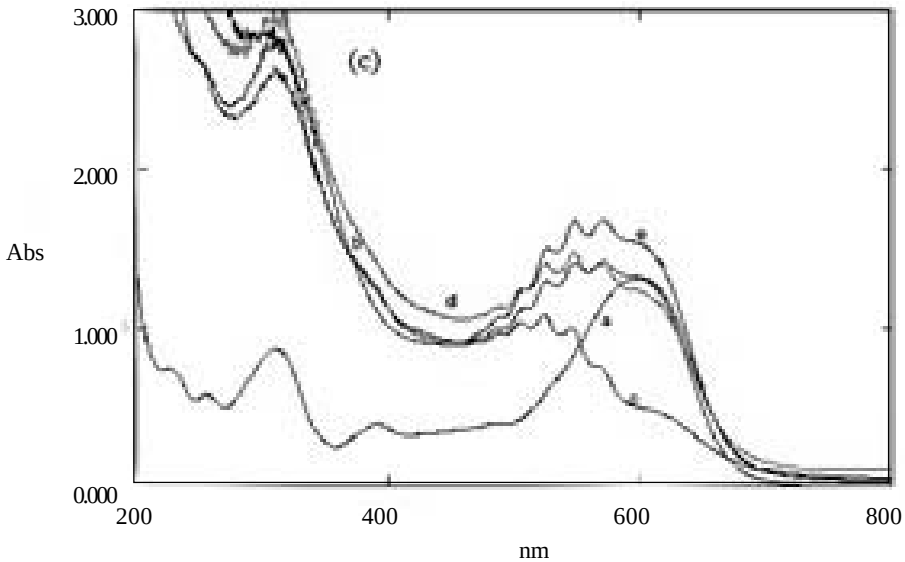

Fig. 3(c) Spectral changes of oxidation of RB5 in the presence of cations in alkaline medium at the start of the reaction

Table 3 Effect of Anions and Cations on oxidation of RB5

[RB5] = $5x10^{-5}$M [Oxidant] = [$KMnO_4$] = $2.5x10^{-4}$M
Temperature=298K [Urea] = 0.075M [H_2O_2] = $7.5x10^{-4}$ M

Ions	dx/dt 10^3 mol.dm^{-3} min^{-1}	$k_{obs}10^3$ min^{-1}	% De-coloration
I^{-1}	9.0	16.3	76.89
NO_3^{-1}	6.4	14.6	81.37
CH_3COO^{-1}	7.2	16.0	81.79
CO_3^{-2}	4.9	11.0	78.68
$C_2O_4^{-2}$	4.7	10.08	79.10
Na^{+1}	2.4	3.19	87.88
Mg^{+2}	0.95	2.02	85.99
Ba^{+2}	1.99	3.05	87.82
Al^{+3}	2.45	4.76	92.55

Mineralization of RB5 dye

The mineralization of Reactive Black 5 dye was confirmed by determination of chemical oxygen demand of the analyte solution after 60 min process time (Table 4). COD is related to the Biological oxygen demand (BOD) of water-bodies which is used for measuring the quality of sustainable marine life. The COD tested in the presence of newly developed ultra-oxidation system displayed the lowest value after oxidation,which indicates that the process is suitable for complete mineralization of the organic dye and is eco-friendly. This can be explained with the release [O] and the formation of a urea-H_2O_2 complex. Reaction with the C-C double bond and N=N bond, leads to complete mineralization according to Equation 2:

$$C_{20}H_{11}N_2O_{10}S_3 + 48H_2O \rightarrow 20CO_2 + 107H^+ + 100e^- + 2NO_3^- + 3SO_4^{2-} \quad (2)$$

Table 4 Comparison of COD removal values of various methods

New advanced oxidation	COD ppm
Dye wastewater	6000-7000
alkaline $KMnO_4$	490
$KMnO_4$ / alkaline H_2O_2 alkaline	470

The filtrate obtained after mineralization was used for seed germination and in fish aquarium containing the recycled water and normal tap water. Zero-order kinetics in aqueous alkaline medium suggests that oxidation was independent of H_2O_2 concentration which was similar to the earlier work reported by Dutta et al. [9] and Varma and Naicker who reported that H_2O_2 acts as a self-scavenger at elevated concentration. For each variable, there was considerable % color removal (Table 1). 60 minutes of permanganate treatment was considered a suitable time, resulting in 95.3 and 94.3% of color removal at each operational parameter. However, after 60 (or even 10) minutes of reaction, significant color removal was seen. This fact opens up a new avenue for further experiments

involving reduced degradative times in the presence of various anions and cations.

The new AOP process showed that it was also effective in the presence of various anions like CH_3COO^-, NO_3^-, $C_2O_4^{2-}$, CO_3^{2-}, I^- in which CH_3COO^- anion in alkaline medium was more effective in comparison to other ions as % decoloration was higher as compared to other ions (Table 3). The UV/Visible spectral change (Fig. 3b) showed that I^- showed less % de-coloration as compared to other ions (76.89%).[11] The following trend of decolorization by anions in alkaline medium was observed:

$$CH_3COO^- > NO_3^- > C_2O_4^{2-} > CO_3^{2-} > I^-$$

The new AOP was also effective in the presence of cations including Al^{3+}, Na^+, Ba^{2+}, and Mg^{2+} and especially in the presence of Al^{3+} which is used in dye fabrication for fastening the color. It was observed that the % decoloration of dye wastewater in the case of Al^{3+} was higher when compared to other ions (Table 3). The UV/Visible spectral change showed that Mg^{2+} showed less % de-coloration as compared to other cations (85.99%). The following trend of decolorization of cations in alkaline medium was observed:

$$Al^{3+} > Na^+ > Ba^{2+} > Mg^{2+}$$

Initially, the rate of oxidation of dye RB5 in aqueous alkaline medium with $KMnO_4$, urea, and H_2O_2 was slow and then increased after 5 min, leading to almost 87% oxidation of dye with reduced time interval when compared with oxidation in the absence of H_2O_2. This suggests that H_2O_2 forms a complex with urea which was helpful in dye degradation as reported earlier.[12]

The rapid decoloration of dye wastewater with Mn/H_2O_2 with additive urea showed that urea – H_2O_2 complex couples with nascent oxygen [O], involved in the dye degradation instead of OH^- ions [13, 14]. Therefore, the rapid decoloration of dye in the presence of urea additive and H_2O_2 proceeded through two oxidative species. Since an increase in the concentration of H_2O_2 and NaOH showed negligible effect on the oxidation[15], OH• is not the oxidizing species in the reaction. The OH• radical was tested by benzoic acid when no bubbles evolved indicating the absence of OH• radical. The nascent release oxygen [O] in current AOP was tested using Mg wire, the formation of white precipitate of MgO showed the presence of nascent oxygen.[9,10]

At high pH, the oxidizing capability of potassium permanganate is less, as fewer electrons are transferred according to Equation 3:

$$2H_2O + M_nO_4^- + 3\bar{e} \rightarrow M_nO_2(s) + 4OH^- \qquad (3)$$

where Mn was reduced to manganite (VI) according to Equation 4:

$$M_nO_4^- + \bar{e} \rightarrow MnO_4^{2-} \qquad (4)$$

In the presence of hydrogen peroxide the cleavage of RB5 takes place according to Equation 5, 6 and 7:

$$2KM_nO_4 + 3H_2O_2 \rightarrow 2KOH + 3O_2 + 4H_2O + 2M_nO_2 \qquad (5)$$

$$NH_2CONH_2 + HOOH \rightarrow \underset{\text{Urea bhydrogen peroxide complex}}{NH_2CONH_2.HOOH} \qquad (6)$$

$$RB\ 5 + NH_2CONH_2HOOH \xrightarrow[OH]{KMnO_4/[O_2]} RCONH_2 + RSR + RSOR \qquad (7)$$

The possible degraded products were presented through the following reaction pathway, as indicated in (Fig.4)

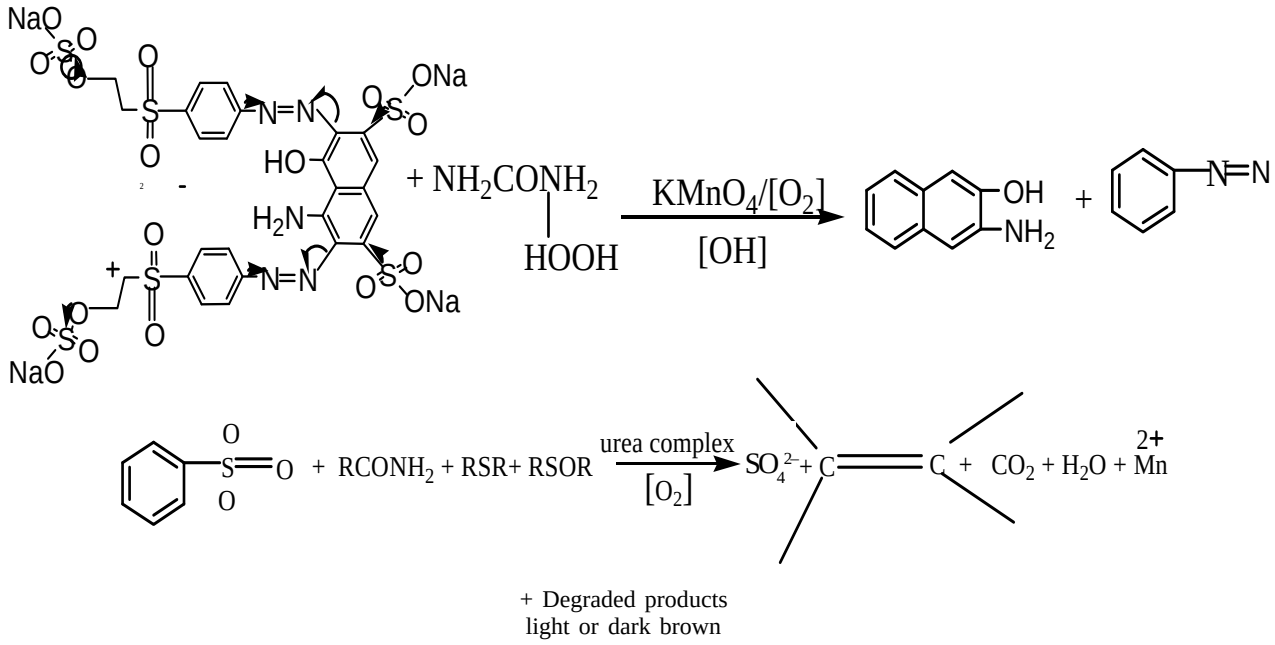

Fig. 4. Reaction Mechanism of RB5 mineralization

UV-visible and IR spectral analysis

The UV-VIS absorption spectra of azo dye RB5 solutions using the new AOP before and after advanced oxidation are presented in (Fig. 2). The characteristic absorption band of the azo group (-N = N-) of RB5 dye is at λ_{max} 597.5 nm, while two low-intensity bands localized between 245 and 360 nm are associated with the $\pi \rightarrow \pi^*$ transitions in aromatic rings in conjugation with the azo bond.[16,17] The reduction in intensity of the 597.5nm band after 60 min of AOP treatment was directly related to the two generated oxidizing species, validating the rupture of the azo bond and complete de-aromatization of dye was associated with new AOP process as reported earlier.[1]

The IR spectral analysis revealed that various peaks of RB5, which had appeared in the RB5 spectrum (Fig. 3d), disappeared in the IR spectrum of dye solution after oxidation (Fig. 3e), indicating the mineralization of dye by the current AOP which was similar to earlier reports.[18,19] The peaks corresponding to 1637.56 cm^{-1} showed the presence of C=C stretch C=O which was also observed in UV/Visible region 190-380 nm which confirmed complete mineralization of dye in the presence of H_2O_2 in alkaline medium. It also suggests that decolorization of the dye is associated with breaking of RB5 aromatic rings and chromophore conjugated unsaturated bonds (–N=N–) in the molecule.[13,19] It also suggests that some aromatic amines like Aniline and 1-Aminonaphthalene may have been produced as interme-diates indicating partial mineralization of RB5.[19] The production of aromatic amines agrees with the results of Kang et. al.,[20] and Wang et. al. [21] However, Azbar et.al.,[1] reported that complete de-aromatization of dye was associated with AOP process. Junnarkar et. al.[22] also reported the cleavage of azo bonds and formation of aromatic amines which are linked to the dyes.[23] This is similar to the work reported by Ullah et. al.[11] while current AOP established complete mineralization in reduced time in comparison to earlier reports.[9,20]

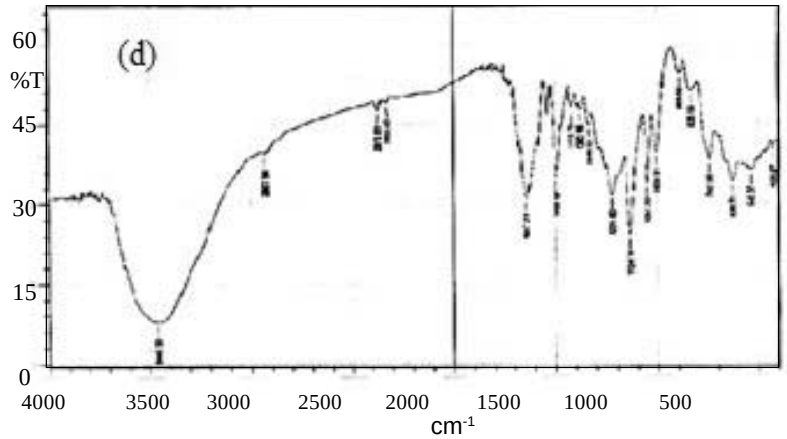

Fig. 3(d) IR spectrum of RB5 showing various intensity peaks

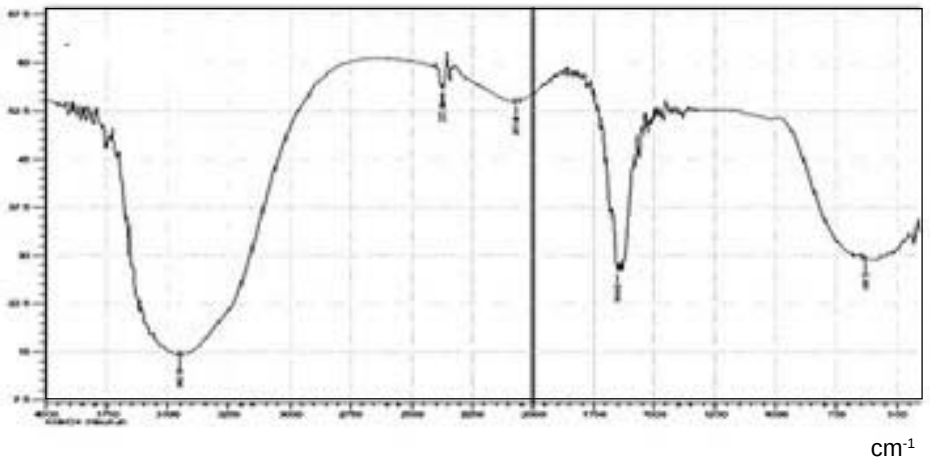

Fig. 3(e) Infra-Red spectrum of RB 5 after oxidation

Mechanism of Rate of reaction in aqueous alkaline medium

$$\text{Dye} + KMnO_4 + \text{Urea} \xrightarrow{k_1 H_2O_2/OH^-} \text{Complex}$$

$$\xrightarrow{k_2} [\text{Complex degradation}] \xrightarrow{k_3} [\text{Mineralization}]$$

$$\frac{d[KMnO_4]}{dt} = k_1[KMnO_4][\text{Dye}][\text{Urea}] \quad (8)$$

It was observed that there was no effect of H_2O_2 concentration on the rate and increase or decrease of Urea also showed no effect on the rate of reduction [Table 1]. Therefore, Equation 8 becomes:

$$\frac{d[KMnO_4]}{dt} = -k_1[KMnO_4] \quad (9)$$

or

$$[KMnO_4] = [KMnO_4]e^{-k_1 t} \quad (10)$$

$$\frac{d[\text{complex}]}{dt} = k_1[KMnO_4] - k_2[\text{Complex}] \quad (11)$$

$$\frac{d[S]}{dt} = k_2[\text{Complex}] \quad (12)$$

k_1 and k_2 are rate-limiting steps. The steady state for above reaction is represented in Equation 11:

$$\frac{d[complex]}{dt}=0$$

Hence,

$$k_1[KMnO_4]-k_2[Complex]=0$$

$$\frac{d[S]}{dt}=k_1[KMnO_4][Dye]^{\frac{1}{2}}$$

From Equation 9,

$$\frac{d[S]}{dt}=-\frac{d[KMnO_4]}{dt} \text{ and } [Sludge]=1-e^{-(k_1t)}$$

or

$$\frac{d[complex]}{dt}=k_1[KMnO_4]e^{-k_1t}-k_2[Complex]$$

According to above equation, the reaction follows first order kinetics:

$$[Complex]=Complex\ e^{-k_2t}+\left(\frac{KMnO_4}{\left(1-\frac{K_2}{k_1}\right)}\right)(e^{-k_2t}-e^{-k_1t})$$

$$[KMnO_4]/[KMnO_4]=e^{-K_1t}$$

$$[Complex]/[complex]=e^{-K_1t}\left(\frac{[KMnO_4]_0/KMnO_4]_0}{1-\frac{K_2}{K_1}}\right)\left(e^{-k_2t}-e^{-k_1t}\right) \qquad (13)$$

since any time,

$$[KMnO_4]+[Complex]+[Sludge] \rightleftharpoons KMnO_4]_0+[complex]_0+[Sludge]_0$$

Combining Equations 10, 11 and 13 we get,

$$[Sludge]=[Sludge]_0+[KMnO_4]_0\left(1-e^{-k_2t}\right)+(Complex)_0[\left(1-e^{-K_2t}\right)--\left(\frac{[KMnO_4]_0/[Complex]_0}{1-\frac{k_2}{k_1}}\right)\left(e^{-k_2t}-e^{-k_1t}\right)$$

$$[KMnO_4]_0+[Complex]=1$$

since [Sludge] = 0

Therefore [Sludge] can be derived as:-

$$[\text{Sludge}]=[KMnO_4]_0-[KMnO_4]_0\,e^{-k_1t}+[\text{Complex}]_0-[\text{Complex}]_0e^{-K_2t}$$
$$-\left(\frac{[KMnO_4]_0\,k_1}{k_1-k_2}\right)e^{-k_2t}+\left(\frac{[KMnO]_0k_2}{k_1-k_2}\right)e^{-k_2t}$$

Conclusions

The new AOP was found to be a self integrated process which required less oxidant, urea and H_2O_2 while being active at higher concentrations of dye with no sludge formation in comparison with the Fenton process in which sludge is formed. 80% degradation of dye occurred in the initgial 10 minutes and complete mineralization in 60 minutes.

Acknowledgement

Authors are very thankful to HEC Pakistan for providing financial support through Research Project No. 20-2282/ NRPU/R&D/HEC/12/5014.

References

1. Azbar, N., Yonar T. and Kestioglu, K., 2004, *Chemosphere*, **55**, 35-43.
2. Pearce, C.I., Lloyd J.R. and Guthrie, J.T., 2003, *Dyes and Pigments*, **58(3)**, 179-196.
3. Barros, L., Ferreira, M.J., Queiros, B., Ferreiraand Baptista, I.C.F.R., 2007, *Food Chemistry*, **103(2)**, 413-419.
4. Hussein, F.H., 2011, *Advances in Treating Textile Effluent*, 117-144.
5. Neamtu, M., Yediler, A., Siminiceanu, I. and Kettrup, A., 2003, *Journal of Photochemistry and Photobiology A: Chemistry*, **161**, 87-93.
6. Burkinshaw, S., Lagonika K. and Marfell, D., 2003, *Dyes and Pigments*, **56**, 251-259.
7. Mills, A., Hazafy, D., Parkinson, J., Tuttle, T. and Hutchings, M.G., 2011, *Dyes and Pigments*, **88**, 149-155.
8. Lucas, M. and Peres, J., 2006, *Dyes and Pigments*, **71**, 236-244.
9. Dutta, K., Bhattacharjee, S., Chaudhuri, B. and Mukhopadhyay, S., 2002, *Journal of Environmental Monitoring*, **4**, 754-760.
10. Varma, R.S. and K.P. Naicker, K.P., 1999, *Organic Letters*, **1**, 189-192.
11. Ullah, I., Ali, S. and Akram, M., 2013, *International Journal of Chemical and Biochemical Sciences*, **4**, 96-100.
12. Lee, I., Kim, C.K. and Lee, B.C., 1989, *Journal of Physical Organic Chemistry*, **2**, 281-299.
13. Bahmani, P., Maleki, A., Ghahramani, E. and Rashidi, A., 2013, *African Journal of Biotechnology*, **12**(26).
14. Meriç, S., Kaptan, D. and Ölmez, T., 2004, *Chemosphere*, **54**, 435-441.
15. Azmat, R., Mohammed, F.V., Ahmed, T. and Tanwir, Q.-U.-A., 2011, *Frontiers of Chemistry in China*, **6**, 84-90.
16. Muruganandham, M., 2004, *Dyes and Pigments*, **63**, 315-321.
17. Zhang, G., Yang, F. and Liu, L., 2009, *Journal of Electroanalytical Chemistry*, **632**, 154-161.
18. Brillas, E., Mur, E., Sauleda, R., Sànchez, L., Peral,

J., Domènech, X. and Casado, J., 1998, *Applied Catalysis B: Environmental*, **16**, 31-42.

19. López-Grimau, V., Vilaseca, M. and Gutiérrez-Bouzán, C., 2015, *Desalination and Water Treatment*, **57**, 2685-2692.

20. Kang, S.-F., Liao, C.-H. and Po, S.-T., 2000, *Chemosphere*, **41**, 1287-1294.

21. Wang, X., Cheng, X., Sun, D., Ren, Y. and Xu, G., 2014, *Environmental Science and Pollution Research*, **21**, 5713-5723.

22. Junnarkar, N., Murty, D.S., Bhatt, N.S. and Madamwar, D., 2005, *World Journal of Microbiology and Biotechnology*, **22**, 163-168.

23. Tantak, N. and Chaudhari, S., 2006, *Journal of Hazardous Materials*, **136**, 698-705.

RNI No. MAHENG/2017/74063
ISSN No. (Print) 2581-5911
ISI Impact Factor 1.022 (2019-2020)

Removal of Methylene Blue from Aqueous Solution Using Peanut Hull as Adsorbent

M.B. Mandake, S.P. Shingare and Advait Swamy*
Department of Chemical Engineering, Bharati Vidyapeeth College of Engineering, (University of Mumbai), Kharghar 400614, New Mumbai, India.
*** Email: advaitv.swamy01@gmail.com**

Abstract
Many industries like the textile industry use dyes to colour their products and thus produce wastewater containing organics with a strong colour. In the dyeing processes, the percentage of dye lost in wastewater is 50% because of the low levels of dye-fibre fixation. To find an effective but cheap method of treatment of wastewater containing dye, peanut hull as agricultural by product was used for adsorption of Methylene Blue (MB) from aqueous solution. The effect of various parameters such as initial Methylene Blue concentration, peanut hull dosage and pH were examined and their optimum experimental conditions were determined. Isotherm studies were done by treatment of Adsorption data using Langmuir and Freundlich isotherm models and it was found that the adsorption data followed Langmuir isotherm. Kinetics was studied using pseudo first order and pseudo second order models and sorption data was found to follow pseudo second order kinetics. Mechanism of rate controlling step was determined by applying intraparticle diffusion for the mass transfer model. Sorption data was found to be controlled by both intraparticle diffusion as well as adsorption step. The results of this study indicate that peanut hull was a good adsorbent for removing Methylene Blue from aqueous solution.

Keywords: *Adsorption, Peanut Hull, Methylene Blue, Adsorption Isotherms, Kinetics, Mechanism.*

Introduction

Dyes are widely used in industries such as textiles, rubber, plastics, printing, leather, cosmetics, etc., to colour their products. Many industries like the textile industry use dyes to colour their products and thus produce wastewater containing organics with a strong colour. In the dyeing processes the percentage of wastewater lost is 50% of the dye because of the low level of dye-fibre fixation. There are more than 10,000 commercially available dyes with over 7×10^5 tonnes of dye stuff produced annually.[5] It is estimated that 2% of dyes produced annually is discharged in the effluents from associated industries. Among various industries, textile industry ranks first in usage of dyes for colouration of fibre. The total dye consumption of the textile industry worldwide is in excess of 10^7 kg/year and an estimated 90% of this ends up on fabrics. Consequently, 1,000 tonnes/year or more of dyes are discharged into waste streams by the textile industry worldwide. Discharge of dye-bearing wastewater into natural streams and rivers poses severe problems to the aquatic life, food web and causes damage to the aesthetic nature of the environment. Discharge of these dyes into effluents affects the people who may use these effluents

for living purposes such as washing, bathing and drinking. Nearly 10-15% of synthetic textile dyes, used yearly are lost to waste streams and about 20% of these losses enter the environment through effluents from waste water treatment plants. Therefore it is very important to verify the water quality, especially when even 1.0 mg/L of dye concentration in drinking water could impart a significant colour, making it unfit for human consumption. Furthermore, dyes can affect aquatic plants because they reduce sunlight transmission through water. Also, dyes may be toxic to aquatic life and may be mutagenic, carcinogenic and may cause severe damage to human beings, such as dysfunction of the kidneys, reproductive system, liver, brain and central nervous system.

The removal of colour from waste effluents becomes environmentally important because even a small quantity of dye in water can be toxic and highly visible. Since the removal of dyes from wastewater is considered an environmental challenge and government legislation requires textile wastewater to be treated, there is a constant need to have an effective process that can efficiently remove these dyes. Numerous techniques were used in the recent past for decolourisation of dyes. Among them adsorption technique has maximum potential for the removal of dyes. Adsorption being a physical process, inexpensive and less time consuming, is widely accepted.[7]

Methods of dye removal from dye-containing industrial effluents have been discussed under three categories[2]:

1. Chemical
2. Physical
3. Biological

Currently the main methods of textile dye treatment are Fenton Process, Photo/Ferri-Oxalate System. Process, Photo - Catalytic and Electrochemical combined treatments, Photo-catalytic Degradation using UV/TiO_2, Sono - Chemical Degradation, Biodegradation, Photo - Fenton processes, Integrated Chemical - Biological Degradation, Electrochemical Degradation, Adsorption Process, ozonation, oxidation, Nano-Filtration, Chemical Precipitation, Ion - Exchange and Reverse Osmosis[3].

Among treatment technologies, adsorption is rapidly gaining prominence as a method of treating aqueous effluents. Some of the advantages of adsorption process are possible regeneration at low cost, availability of known process equipment, sludge-free operation and recovery of the sorbate[4]. Adsorption is a well-known equilibrium separation process and an effective method for water decontamination applications. Adsorption has been found to be superior to other techniques for water re-use in terms of initial cost, flexibility and simplicity of design, ease of operation and insensitivity to toxic pollutants. Adsorption also does not result in the formation of harmful substances. Activated carbon is the most widely used adsorbent for dye removal because of its extended surface area, micro-pore structure, high adsorption capacity and high degree of surface reactivity. However adsorption by activated carbon has some drawbacks such as the cost of the activated carbon, the need for regeneration and the loss of adsorption efficiency after regeneration. This has led to the search for cheaper alternatives[9].

There have been many attempts to find inexpensive and easily available adsorbents to remove the pollutants such as the agricultural solid wastes which may be good potential adsorbents due to their physic-chemical characteristics and low cost. Agricultural waste materials have little or no economic value and often pose a disposal problem. The utilization of agricultural waste is of great significance. A number of agricultural waste materials are being studied for the removal of different dyes from aqueous solutions under different operating conditions[4]. Agricultural wastes are renewable, available in large amounts and less expensive as compared to other adsorbent materials. Agricultural wastes are better than other adsorbents because the agricultural wastes are usually used without or with a minimum of processing

(washing, drying, grinding) and thus reduce production costs by using a cheap raw material and eliminating energy costs associated with thermal treatment. [5] Agricultural waste includes (but not limited to) banana peel, peanut hull, peanuts hull, orange peel, date pit, broad bean peel, almond shells, etc. The use of these low-cost bio-sorbents is recommended since they are relatively cheap or of little cost, easily available, renewable and show high affinity for dyes.

Material and Methods

Methylene Blue was chosen in this study because of its known strong adsorption onto solids. Methylene Blue has a molecular weight of 373.9 g, which corresponds to Methylene Blue hydrochloride with three groups of water. The structure of Methylene Blue is given below:

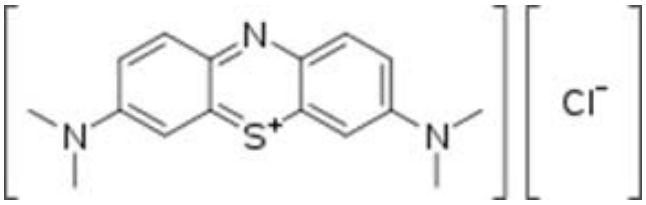

Methylene Blue, a cationic dye, is not regarded as acutely toxic, but it has various harmful effects. On inhalation, it can give rise to short periods of rapid or difficult breathing, while ingestion through the mouth produces a burning sensation and may cause nausea, vomiting and gastritis problems[14].

Materials

Peanut hull used in the present investigation was collected directly from local farms. The collected material was then washed with distilled water for several times to remove the dirt particles. The washing process was continued until the washing was colourless. The washed materials were then dried in hot air oven at 80°C for 8 hours. Dried materials were then ground using a domestic mixer and then sieved to obtain a mixture of constant particle size of 100 mesh. This mixture was later stored in glass bottle for use.

Equilibrium Studies

Equilibrium experiments were carried out by contacting 1g of peanut hull particles with 100 mL of dye solution of different initial dye amounts, 500, 250 and 100 mg/L. The contact was made in 300 mL stopper bottles using shakers at a constant agitation speed. The agitation was made for 4 hours until equilibrium was reached. Amount of adsorption at equilibrium q_e (mg/g) is calculated by Equation 1:

$$q_e = \frac{(C_0 - C_e)V}{W} \quad (1)$$

where, C_o and C_e (mg/L) are the liquid phase concentration of dye at initial time and equilibrium time t, respectively. V (L) is the volume of the solution and W (g) is amount of adsorbent used.

The dye removal can be calculated as follows:

$$\text{Adsorption Percent (\%)} = \frac{C_0 - C}{C_0} \times 100 \quad (2)$$

where C (mg/L) is liquid phase concentration at any time t.

Effect of Adsorbent Dosages

The effect of peanut hull mass on the amount of colour adsorbed was obtained by contacting 100 mL of dye solution of initial dye concentration 100 mg/L with different weighed amounts (0.5, 1 and 1.5 g) of peanut hull using shakers at room temperature (32°C) for 4 hours until equilibrium was reached. At equilibrium, the samples were then centrifuged and the concentration in the supernatant dye solution was analysed using COD.

Effect of pH

The effect of pH on the amount of colour removal was analyzed at different pH values i.e. 4, 7 and 10. The pH was adjusted using 1 N NaOH and 1 N HCl solutions. In this study, 100 mL of dye solution of 100 mg/L was

agitated with 1g of peanut hull using shakers at room temperature (32°C). Agitation was done for 4 hours which was sufficient to reach equilibrium at a constant agitation speed. The samples were then centrifuged and the concentration in the supernatant solution was analysed using COD reduction.[42]

Isotherm Studies

Adsorption isotherm is characterized by certain constant values which express the surface properties and affinity of the adsorbent and can also be used to compare the adsorptive capacities of the adsorbent for different pollutants. The Langmuir model is valid for monolayer adsorption onto a surface with a finite number of identical sites which are homogeneously distributed over the adsorbent surface. The well-known expression of the Langmuir model is given as:

$$q_e = \frac{q_{max}\, K\, C_e}{1 + K\, C_e} \qquad (3)$$

where q_e is the amount of MB adsorbed on adsorbent at equilibrium, C_e is the equilibrium concentration in the solution, q_{max} is the maximum adsorption capacity and K is the adsorption equilibrium constant. The linear form of this equation is written as:

$$\frac{C_e}{q_e} = \frac{1}{k\, q_{max}} + \frac{C_e}{q_{max}} \qquad (4)$$

A plot of C_e/q_e versus C_e is a straight line with slope $1/q_{max}$ and an intercept of $1/K\, q_{max}$. The Freundlich model is an empirical equation based on adsorption on a heterogeneous surface suggesting that binding sites are not equivalent and/or independent. The Freundlich equation is expressed as:

$$Q_e = K_F\, C^{1/n} \qquad (5)$$

where K_F is an indicator of the adsorption capacity and n is indicator of the adsorption intensity. The logarithmic form of this equation is given by the following equation:

$$\ln(q_e) = \ln(K_F) + \frac{1}{n} \ln C_{eq} \qquad (6)$$

From the plot of ln (q_{eq}) versus ln (C_{eq}), K_F and 1/n values are obtained.

Adsorption Kinetics

Kinetic models have been proposed to determine the mechanism of adsorption which depends on the physical and/or chemical characteristics of the adsorbent as well as on the mass transport process. In order to determine the mechanism of adsorption of adsorption of MB onto DPH, pseudo-first and pseudo-second order kinetic models have been proposed as follows:

Lagergren Model

The integrated form of the model is

$$ln\ (q_e - q) = ln\ (q_e) - k_1 t \qquad (7)$$

where q is the amount of MB adsorbed at time t (min), q_e the amount of MB adsorbed at equilibrium and k_1 is the rate constant of pseudo-first order adsorption.

Pseudo-Second Order Model

The adsorption kinetics can also be given by a pseudo-second order reaction. The integrated linear form of this model is

where k_2 is the pseudo-second order rate constant of MB adsorption. The plot of t/q versus t (Eq. 8) should give a linear relationship, from which q_e and k_2 can be determined from the slope and intercept respectively of the plot, if second order kinetic equation is applicable.

Since the models mentioned above cannot identify a diffusion mechanism, the intraparticle diffusion model was also tested to find the rate controlling step. In this model, the rate of intraparticular diffusion is a function of $t^{1/2}$ and can be defined as shown below and calculated by linearization of the given curve

$$q = f\left(\frac{Dt}{rp}\right)^{(1/2)} = k_i t^{1/2} \qquad (9)$$

where r_p is the particle radius, D the effective diffusivity of MB within the particle and k_i is the intraparticular diffusion rate.

Results and Discussion

Effect of Initial Dye Concentration

Fig.1 shows the effect of initial MB concentration on MB adsorption. Fig.1 is the graph of % COD reduction verses contact time. As shown in Fig.1, initially %COD reduction is slightly greater for 500 mg/L solution. This indicates that adsorption i.e. dye uptake (mg/g) increases with increase in initial dye concentration. The concentration is an important driving force to overcome all the mass transfer resistance of the dye between aqueous and solid phase. Hence, initial dye concentration will enhance the adsorption process. But, at equilibrium time, %COD reduction decreases with increase in dye concentration. This means % removal of dye decreases with increase in initial dye concentration because the capacity of 1 gm of dye is fixed and as initial dye concentration increases, the capacity goes on decreasing and after some time there is no free surface left for further adsorption of dye. As initial MB concentration increases from 100 to 500 mg/L, % COD reduction decreases from 50.3% to 41.2%.[43]

Effect of Adsorbent Dosage

The effect of adsorbent dosage on the adsorption rate of Methylene Blue was studied, while other experimental conditions were kept constant, as the adsorbent concentration was varied from 0.5 to 1.5 g/L. Results obtained for the adsorption of Methylene Blue are shown in Fig. 2. It is clear from the plot of % COD reduction verses contact time that %COD reduction for 1.5 gram adsorbent is maximum (47.83%) and decreases as the adsorbent dose decreases. For 0.5 gram dosage, it is 34.4%.[44] Hence, it can be concluded that the % dye removal increases with increase in adsorbent dosage. COD reduction for 1 gm (44.73 %) and 1.5 g (47.83 %) dosage is:

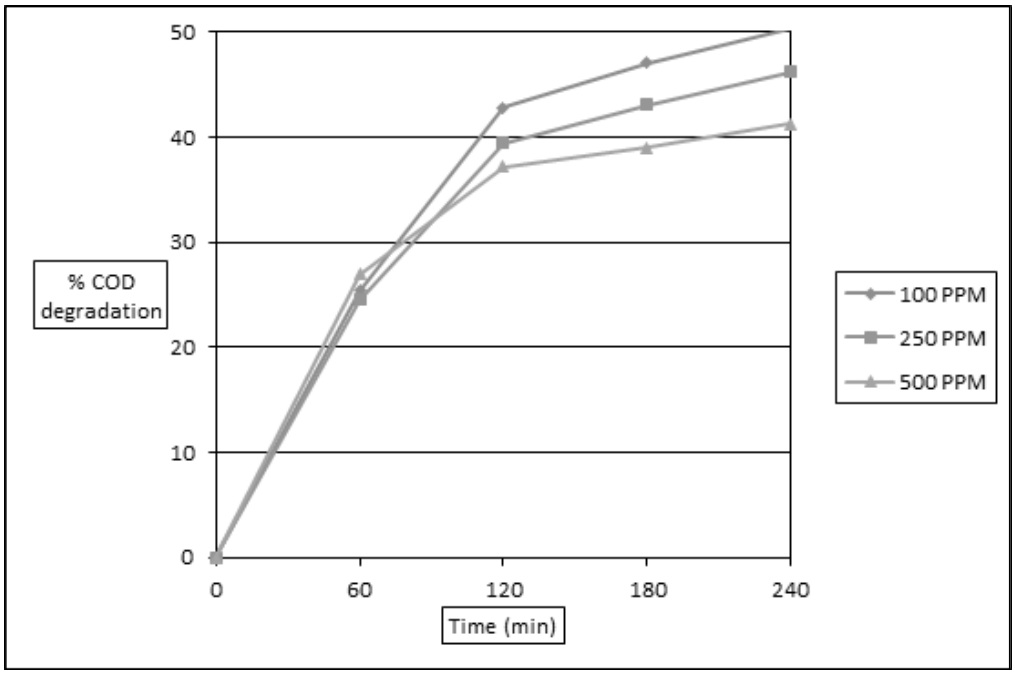

Fig. 1: Effect of initial concentration on removal of MB by Peanut Hull (Conditions: W = 1g/100 mL. at Room Temp.)

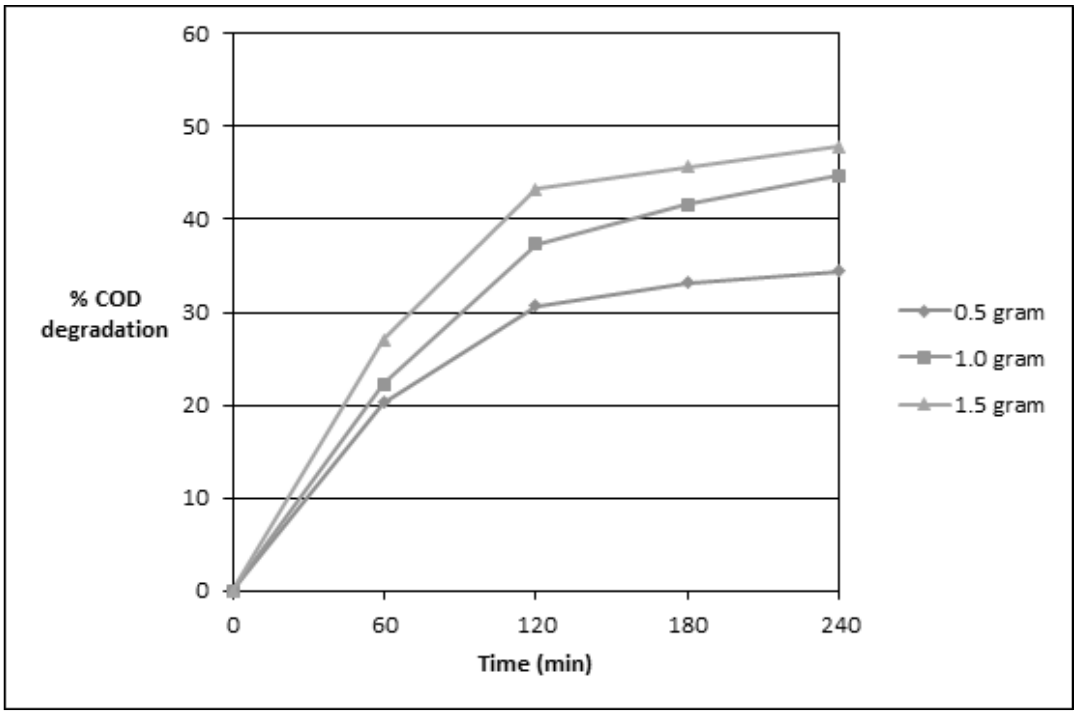

Fig. 2: Effect of Adsorbent mass on adsorption of MB on Peanut Hull (Conditions SC_o=100mg/L, V=100 mL, at Room Temp.)

approximately equal but equilibrium time for 1.5 g is 3 hours while that for 1 g, 4 hours.[43] Hence, high adsorbent dosage may reduce equilibrium time. But as adsorbent mass increases and dye concentration remains constant, more adsorbent surface remain unoccupied and dye uptake decreases.

Effect of pH

The effect of pH on adsorption of MB solution was studied by varying pH, keeping other conditions constant. Fig. 3 shows the plot of % COD reduction verses contact time. As shown, the % COD reduction increases with increase in pH in the range 2-7, after which pH does not have any influence on the adsorption process. The % COD reduction values for 4, 7 and 10 pH solution are 46.53%, 50.65% and 52.16% respectively. That means the adsorption and dye uptake increase as pH of solution increases up to 7 after which increase in pH does not show any significant effect. Several reasons may be attributed to dye sorption behaviour of the sorbent relative to solution pH. The surface of peanut hulls may contain a large number of active sites and the solute (dye ions) uptake can be related to the active sites and also to the chemistry of the solute in the solution.

At lower pH, the surface charge may get positively charged, thus making H^+ ions compete effectively with dye cations causing a decrease in the amount of dye adsorbed. At higher pH, the surface of peanut hull particles may get negatively charged, which attract the positively charged dye cations through electrostatic forces of attraction, hence dye adsorption increases and as pH increases continuously, the surface becomes saturated and dye uptake remains constant.[43]

Adsorption Isotherms

In order to establish the most appropriate correlation for

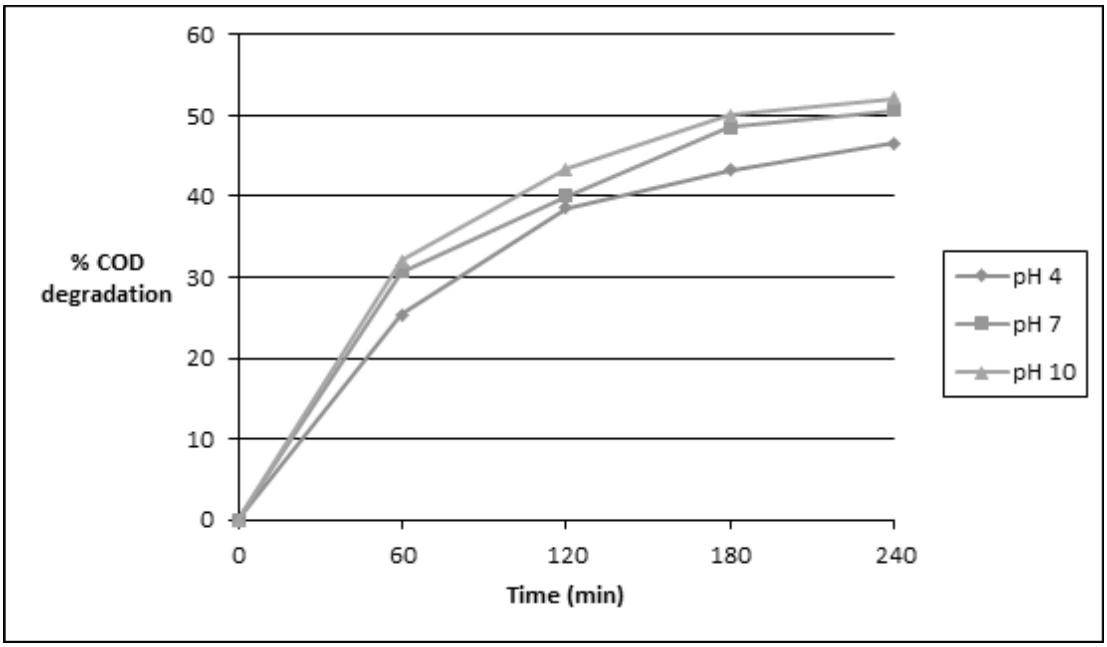

Fig. 3: Effect of solution pH on MB Adsorption on Peanut Hull (Condition: C_o=100 mg/L, W=1g/100 mL. at Room Temp.)

the equilibrium data in design of adsorption system, two isotherms models were tested Langmuir and Freundlich isotherms.

The Langmuir adsorption model is based on the assumptions that maximum adsorption corresponds to the saturated monolayer of solute molecules on adsorbent surface. The linear form of the Langmuir isotherms is given by Eq. (4). As shown in Fig. 4, the adsorption obeys the Langmuir isotherm and Langmuir constants q_{max} and b are determined from the slope and intercept respectively of the plot and are presented in Table 1. The R^2 value (0.9958) suggests that Langmuir isotherm provide a good fit for the adsorption data.[44]

Table 1. Langmuir Isotherm Constants and Correlations for MB adsorption on Peanut Hull

q_{max} (mg/g)	b (l/mg)	R^2
56.4971	$1.94x10^{-3}$	0.9958

The essential characteristics of Langmuir isotherms can be expressed in the terms of the dimensionless constant separation factor R_L describe by Eq. 10.

$$R_L = \frac{1}{1 + bC_0} \qquad (10)$$

where C_o (mg/L) is the highest initial concentration of adsorbent. The parameter R_L indicates the nature of the adsorption as shown below:

$R_L > 1$	Unfavourable adsorption
$0 < R_L < 1$	Favourable adsorption
$R_L = 0$	Irreversible adsorption
$R_L = 1$	Linear adsorption

The value of R_L in the present investigation was found to be 0.8375, showing that the adsorption of MB on peanut hull is favourable under the experimental conditions.

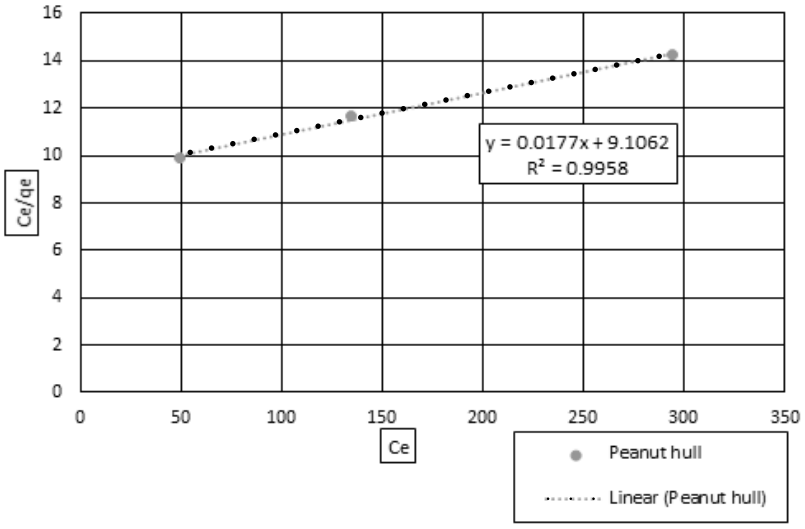

Fig. 4: Langmuir Isotherm for MB Adsorption on Peanut Hull

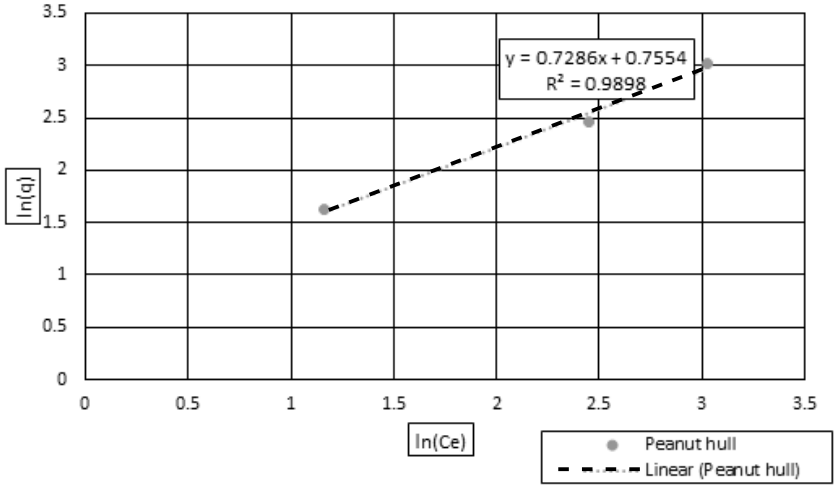

Fig. 5: Freundlich Isotherm MB Adsorption on Peanut Hull

The Freundlich isotherms is used for non-ideal sorption that involves the heterogeneous surface energy and is described by Eq. 5. The magnitude of the exponential 1/n gives an indication of the favourability of absorption. Value n > 1 represents favourable adsorption process. The linear form of the Freundlich isotherm is shown in Eq. 6.

The value of K_F and n can be calculated from the intercept and slope respectively of linear plot as shown in Fig. 5. Since the intercept of the linear plot is negative, Freundlich isotherm does not describe the adsorption of MB on peanut hull. It was observed that the equilibrium sorption data was best represented by Langmuir isotherm. The best fit isotherm expressions confirm the monolayer coverage process of MB on peanut hull.

Adsorption Kinetics

In order to investigate the adsorption process of MB on peanut hull, pseudo-first order, pseudo-second order and

intraparticle diffusion model were used. The plots of the linearized form of the pseudo-first order equation are shown in Fig. 6. The values of k_1, q_e and correlation coefficients are compared in Table 2. The results showed that the correlation coefficients obtained for the first order kinetic model is 0.9896. The theoretical q_e values found from this model did not give reasonable values, so pseudo-first order model could not describe the adsorption results of MB on peanut hull.

The linearized form of the pseudo-second order model is presented in Fig. 7. The values of correlation coefficient of the model were very high and the theoretical q_e values were much close to the experimental q_e values given in Table 2.

The constant k_2 is used to calculate the initial sorption rate, h (mg/g min), as $t \rightarrow 0$ as follows:

$$h = k_2 q_e^2 \quad (11)$$

The value of h in the present investigation was found to be 0.06073 mg/g min.

Table 2: Comparison of the pseudo-first order and pseudo-second order adsorption rate constants and calculated and experimental q_e values.

$q_{e\ exp}$ (mg/g)	Pseudo first order model		Pseudo second order model	
	K_1 (1/min)	q_e (mg/g)	K_2 (g/mg.min)	q_e (mg/g)
5.192	2.158	1.496×10^4	2.101×10^{-3}	6.845

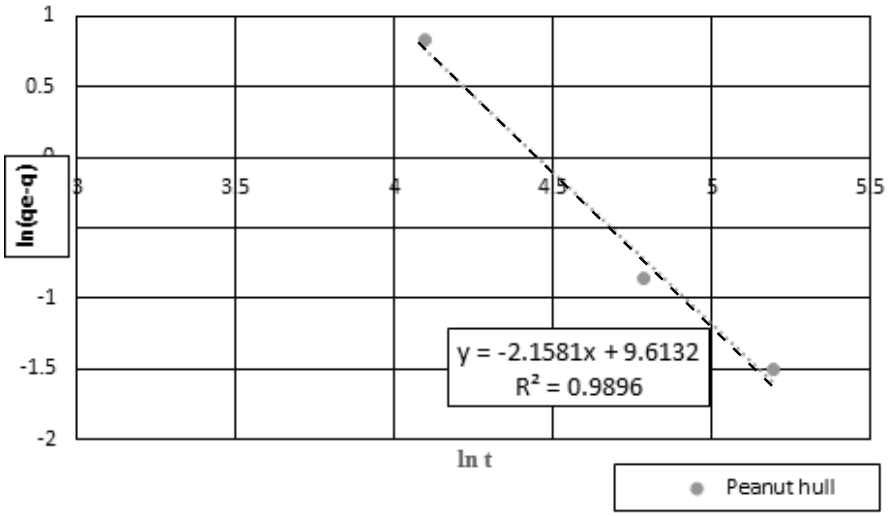

Fig. 6: Pseudo-First Order Kinetics for MB adsorption on Peanut Hull (C_0=100 mg/L, V= 100 mL, W=1g, at Room Temp.)

In the view of these results, it can be said that the pseudo-second order kinetic model as compared to the pseudo-first order model provides a better correlation for the adsorption of MB on peanut hull.

The adsorption of MB on peanut hull follows generally three consecutive steps of external diffusion, intraparticle diffusion and adsorption. One or more of these steps can control the adsorption kinetics altogether or individually. In the simplified model, it is assumed that the first sharp

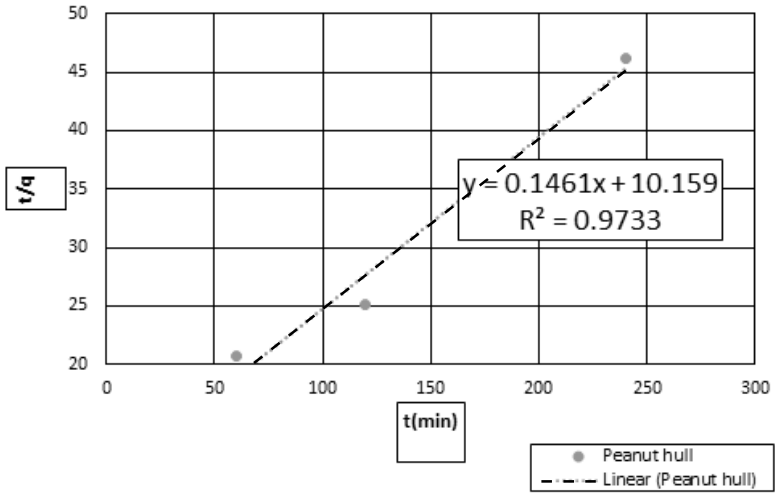

Fig. 7 Pseudo-Second Order Kinetics for Methylene Blue on Peanut Hull (C_0=100 mg/L, V= 100 mL, W = 1g, at room temp.)

linear stage is a rapid external diffusion and surface adsorption which is neglected, the second linear stage is a gradual adsorption stage where the intraparticle diffusion is rate limited, and the final stage is the equilibrium stage[14]. The intraparticle diffusion parameter, K_i for this region was determined from the slope of the plots of q versus $t^{1/2}$ at varying temperatures. As illustrated in Fig. 8 the curves reveal linear characteristics. However, the linear plots did not pass through the origin. This indicates that the intraparticle diffusion is not the only rate controlling step. Since, in a well-agitated batch system, the external diffusion resistance is much reduced, intraparticular diffusion along with the adsorption is more likely to be rate controlling step.

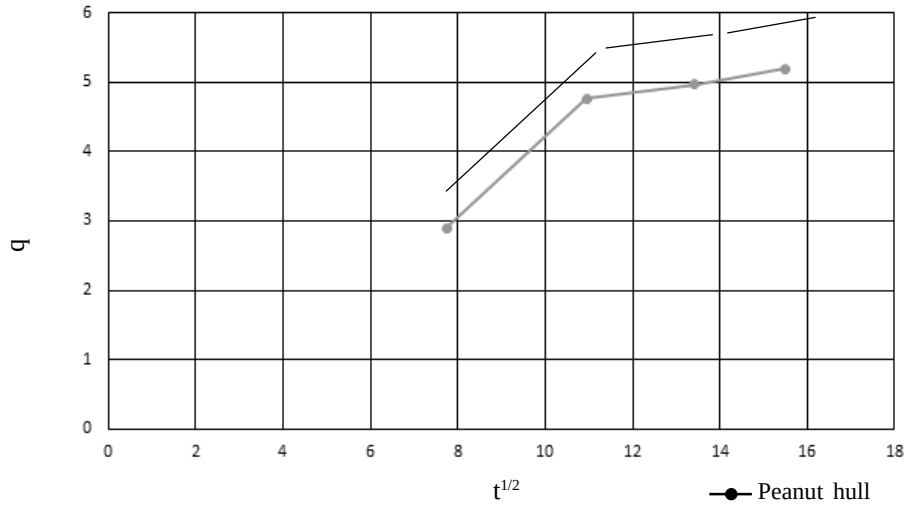

Fig. 8: Intraparticle Diffusion (C_0=100 mg/L, V= 100ml, W=1g, at Room Temp.)

Conclusions

The present study shows that peanut hull, an agricultural waste biomaterial can be used as an adsorbent for the removal of Methylene Blue from its aqueous solutions. The amount of dye adsorbed was found to vary with initial solution concentration, pH and adsorbent dose. The amount of dye uptake (mg/g) was found to increase with increase in solution concentration and pH, and found to decrease with increase in adsorbent dosage. The equilibrium data agreed well with Langmuir isotherm model with monolayer adsorption capacity of 56.497 mg/g at room temperature. The value of the separation factor, R_L, indicated that the dye/peanut hull system favours adsorption. The suitability of pseudo-first order kinetic and pseudo-second-order kinetic models for the adsorption of MB onto peanut hull was also discussed. The adsorption data were found to follow pseudo-second order kinetics. The dye uptake process was found to be controlled by external mass transfer in earlier stages and by intraparticle diffusion in later stages.

References

1. Bharathi, K.S. and Ramesh, S.T., 2013, *Applied Water Science*, **3(4)**, 773-790.
2. Tim Robinson, Geoff Mcmullan, Roger Marchant and Poonam Nigam, 2001, *Bioresource Technology*, **77(3)**, 247-255.
3. Mohamad Amran, Mohd Salleh, Dalia Khalid Mahmoud, Wan Azlina Wan Abdul Karim and Azni Idris, 2011, *Desalination*, **280(1–3)**, 1-13.
4. Bhatnagar, Amit and Sillanpaa Mika, 2010, *Chemical Engineering Journal*, **157(2-3)**, 277-296.
5. Kayode Adesina Adegoke and Olugbenga Solomon Bello, 2015, *Water Resources and Industry*, **12**, 8-24.
6. Seghier Abdelkarim, Hadjel Mohammed and Benderdouche Nouredine, 2017, *Trends in Green Chemistry*, **3(1:4)**.
7. Neetu Sharma, Tiwari, D.P. and Singh, S.K., 2012, *International Journal of Scientific and Engineering Research*, **3(2)**, 1-10.
8. Dinesh Mohan, Kunwar P. Singh, Gurdeep Singh and Kundan Kumar, 2002, *Eng. Chem. Res.*, **41(15)**, 3688-3695.
9. Mohd. Rafatullah, Othman Sulaiman, Rokiah Hashim and Anees Ahmad, 2010, *Journal of Hazardous Materials*, **177(1-3)**, 70-80.
10. Renmin Gong, Mei Li, Chao Yang, Yingzhi Sun and Jian Chen, 2005, *Journal of Hazardous Materials*, **B121**, 247-250.
11. Renmin Gong, Yi Ding , Mei Li , Chao Yang , Huijun Liu and Yingzhi Sun, 2005, *Dyes and Pigments*, **64**, 187-192.
12. Nevin Yalcin and Vahdettin Sevinc, 2000, *Carbon*, **38**, 1943-1945.
13. Namasivayam, C., 1998, *Bioresource Technology*, **64,** 77-79.
14. Dursun Ozer, Gulbeyi Dursun and Ahmet Ozer, 2007, *Journal of Hazardous Materials*, **144,** 171-179.
15. Namasivayam, C. and Kanchana, N., 1992, *Chemosphere*, **25(11)**, 1691-1705.
16. Pankaj Sharma, Ramnit Kaur, Chinnappan Baskar and Wook-Jin Chung, 2010, *Desalination*, **259**, 249-257.
17. Hameed, B.H., Krishni, R.R. and Sata, S.A., 2009, *Journal of Hazardous Materials*, **162(1)**, 305-311.
18. Dursun Özer Gülbeyi and Dursun Ahmet Özer, 2007, *Journal of Hazardous Materials*, **144(1-2)**, 171-179.
19. Vadivelan, V. and Vasanth Kumar, K., 2005, *Journal of Colloid And Interface Science*, **286(1)**, 90-100.
20. Gurusamy Annadurai Ruey-Shinjuang Duu-Jonglee, 2002, *Journal of Hazardous Materials*, **92(3)**, 263-274.

21. Nevin Yalçýn Vahdettin Sevinç, 2000, *Carbon*, **38(14)**, 1943-1945.

22. Namasivayam, C., Prabha, D. and Kumutha, M., 1998, *Bioresource Technology,* **64(1)**, 77-79.

23. Renmin Gong, Yingzhi Sun, Jian Chen, Huijun Liu and Chao Yang, 2005, *Dyes and Pigments*, **67(3)**, 175-181.

24. Nagarethinam Kannan and Mariappan Meenakshi Sundaram, 2001, *Dyes And Pigments*, **51(1)**, 25-40.

25. Runping Han, Yuanfeng Wang, Weihong Yu, Weihua Zoujie and Shihongminliu, 2007, *Journal of Hazardous Materials,* **141(3)**, 713-718.

26. Mokhtar Arami, Nargess Yousefi Limaee, Niyaz Mohammad Mahmoodi and Nooshin Salmantabrizi, *Journal of Colloid And Interface Science,* **288(2)**, 371-376.

27. Hosein Nadia, Mostafa Alizadeha, Morteza Ahmadabadia, Ahmad Reza Yarib and Sara Hashemid, 2012, *Arch. Hyg. Sci.,* **1(2)**, 41-47.

28. Doungkamon Phihusut and Monruedee Chantharat, 2007, *Environment and Natural Resources*, **15(2)**, 30-38.

29. Malik, D.S., Jain, C.K., Anuj K. Yadav, Richa Kothari and Vinayak V. Pathak, 2016, *International Research Journal of Engineering and Technology,* **3(7)**, 864-880

30. Robinson, T., Chandran, B. and Nigam, P., 2000, *Corncob and Barley Husk, Environment International,* **28(1-2)**, 29-33.

31. Million Mulugeta and Belisti Lelisa, 2014, *Modern Chemistry and Applications*, **14,** 6798.

32. Santhy, K. and Selvapathy, P., 2005, *Bioresource Technologies*, **97(11)**, 1329-36.

33. Malik, P.K., 2004, *Journal of Hazardous Materials*, **113(1-3),** 81-8.

34. Nasuha, N., Hameed, B.H. and Azam T. Mohd Din., 2009, *Journal of Hazardous Materials*, **175(1-3)**, 126-32.

35. Shalini Gautam and Saima H. Khan., 2016, *International Journal of Science, Environment and Technology*, **5(5)**, 3230-3236, 2277-663X.

36. Senthil Kumar, P., Abhinaya, R.V., Gayathri Lashmi, K., Arthi, V., Pavithra, R., Sathyaselvabala, V., Dinesh Kirupha, S. and Sivanesan, S., 2011, *Colloid Journal,* **73:651**, 1608-3067.

37. Bhatnagar, Amit, Minochaa, A.K. and Sillanpaa, Mika., 2010, *Biochemical Engineering Journal,* **48(2)**, 181-186.

38. Kayode Adesina, Adegoke and Olugbenga Solomon Bello, 2015, *Water Resources and Industry*, **12**, 8-24.

39. Ponnusamy Senthil Kumar, Subramaniam Ramalingam and Kannaiyan Sathishkumar, 2011, *Korean Journal of Chemical Engineering*, **28(1)**, 149-155.

40. Malik, P.K., 2003, *Dyes and Pigments*, **56(3)**, 239-249.

41. Chuah, T.G., Jumasiah, A., Azni, I., Katayon, S. and Thomas Choong, S.Y., 2005, *Desalination*, **175(3)**, 305-316.

42. M. Saban Tanyildizi, 2011, *Chemical Engineering Journal*, **168(3)**, 1234-1240.

43. Rohit R. Gurav, Atish P. Limbare, Nitesh B. Pardeshi and Manoj B. Mandake, 2019, *GP Globalize Research Journal of Chemistry*, **3(1)**, 72-79.

44. Advait Swamy, Ajay S. Nirmal, Omkar V. Sakpal and Manoj B. Mandake, 2019, *GP Globalize Research Journal of Chemistry*, **3(1)**, 80-87.

RNI No. MAHENG/2017/74063
ISSN No. (Print) 2581-5911
ISI Impact Factor 1.022 (2019-2020)

Analytical Method Development and Validation of Lurasidone by RP-HPLC

Pranav P. Kulkarni* and Rajendra B. Kakde
Department of Pharmaceutical Sciences, RTMNU, Nagpur, India
Email: pranavkulkarni95@yahoo.com; drkakde@yahoo.com

Abstract
The present study describes the development of a validated RP-HPLC method for the determination of Lurasidone. The separation was carried out at 40°C on a Princeton C18 (5 µg, 250×4.6 mm) column with Acetonitrile : Methanol (90:10 %v/v) as a mobile phase at a flow rate of 0.8 mL/min. The wavelength of detection was 210 nm. Retention time of nearly 3.5 minutes was obtained. Analytical validation parameters such as specificity and selectivity, linearity, accuracy and precision were evaluated. The calibration curve was linear in the range of 2–20 µg/mL with a correlation co-efficient of 0.999. Relative standard deviation values for all key parameters, was less than 2.0%. The method was validated according to ICH guidelines and the acceptance criteria for accuracy, precision, linearity, specificity and system suitability were met in all cases.

Keywords: *Lurasidone, RP-HPLC, Analysis, Acetonitrile (ACN), Validation.*

Introduction

Lurasidone (trade name Luramax) is an antipsychotic medication used to treat schizophrenia and bipolar disorders. Chemically it is 2{2-[4-(1,2-benzisothiazol-3-yl)piperazin-1-ylmethyl] cyclohexylmethyl}hexahydro-4,7-methano-isoindole-1,3-dione. The drug was approved for use in India by the Drug Controller General of India. Lurasidone is indicated for the treatment of schizophrenia and bipolar disorders by acting as antagonist of Dopamine D_2 and D_3 receptors. It is commercially available in tablet dosage form as Luramax in India. [1] Literature survey revealed that few analytical methods like UV spectrophotometric method have been used for estimation of Lurasidone in bulk and tablet dosage form, The Liquid Chromatography/Mass Spectrometry (LC/MS) method has been reported for the determination of Lurasidone in human plasma. The present work describes an analytical method and validation of Lurasidone using reverse phase HPLC. [2] The proposed method was found to be suitable for routine determination of the drug in pharmaceutical formulations.

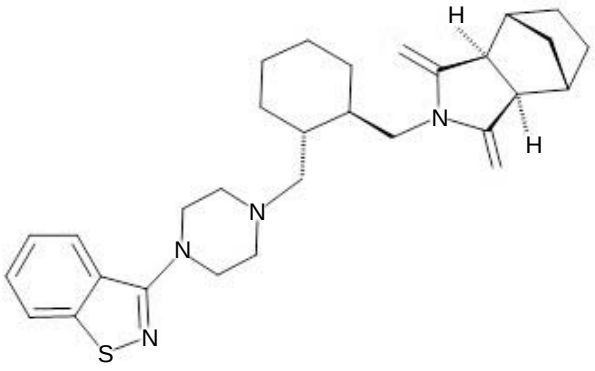

Fig.1: Chemical structure of Lurasidone

Materials and Methods

Chemicals

Standard bulk drug sample of Lurasidone was provided by Glenmark Pharmaceuticals Ltd., India. Pharmaceutical dosage form used in this study was **LURAMAX** tablets labeled to contained 40 mg (Sun Pharmaceuticals Mumbai, India). Acetonitrile (Merck), Methanol (Merck) and HPLC grade water were used. The solvents were further filtered through nylon membrane filter (0.22µ) and vacuum degassed. The 0.22 µ nylon filter paper were purchased from Pall India Pvt. Ltd, Mumbai (India). All the glassware used during experimentation were of Analytical grade-I.

Apparatus and chromatographic conditions

HPLC method development and validation was done on a Shimadzu (Japan) Liquid chromatography set equipped with (LC- 6AD pump), SPDM-20A prominence PDA detector, Rheodyne 7725µ injection with 20µL loop and LC-Solutions software. Stationary phase used was Symmetry→ C-18 5ìg Column (4.6 mm × 250 mm) and the mobile phase used was ACN: Methanol (90:10v/v). The mobile phase was filtered using 0.22µ nylon filter paper purchased from Pall India Pvt. Ltd, Mumbai, India. The mobile phase flow rate was 0.800mL min-1 and injection volume was 20µL.[3]

HPLC Method

Preparation of stock standard solution

Standard stock solution of Lurasidone (1000 µg/ mL) was prepared in Methanol.

Working Standard Solution

A volume of 100 µL Lurasidone stock standard solution was transferred into a volumetric flask of 10 mL capacity using micro-pipette and the volume was made up to the mark using diluent. The resulting solution was then sonicated for 15 min. and contained 10 µg/mL of Lurasidone (10 ppm).

Working Sample Solution

Twenty tablets were weighed and the average weight of tablet was determined. Ten tablets, equivalent to about 10 mg of Lurasidone were crushed, triturated and weighed accurately and transferred to a 10 mL volumetric flask. About 5 mL of methanol was added and sonicated for minimum 30 min. with intermittent shaking. Then the contents were brought back to ambient temperature and diluted to volume with water. The sample was filtered through 0.45 µm nylon syringe filter. 100 µL of this solution was pipetted out and made up to 10 mL using diluent to obtain concentration of 10 µg/mL of Lurasidone (10 ppm).

Validation

The developed method was validated according to ICH guidelines. The linearity was evaluated by linear regression analysis. The calibration graph was plotted for the HPLC method (2-20 µg/mL)[4,5].

Precision studies were done in terms of repeatability (intra-day precision) and intermediate (inter-day precision) and expressed as relative standard deviation (RSD) for a series of measurements. Intra-day precision was calculated from six replicate readings at 3 concentration levels within the linearity range. Inter - day precision was studied by comparing the results on three different days.

To study the accuracy of the method, recovery studies were carried out by addition of standard drug solution to preanalyzed sample at 3 different levels i.e. 80, 100 and 120%. The resultant solutions were then reanalyzed by the proposed method.

LOD and LOQ was calculated using single-to-noise (S/N) ratio method. LOD was taken as a concentration of analyte where S/N is 3 and LOQ was taken as a concentration of analyte where S/N is 10. Robustness was evaluated by studying the influence of small deliberate changes in the analytical parameters on

retention times and peak shapes. The method should be robust enough with respect to all critical parameters so as to allow routine laboratory use. Specificity of the method towards the drug was studied.

Results and Discussion

Development and Optimization of HPLC method

Chromatographic studies were performed on Princeton C18 analytical column. Initially, different mobile phases were tried in isocratic mode to get an adequate retention of Lurasidone. Mobile phases containing methanol, methanol: water, methanol: ammonium acetate, methanol: 0.01% formic acid etc. were tried, but retention time of Lurasidone was not satisfactory nor adequate resolution was obtained. Different columns were used like ODS (Octadecyl silane), C8 and C18 (Thermo-BDS Hypersil) but tailing, broadening and low retention time were observed. Then different ratios of acetonitrile: water (90:10, 80:20, 70:30, 60:40, 50:50 v/v) were tried and it was observed that the retention times of Lurasidone were between 1-15 min and also tailing was observed. However, acetonitrile: methanol (90:10 v/v) at flow rate of 0.8 mL/min. gave a retention time of 3.5540±0.10 min. with sharp peak, good peak symmetry and minimum tailing factor.[6]

Table 1: Optimized Chromatographic Conditions for Lurasidone on HPLC

Column	Princeton C18 (4.6 mm X 250mm, 5µg)
Mobile phase	ACN : Methanol (90:10 v/v)
Pump mode	Gradient
Flow rate	0.8 mL/min.
Injection volume	20 µL
Operating Wavelength	210 nm
Run time	20 min.
Temperature	40°C

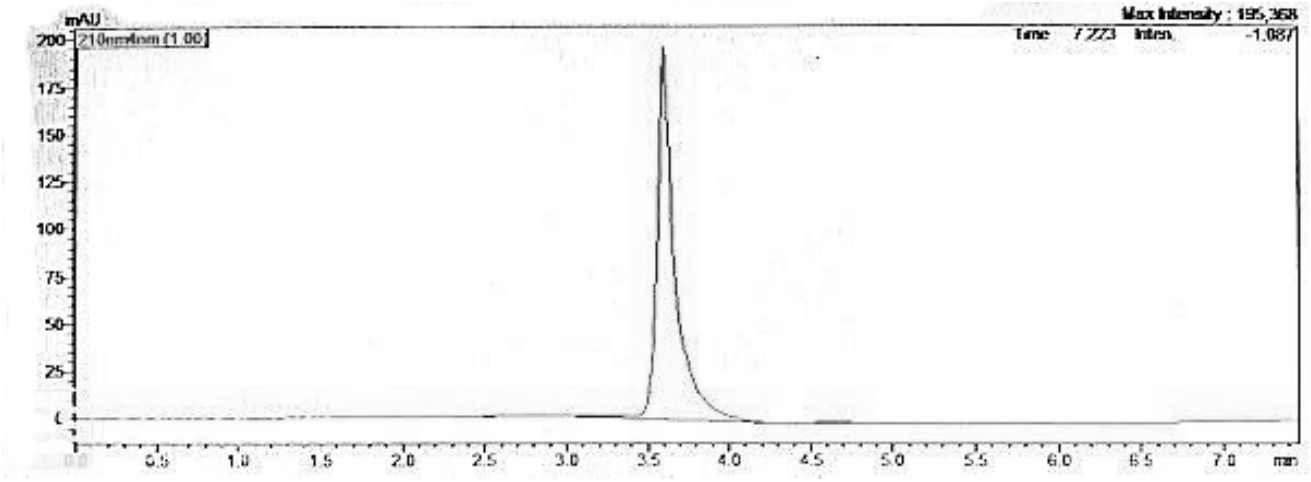

Fig 2: HPLC chromatogram of Lurasidone

Pre-validation Performance

Before starting the validation of method, it is necessary to check suitability of the system to carry out experiment as well as the robustness of developed method.

System Suitability

The chromatographic conditions were set as per the optimized parameters and mobile phase was allowed to equilibrate with stationary phase to get a steady baseline. Six replicate injections of working standard solution B were made separately and the chromatograms were recorded.[7] One of the standard chromatograms is depicted in Figure 2 and the results of system suitability parameters are given in Table 2.

Table 2: Study of System Suitability Parameters

Sr. No.	Retention time (min)	No. of Theoretical Plates	Capacity Factor	Peak Area
1	3.797	5270	0.667	186521
2	3.751	5274	0.66	179842
3	3.734	5280	0.64	183987
4	3.722	5334	0.652	182584
5	3.701	5245	0.659	182686
6	3.723	5203	0.651	182489
Mean	3.738	5267	0.654	183018
SD	0.033	43.112	0.009	2185
%RSD	0.888	0.818	1.424	1.193

Robustness Test

This test was done to investigate the performance when small, deliberate changes were made to the already established chromatographic conditions.[8] For the evaluation of the method robustness, one chromatographic parameter was changed while all the other parameters were kept constant. The studies were carried out for by changing the wavelength of detection and results are shown in Table 3.

Table 3: Results of Robustness Study

Luramax Tablets (Avg. Wt. 165.21mg for 40mg of Lurasidone)				
	Wavelength (210±2nm)		**Acetonitrile content in mobile phase [ACN : Methanol(90 : 10 v/v)]**	
	208nm	**212nm**	**88ml ACN**	**92ml ACN**
Mean*	99.81	100.78	15.37	100.08
±SD	0.82	0.81	0.58	0.45
%RSD	0.15	1.03	0.53	0.87

* Each value is the mean of three observations

Analytical Method Validation

Specificity

A working sample solution was used for specificity study

1) Normal (control) for 24 hr.
2) Addition of 1N HCl up to 10.0 mL mark for 24 hr.
3) Addition of 1N NaOH up to 10.0 mL mark for 24 hr.
4) At room temperature in dark after addition of 6% H_2O_2 up to 10.0 mL for 3 hr.
5) At 80°C (dry heat) for 4 hr.
6) In sunlight for 24 hr.

After the stipulated time of each stress condition, the volume was made up to 10 mL with diluent and one mL of this solution was diluted to 10 mL with diluent. One mL of the second dilute solution was again diluted to 10.0 mL mark with the diluent.[9] Then these samples are injected to get chromatograms and the results are shown in Table 4.

Table 4: Results of Specificity Study

	Acid	Base	Peroxide	Photo	Thermal	Neutral
Concentration	1N HCL	1N NaOH	6% H_2O_2	UV	80ºC (oven)	Water
Stress condition (R.T.)	24 hr	24 hr	3 hr	24 hr	4 hr	24 hr
Result	98.54%	97.36%	93.64%	98.56%	100.00%	100.00%

Linearity of Response

Aliquots of Lurasidone working standard solutions were transferred to a series of 10mL volumetric flask and diluted to volume with the diluents to yield solutions in the concentration of 2 to 20µg/mL. A 20 µL volume of each solution was injected in triplicate under previously mentioned optimized chromatographic conditions.[10] The peak area was measured electronically and plotted against their respective concentrations.

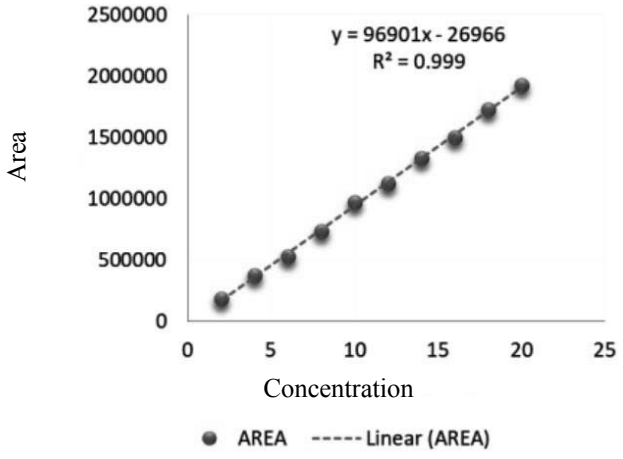

Fig. 3: Calibration curve shows Linearity of Lurasidone

Table 5: Results of Linearity Study

Parameters	Result
Concentration range	2.0-20 µg/mL
Equation for straight line	y = 96901 x - 26966
Slope	96901
Y-intercept	13421.08
Correlation coefficient	0.999

Linearity was confirmed by excellent correlation coefficient 0.999.

Accuracy

Accuracy of the proposed method was ascertained on the basis of recovery studies performed by standard addition method at three different levels 80, 100 and 120%). The recovery results were obtained in the range

of 93.89 - 95.46% indicated excellent accuracy for the developed method and are summarized in Table 6.

Table 6: Results of Accuracy Study

Luramax tablets (Avg. Wt. 165.21 mg for 40 mg of Lurasidone)						
Level	**Weight of Sample Taken**	**Amount of Standard Added**	**Area***		**Total Estimated Weight of Drug**	**% Recovery**
			Sample	**Standard**		
80%	165.21	8	1726313	788649	17.512	93.895
100%	165.28	10	1541112		19.541	95.412
120%	165.30	12	1410112		21.456	95.468
*Each value is mean of Three observations				**Overall**	**Mean**	94.925
					±SD	0.729
					%RSD	0.767

Precision

Table 7: Results of Precision Study

Sr. No.	**Obs.**	**% Drug estimation**		
		Interday*	**Intraday***	**Different Analysts***
1	I	98.89	98.91	98.87
2	II	98.64	98.98	98.86
3	III	98.03	98.93	98.88
4	IV	98.55	98.88	98.91
5	V	98.06	98.85	98.92
6	VI	98.53	98.92	98.85
* Each value is mean of Six observations	**Mean**	**98.45**	**98.91**	**98.88**
	±S.D.	**0.3102**	**0.041**	**0.025**
	%R.S.D.	**0.3151**	**0.0410**	**0.0257**

a. Repeatability

Precision of proposed method was ascertained by replicate analysis of homogeneous samples of formulation.

b. Intermediate Precision

The samples were analysed by proposed method on different days (intra-day & interday) and by different analysts. The results of study are given in Table 7.

Limit of Detection (LOD) and Limit of Quantitation (LOQ)

LOD and LOQ were determined by the method based on standard deviation of the response and the slope of calibration curve as per ICH guidelines (Table 8).

Table 8: Results of LOD and LOQ Studies

Sr. No.	**Parameters**	**Value**
1	LOD(µg/mL)	1.444
2	LOQ(µg/mL)	4.376

Conclusions

A simple, accurate, precise and economical method was developed for the analysis of Lurasidone. The developed method was validated according to ICH Q2R1 guidelines. The drug was confirmed by performing IR and LC-MS study.

Acknowledgement

The authors would like to thank the Head, Department of Pharmaceutical Sciences, RTMNU, Nagpur, India for giving an opportunity to carry out our dissertation work in the institute. We greatly acknowledge Glenmark Pharmaceuticals, Mumbai, India for providing the gift sample of Lurasidone.

References

1. https://en.wikipedia.org/wiki/Lurasidone

2. Pavia D.L., Lampman, G.M. and Kriz G.S., 2006, Introduction to Spectroscopy, 3rd ed., Harcourt College Publishers, p.353.

3. Snyder R.L., 1997, In practical HPLC Method Development, II edition, p.292.

4. ICH, Q1A (R2), 2003, Stability Testing of Drug Substances and Products, International Conference of Harmonization, IFPMA, Geneva.

5. ICH, Q2 (R1), 2005, Validation of Analytical Procedures: Text and Methodology, In Proceedings the International Conference on Harmonization, IFPMA, Geneva.

6. Kealey D. and Haines J.P., 2002**,** U.K., Analytical Chemistry, BIOS Scientific Publishers Limited, p.1-2.

7. Skoog D.A. and West D.M., 1980, In Principles of Instrumental Analysis. 2nd edition, Holt Saunders Golden Sunburst Series, p.667.

8. Jeffery G.H., Besset J., Men. Dham, J. and Denney, R.C., 1989, Vogel's Text Book of Quantitative Chemical Analysis, 5th ed. English Language Society/ Longman, p.216.

9. Beckett H. and Stenlake J.B., 1997**,** Practical Pharmaceutical Chemistry, 4th ed., Part II, CBS Publisher and Distributor, New Delhi, p.277.

10. Prathap B., Dey A., Rao G. S., Sundarrajan T. and Hussain S., *Journal of Pharmacy and Pharmaceutical Sciences*.

RNI No. MAHENG/2017/74063
ISSN No. (Print) 2581-5911
ISI Impact Factor 1.022 (2019-2020)

Studies on m-Nitrobenzaldehyde Derivative of 1, 2-Diphenylethane-1, 2-Diene Hydrazone Oxime

Madhuree K. Jagare[1*], Raj R. Badekar[2] R.S. Lokhande[1] and Vijay Ghodvinde[3]
[1]School of Basic Sciences Jaipur National University, Jaipur, India
[2]RIVA Industries, Ambernath MIDC, Thane, Maharashtra, India
[3]Department of Chemistry S.V. Junior College, Vasind,
Dist. Thane, Maharashtra, India
Email: badekarrr@gmail.com

Abstract
Reaction between hot ethanolic solution of α-benzilmonoximehydrazide (HBMOH) and m-nitrobenzaldehyde (m-NBA) yields Benzilmonoximehydrazide-m-nitrobenzaldehydes (HBMHMNB). Synthesized compound was characterized on the basis of various physico-chemical and spectral techniques such as UV-Visible, PMR and IR spectra.

Keywords: *α-benzilmonoximehydrazide (HBMOH), m-nitrobenzaldehyde, UV-Visible, PMR and IR spectra*

Introduction

Schiff bases[1] and their metal complexes are used in various biological systems as catalysts as well as in the manufacture of polymers and dyes.[2-6] α-Benzilmonoximehydrazone is one of the examples of Schiff base derived compounds and its various metals complexes have been studied recently[3-8]. In our previous work[9], we synthesized o-nitrobenzaldehyde derivative of 1, 2-diphenylethane-1-2-diene hydrazone oxime and prepared compound was characterized by different physico-chemical and spectral techniques. In this paper, we report the synthesis of m-nitrobenzaldehyde derivative of 1, 2-diphenlyethane-1-2-diene hydrazone oxime. The structure of the synthesized compound was elucidated by physico-chemical and spectral studies. The IUPAC name of the title compound is 2-[(3Nitrobenzylidene) hydrazinylidene]-1,2-diphenylethanimine (HBMHmNB).

Materials and Methods

All chemical used were of Analytical Reagent grade. Distilled water was obtained from a glass distillation unit. UV- visible spectra of the compound were recorded on JASCO V-650 spectrophotometer, methanol was used as a solvent to record the UV- spectrum of the compound. FTIRspectra (KBr discs) were recorded on Perkin-Elmer spectrum 100 model. PMR spectra were recorded on Brucker AV300 NMR spectrometer using TMS as internal standard.

Preparation of Compound

α-Benzilmonoxime was prepared by reported method[4-8]. The title compound was prepared by taking a hot ethanolic solution of 2.39 gm. (0.01 mol) of

α-benzilmonoximehydrazide (HBMOH) in a 100mL three necked round bottom flask, stirred for 15min and then ethanolic solution of m-nitrobenzaldehyde (mNBA) (1.863gm) (0.0125mol) was added. The final mixture was then refluxed for 7 hours, cooled and filtered. The resulting precipitate was washed with hot distilled water.

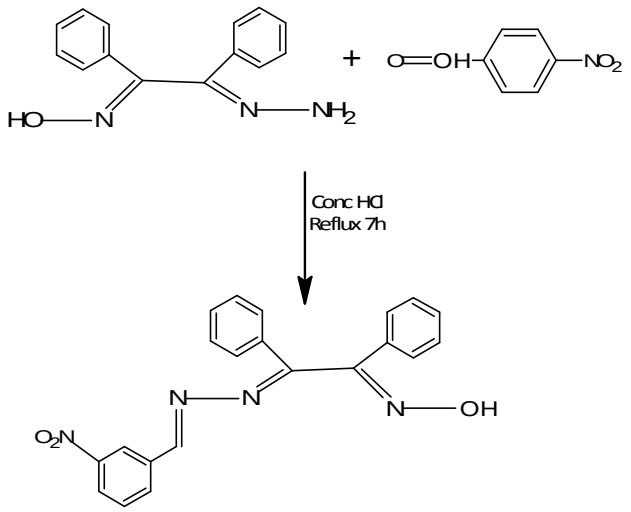

Results and Discussion

Characterization of the prepared compound was done by using analytical data obtained from UV-visible, FTIR, ^{1}HNMR spectroscopy and elemental analysis. The molecular weight of the compound (372gmol^{-1}) was determined by Rast method[9]; m.p. 210-215^{0}C. It is a yellowish brown crystalline solid, soluble in common organic solvents such as methanol, chloroform, acetone, DMF, DMSO, etc. Structural studies of the synthesized compounds was done by FTIR, PMR, UV-visible spectroscopy and elemental analysis. The prepared compound was monobasic in nature.

Elemental Analysis

%	C	H	N	O
Theoretical	67.7	4.3	15.0	12.8
Observed	66.0	4.4	14.9	12.7

Spectral Measurements

A) *UV- Visible spectrum (In Methanol solvent)*

The electronic spectrum of HBMHmNB in methanol for the UV region shows two high intensity bands at 298nm and 247nm respectively. These bands are due to π→π* transitions for azomethine and oximino group respectively in the synthesized compound.

Table 1: UV-Visible spectra of HBMHmNB

λ nm	Abs.	ε	Transition	Assignment
298	1.077	14379	π→π*	Azomethine group > C=N-O
247	0.310	4138	π→π*	Oximinio group > C=N-N

B) *FT(IR) Spectrum*

In FTIR spectrum of HBMHmNB compound should show the absence of band between 3300 – 3350cm^{-1} due to the –NH_2 vibration reported[8] at 3387cm^{-1} in α-Benzilmonoximehydrazide, indicating a successful replacement of the amino group by the hydrazoyl group during Schiff base formation. The spectrum of HBMHmNB shows peak at 3314cm^{-1} which is assigned to the hydroxyl group of the oxime. The bands at 1588cm^{-1} and 1531cm^{-1} are due to (C=N-N) azomethine and (C=N-O) oximono group respectively.

Table 2: FT(IR) spectra of HBMHmNB in cm^{-1}

Bands	Assignments
3314	-OH (Oximino)
2902	-Ar (C=C)
2794	-Ar (C-H)
1588	>C=NN (Azomethine)
1531	>C=NO (Oximino)
1393/1334	-NO2 (Two bands)

C) *PMR- Spectrum*

^{1}H NMR spectra of the synthesized compound was recorded in d_6 DMSO solvent and important bands are summarized in **Table 3**. The pmr spectrum of HBMHmNB reveals a broad singlet at δ 9.003 due to –OH of oximino group. A multiplet was observed around δ 7.449-8.67 due to phenyl rings in the compound. Another singlet observed at δ 2.51 was assigned to –CH = group of the title compound.

Table 3: PMR data of HBMHmNB in ppm

δ (PPM)	Assignments
9.003	-OH (oximino proton)
7.449-8.670	Phenyl rings
2.507	-CH=(methane group)

Conclusions

The synthesized compound is insoluble in water but it is soluble in dilute alkali and common organic solvents. Its structure was elucidated by spectral studies such as UV-visible, PMR and FTIR spectra.

Acknowledgment

The authors are thankful to Dr. Santosh Kulkarni, Agrawal College, Kalyan, Dist. Thane, Maharashtra, India for providing instrumentation facilities and moral support.

References

1. Karthikeyan S., Prasad M. J., Poojary D. and Bhat B. S., 2006, *Bioorg. Med. Chem.,* **14**, 7482.

2. Cacic M., Molnar M., Sarkanj B., Has-Schon E. and Rajkovic V., 2010, Molecules, **15**, 6795-680.

3. Badekar R.R., 2012, M.Sc. Thesis, University of Mumbai.

4. Badekar, R.R., Kulkarni, S.W., Lokhande, R.S. and Thawkar, B.S., 2016, *International Journal of Applied Research*, **2(9)**, 175-179.

5. Badekar R.R., Kulkarni S.W., Lokhande R.S. and Patil R.M., 2016, *International Journal of Advanced Research*, **4(7),** 1093-1097.

6. Badekar R.R., Kulkarni S.W., Lokhande R.S. and Patil R.M., 2016, *International Journal of Advanced Research*, **2(9)**, 796-800.

7. Singh V., Badekar R. and Mane R., 2018, *International Journal of Advance and Innovative Research*, 5(3).

8. Kamble P.S., Badekar, R.R. and Singh, V.H., 2018, *International Journal of Research and Analytical Reviews*, **5I(3I)**, 2348-1269.

9. Jagare, M., Badekar, R., Kulkarni, S. and Lokhande, R., 2019, *International Journal of Advance and Innovative Research*, **6(2),** (XVII), 97-99.

10. Vogel A.I., 1964, "A Textbook of Quantitative Inorganic Analytical"; Longmans Green and Co. Ltd., 3rd Ed., London.

11. Vogel A.I., 1964, "A Textbook of Quantitative Inorganic Analytical"; Longmans Green and Co. Ltd., 3rd Ed., London.

12. Bhargava, P.P. and Tyagi, M., 1986, *Ind. J. Chem*., **25A,** 193.

13. Chakrabarti, A. and Sahoo, B., 1981, *Ind. J. Chem*., **20A,** 431.

14. Ugarkar, B.G., Cottam, H.B., McKernan, P.A., Robins, R.K. and Revankar, G.R., 1984, *J. Med. Chem.*, **27,** 1026-1030.

15. Hussen, A.I., 2006, *J. Coord. Chem*., **59,** 157.

16. Karthikeyan, S., Prasad, M.J., Poojary, D. and Bhat, B.S., 2006, *Bioorg Med. Chem*., **14**, 7482.

17. Cacic, M., Molnar, M., Sarkani, B., Hutschon, E. and Rajkovic, V., 2000, *Molecules*, **13**, 6793-680.

18. Dave, S. and Bansal, 2013, *Internationl Journal as Pharmaceutical Research*, **5C1**, 6-7.

19. Jeffery, G.H. and J. Bassett., 1996, Vogel's Textbook of Quantititive Chemical Analyses; 5th edition, Longman Publication.

20. Datta, R.L. and Syamal, A., 1982, Elements of Magnetochemistry, S. Chand and Company Ltd., Ramnagar, New Delhi.

21. Belavale, P., Badekar, R., Kulkarni, S. and Lokhande, R., 2019, *International Journal of Advance and Innovative Research*, **6(2) (IX)**.

RNI No. MAHENG/2017/74063
ISSN No. (Print) 2581-5911
ISI Impact Factor 1.022 (2019-2020)

Analysis of Heavy Metal Content (Zn, Cu, Pb, Cr, Cd) in Sediment and *Corbicula* sp. Samples : A Case Study in Cau River, North Region, Vietnam

Bui Thi Thu[1*], Nguyen Thi Hong Hanh[1], Trinh Kim Yen[1], Pham Phuong Thao[1], Le Dac Truong[1], Pham Hong Tinh[1], and Dao Van Bay[2]
[1]Faculty of Environment, Hanoi University of Natural Resources and Environment, 41A, Phu Dien, Bac Tu Liem, Hanoi, Vietnam
[2]Faculty of Chemistry, Hanoi National University of Education, 136 Xuan Thuy, Cau Giay, Hanoi, Vietnam
[*]**Email: buithu84@gmail.com**

Abstract
This paper presents some results of heavy metal content (Zn, Cu, Pb, Cr, Cd) analysis in sediment and mussel samples (Corbicula sp.) *collected from 28 points in Cau River, Bac Kan to Hai Duong section, North Region, Vietnam. The study showed that heavy metal content in sediment ranged from 17.333 - 66.601 mgCu/kg dry sediment; 21.208 - 196.470 mgPb/kg dry sediment; 40.876 - 365.777 mgZn/kg dry sediment and 29.357 - 120.046 mgCr/kg dry sediment. The result show that most of the high heavy metal content (Cu, Pb and Zn) were in the lower reach of the river where there are many industrial zones. Most of the points having heavy metal content in Cau River sediments were in the range of TEC-PEC compared with the US-EPA standard of US. The analysis of the dried mussel sample* (Corbicula sp.) *showed that the metal content decreased in the sequence Zn > Cu > Pb > Cr > Cd. The average concentration of Zn, Cu, Pb, Cr and Cd were 52.932 mg/kg, 19.343 mg/kg, 18.496 mg/kg, 7.549 mg/kg and 4.536 mg/kg, respectively. In addition, the analysis revealed that the Cr content of 10 out of 28 observed sites exceeded the permitted limit of Hong Kong standard. This study of determining the relationship between the heavy metal content in* (Corbicula sp.) *and sediments of Cau river shows that metals such as Cu, Pb, Zn and Cd have a positive and close correlation ($r > 0.5$; $p < 0.05$) while Cr indicates a low and not close correlation ($r < 0.5$; $p > 0.05$). The results of this study show that initially,* (Corbicula sp.) *could be used as an indicator organism to monitor heavy metal pollution in river sediments.*

Keywords: *Content, heavy metal, river mussel* (Corbicula sp.)*, sediment, Cau River, Vietnam*

Introduction

In recent years, the development of industrial zones in developing countries including Vietnam has released a significant amount of waste water and caused heavy water pollution in large rivers. Heavy metal pollution poses a serious threat to people's daily life and has negative impact on social activities. The accumulation of heavy metal affects not only the life of aquatic organisms but also other animals and humans through the food chain[1]. Research studies have shown that heavy metals such as As, Hg, Cd and Pb are difficult to decompose and able

to cause immediate poison or long-term effects on human and living thing health[2]. The World Health Organization (WHO)[3] identified these metals as 4 out of 10 pollutants affecting public health[4]. Heavy metals are usually highly toxic and remain for a long period in the environment[5]. Heavy metal pollution is a serious threat to the environment[6]. In monitoring heavy metal pollution, physicochemical analysis methods are commonly used[7]. However, these method are costly. In order to fully evaluate the level of heavy metal pollution, the determination of their concentrations should be carried out not only in water but also in samples of sentiment and benthic species.

For analysis of benthic species samples, Nguyen Van Khanh et al.[1,8] suggested that bivalve animal is a species with good resistance to pollution and high accumulation of pollutants from water and sediment. Therefore, they are used as indicators for poisonous metal pollution such as As, Hg, Cd, Pb, etc. This method has proved to be able to detect very small metal content in contrast to the other analytical methods. Percy[9] and Jonna[10] have used this tool for monitoring heavy metal pollution in estuary and seaside areas. Fang et al.[11], Ming Li[12] and Xiaoling Ma et al, [13] have shown applications of benthic species analysis in heavy metal research. Analysis of the sediment samples was studied by Hakanson[14] and Ming Li et al.,[12] In this work, we present some analysis results of heavy metals content (Cu, Pb, Zn, Cd and Cr) from 28 sediment and mussel (*Corbicula* sp.) samples in Cau river basin, Vietnam where many industrial zones such as mining, metallurgy, electroplating, plastic production, detergent production, etc. are located.

Materials and Methods

Heavy metals, Cu, Pb, Zn, Cd and Cr in mussel species (*Corbicula* sp) and sediments found in Cau river which flows through, 5 provinces, Bac Kan, Thai Nguyen, Bac Giang, Bac Ninh and Hai Duong, Northern Vietnam[15] were analysed. Samples of sediment and benthic samples were taken by specialized sampling equipment (bucket type: Ekman, U.S., the sampling area was 20cm x 20cm x 20cm).

Samples were collected at 28 sites on the Cau River of length 288.5 km (Figure 2). At one location, one sample of sediment and one sample of mussel (*Corbicula* sp.) were taken in the middle of the river or near the river bank depending on the area related to the industrial zone, residential zone and river bottom. The size of each sample was 20cm x 20cm x 20cm.

At each sampling site, three large samples were taken. Each large sample consisted of three small samples taken 1 m apart and mixed into a representative sample). Large samples were 2-3 m apart around the first sampling site. A representative composite sample was taken after mixing these three large samples. The sample was kept in a zip bag refrigerated and transported to the laboratory[16].
The sampling site is shown in Figure 1.

Research Methods

The US - EPA 3050B standard in 1996[17] was referenced to carry out the process of sediment sample treatment for identifying heavy metals. The content of heavy metals in sediment and mussel samples was analysed on AAS - Themo Fisher M6 Environment Laboratory, Hanoi University of Natural Resources and Environment (Vilas 955) as follows:
Sediment samples were allowed to dry naturally in ambient air at room temperature (28-30^{o}C), and then ground and filtered through a 0.2 nm sieve. 1.0 g of dry sediment was weighed and treated with HNO_3 solution and 30% H_2O_2 solution at 95°C.

The amount of heavy metals in sediment was calculated by the formula:

$$X = \frac{C_m \times V_s}{m} \times K$$

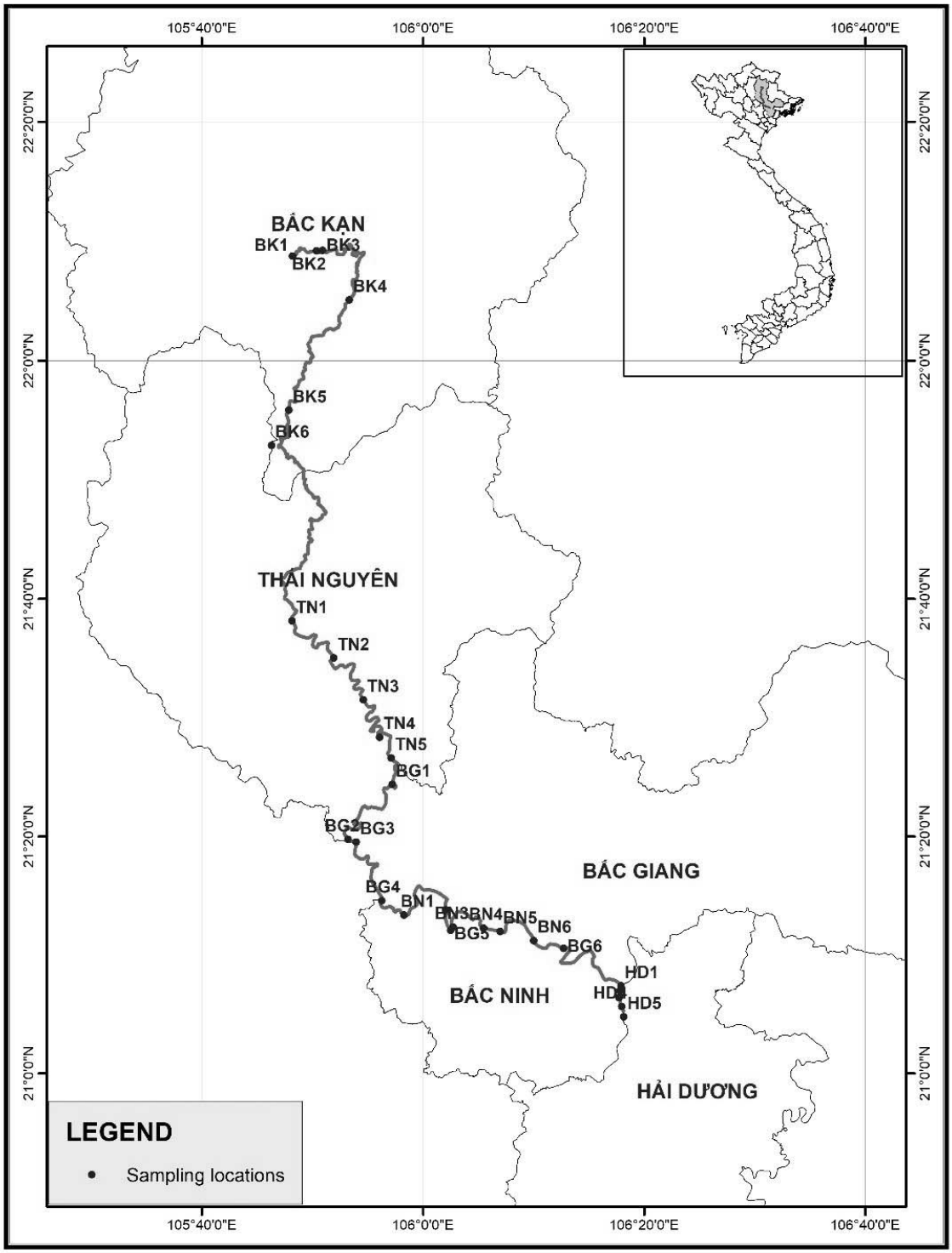

Fig. 1: Sampling sites of sediment and mussel (*Corbicula sp.*) samples in Cau river, Vietnam

where X is heavy metal content (mg/kg of dry sediment) C_m is the measured heavy metal concentration (mg/L), $V_{volumetric}$ is sample volume ($V_{volumetric}$ = 50mL), m is sample weight (g) and K is dry coefficient of sediment.

The mussel sample was stored in a cooler at 4°C. The mussel sample was removed from the intestines, weighed and freeze dried in the laboratory of Hanoi University of Technology, Vietnam. The lyophilized benthic animal samples were completely decomposed with strong acids (HNO_3 and concentrated $HClO_4$) and H_2O_2 at 90°C.

The metal content in the animal sample was calculated using the following formula:

$$X_k = \frac{C_m \times V_m}{m} \text{ (mg/kg dry organisms)}$$

which X_k is content of heavy metals (mg/kg), C_m is metal concentration measured on AAS (mg/L), $V_{volumetric}$ is volume of solution (mL), m is benthos sample weight (g).

The metal content calculated by fresh weight is given by the formula $X_t = \frac{X_k}{K}$ (mg/kg of fresh organism)

The research data was processed statistically, comparing the average values by variance analysis[18], and checking the smallest significant difference (LSD) with $\alpha = 0.05$. The content of heavy metals in sediments was compared with Vietnamese standards QCVN 43:2017/BTNMT - National Technical Regulation on sediment quality[19] and Canadian National Standards (Sediment Quality Guideline - sediment quality guidelines) (2002)[20] and US EPA standards (1997)[21].

The heavy metal content in benthic was compared with QCVN 08-2:2011/BYT[22] for Hg, Cd, and Pb and Hong Kong heavy metal pollution regulation on public health and urban services for Cr (Metallic Contamination Regulations of Public Health and Municipal Services Ordiance, Laws of Hong Kong)[23].

Results and Discussion

Heavy metals contents (Cu, Pb, Zn, Cd and Cr) in Cau river sediment

The results of determining the concentrations of Cu, Pb, Zn, Cd, and Cr metals in Cau river sediments are presented in Table 1.

Table 1. Heavy metal content in Cau river sediment

Monitoring site	Heavy metal content (m ± sd) * (mg/kg dry sediment)				
	Cu	Pb	Zn	Cd	Cr
Bac Kan (n = 6)	31.062 ± 8.131	44.061 ± 12.396	47.951 ± 6.162	0.803 ± 0.315	57.530 ± 10.093
Thai Nguyen (n = 5)	53.828 ± 10.987	70.029 ± 9.863	316.930 ± 28.835	3.833 ± 1. 362	106.080 ± 13.301
Bac Giang (n = 6)	31.654 ± 5.396	124.750 ± 15.120	135.440 ± 22.183	0.878 ± 0.297	105.480 ± 10.276
Bac Ninh (n = 6)	40.304 ± 13.015	150.480 ± 31.485	124.050 ± 15.514	0.670 ± 0.225	101.150 ± 11.103
Hai Duong (n = 5)	39.793 ± 9.114	54.167 ± 28.421	91.329 ± 21.229	1.345 ± 0. 477	85.277 ± 3.586
QCVN 43:2017/BTNMT	**197**	**91.3**	**315**	**3.5**	**90**
PEC	**77.7**	**396**	**1532**	**11.7**	**159**
TEC	**28**	**34.2**	**159**	**0.592**	**56**
ISQG	**35.7**	**35**	**123**	**0.6**	**37.3**

(*) m: Average value; SD is the standard deviation

Comparisons with global studies are presented in Table 2. The differences in the total content of Cu, Pb, Zn, Cd and Cr metals in the sediments show that the total content and the distribution of metals depend on the conditions of the study area.

The Cau river basin, which runs through Thai Nguyen and Bac Ninh provinces, has specific characteristics in terms of geographical and socio-economic conditions, especially many mineral mines and industrial zones, Cu, Pb and Zn in Cau river sediment in Thai Nguyen tend to be higher than in other research areas (Table 2).

Table 2. Metal content in sediments of some rivers in the world

Reference	Monitoring site	Total metal content (mg / kg dry sediment)				
		Cu	**Pb**	**Zn**	**Cd**	**Cr**
Akcay et al.[24]	Buyak Menderes and Gediz Rivers, Turkey	108 - 152	35-140	85 - 185	-	-
Yan wu Zhou et al.[25]	Yifeng River Mouth, Southeast China	10 - 40	40 -100	60 -140	-	-
Shou Zhao et al. [26]	Duong Tu River mouth, China	10.64 – 34.91	17.37 – 109.4	57.89 -107.7	-	-
Xiaoling Ma et al. [13]	Golden River, China	14.1-30.3	15.5 -24.6	39.9 -74.6	0.1 – 0.3	-
Bui Thi Thu et al.	Cau River, Northern Vietnam	33.96 – 66.601	9.863 – 196. 470	6.161 – 365.780	0.225 – 4.955	3.586 – 120.050

Heavy metal contents (Cu, Pb, Zn, Cd and Cr) in Cau river benthos

The results of determining heavy metal content (Cu, Pb, Zn, Cd and Cr) in the mussel (*Corbicula* sp.) of Cau River are presented in Table 3.

Table 3. Cu, Pb, Zn, Cd and Cr content in mussel samples (*Corbicula* sp.) in Cau river sediment

Monitoring site	**Metal content in mussels (mg/kg fresh organisms)**				
	Cu	**Pb**	**Zn**	**Cd**	**Cr**
Thai Nguyen	2.822 ± 0.927	2.198 ± 0.714	9.620 ± 1.306	1.056 ± 0.211	0.029 ± 0.209
Bac Giang	2.452 ± 0.352	2.556 ± 0.667	6.393 ± 1.290	0.364 ± 0.142	1.032 ± 0.150
Bac Ninh	2.250 ± 0.635	2.431 ± 0.597	6.226 ± 1.826	0.526 ± 0.153	1.012 ± 0.170
Hai Duong	2.590 ± 0.549	2.196 ± 0.200	4.562 ± 0.511	0.419 ± 0.050	0.835 ± 0.108
QCVN 8-2:2011/BYT	**-**	**1.5**		**2.0**	
Hong Kong Standard	**-**	**-**	**-**	**-**	**1.0**

Results of determining the relationship between heavy metal content in (*Corbicula* sp.) and sediment of Cau river

The relationship between Cu, Pb, Zn, Cd and Cr content in mussels (*Corbicula* sp.) and sediments of Cau river are shown in Figure 2 and Table 4 as follows:

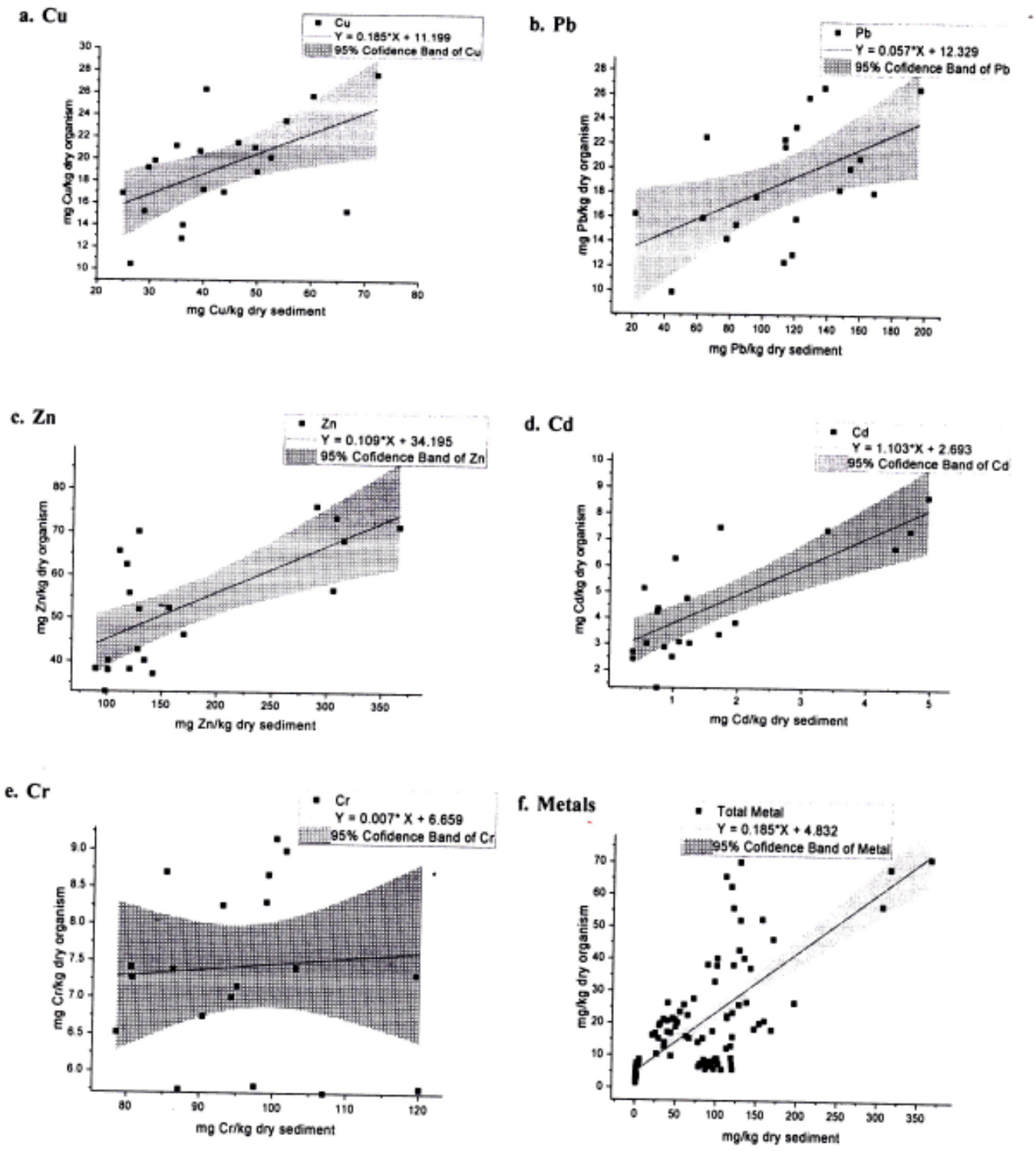

Fig. 2 : The relation between heavy metal content (Cu, Pb, Zn, Cd and Cr) in mussel tissue and sediment in Cau river

Figure 2 shows the relation between the heavy metal content (Cu, Pb, Zn, Cd and Cr) in mussel (*Corbicula* sp.) and sediment in Cau river. It can be seen that for most of them (except Cr) at positions where the heavy metal content in sediment is high, the concentration in mussel tissue (*Corbicula* sp.) is also high and vice versa (Table 4). This means that heavy metal accumulation in mussel tissue depends on its content in sediment. This relationship is expressed through a linear regression function Y = aX + b, where Y is the value of heavy metal content contained in mussel tissue tissue (*Corbicula* sp.) and X is the value of heavy metal content contained in the river bottom sediment.

Table 4. Relationship between metal concentrations in mussels and sediments in Cau river

Metal	Relationship [In mussels (X)] and in sediments (Y)]	Correlation coefficients (*) Pearson (r)	(p-value)
Cu	Y = 0.185*X + 11.199	0.54	0.01
Pb	Y = 0.057*X + 12.329	0.52	0.02
Zn	Y = 0.109*X + 34.195	0.68	0.0009
Cd	Y = 1.103*X + 2.693	0.77	0.00006
Cr	Y = 0.007*X + 6.659	0.08	0.72
Heavy metal	Y = 0.185*X + 4.832	0.73	0.00

(*) Significant correlation p <0.05 (95% confidence level)

Table 4 illustrates that the relation between heavy metal content (Cu, Pb, Zn, Cd) and their total content in mussel tissue and sediment in Cau river are increasing functions with r>0.5 with a high correlation between them (Figure 2 a-d and f). As for Cr metal, the value of r = 0.084 < 0.5 indicates a low, loose relation between them (Figure 2e).

In comparison with the study of Vo Van Minh[27], the accumulation of Cd and Pb is seen in mussels (*Corbicula* sp.) in the Cu De estuary in Da Nang city, in the central region of Vietnam. The content of Cd and Pb in mussel species in Cau river tends to increase. The results show that the correlation between the metals (Pb, Cd) in mussel and sediment of Cau river closely correlated with the results of the study to determine the relationship in sediments of some rivers in Middle Region, Vietnam. Thus, it is possible to use mussels (*Corbicula* sp.) as an indicator organism to monitor heavy metal pollution in Cau river sediments.

Conclusions

The results of heavy metal content analysis (Zn, Cu, Pb, Cr, Cd) in sediment and mussel (*Corbicula* sp.) from 28 samples collected along Cau river (Bac Kan to Hai Duong section, North Vietnam) have been analysed.

Acknowledgement

This work was financially supported by the Ministry of Natural Resources and Environment of Vietnam under project TNMT.2017.04.13.

References

1. Nguyen Van Khanh, Vo Van Minh, Pham Thi Hong Ha and Duong Cong Vinh, 2010, *Journal of Marine Science and Technology*, **10**, 1.

2. Le Huy Ba, 2002, Environmental toxicology, Ho Chi Minh City National University Publishing House.

3. WHO, 2011, 10 chemicals of major public health concern.

4. Jarup, L., 2003, *Br. Med. Bull*. **68**, 67-182.

5. Maanan, M., 2007, *Morroco. Envir. Toxic*., **10 (1002)**, 525-531.

6. Ming Li, Wei Yang, Tao Sun and Yuwan Jin, 2016, *Marine Pollution Bulletin* **103**, 227-239.

7. Phillips, D.J.H., 1977, *Environment Pollut.,* **13**, 281-313.

8. Nguyen Van Khanh, Tran Duy Vinh and Le Ha Yen Nhi, 2014, *Journal of Marine Science and Technology*, **14(4)**.

9. Percy, P., 2004, Heavy metal concentrations in the Pacific oyster; Crassostre gigas. Aukland Univeristy of Technology, p.116.

10. Jonna P. and Sokolowski, A., 2011, Mussel as a tool in metal pollution biomonitoring - current status and perspective. In: Mussel - Anatomy, Habitat and Environmental Impact, Nova Science Publishers, Inc, p.379-394.

11. Fang, Z.Q., Cheung, R.Y.H. and Wong, M.H., 2001, *Journal of Environmental Sciences*, **13(2)**, 210-217.

12. Ming Li,Wei Yang, Tao Sun and Yuwan Jin, 2016, *Marine Pollution Bulletin* **103**, 227-239.

13. Xiaoling Ma, Hang Zuo, Mengjing Tian, Liyang Zhang, Jia Meng, Xuening Zhou, Na Min, Xinyuan Chang and Ying Liu, 2016, *Chemosphere,* **144**, 264-272.

14. Hakanson, L., 1980, *Water Res.* **14**, 975-1001.

15. Cau river environmental protection committee, 2017, Report on the implementation of project for protection and sustainable development of ecological environment, landscape of Cau river basin in 2016, implementation plan proposal for 2017.

16. ISO 5667-15, 1999, Water quality - Sampling - Part 15: Guidance on preservation and handling of sludge and sediment samples.

17. US EPA, 1996, EPA 3050B Acid digestion of sediments, sludges and soils.

18. Mai Van Nam., 2006, Economic Statistics Principles textbook, Culture and Information Publishing House.

19. Ministry of Natural Resources and Environment, 2017, QCVN 43:2017/BTNMT - National Technical Regulation on sediment quality.

20. Canadian Council of Ministers of the Environment, 2002, Canadian sediment quality guidelines for the protection of aquatic life, Summary tables, Updated. In:Canadian Environmental Quality Guidelines 1999, Canadian Council of Ministers of the Environment, Winnipeg.

21. US EPA, 1997, Toxicological Benchmarks for SCdeening Contaminants of Potential concern for Effects on Sediment - Associated Biota, Report of the Sediment Cditeria Subcommittee, Science Advusory Board, ES/ER/TM-95/R4, U.S environmental Protection Agency, Washington, DC.

22. Ministry of Health, 2011, QCVN 08-2:2011/BYT - National technical regulation on heavy metal pollution in food.

23. Laws of Hong Kong, Part V (Food and Drugs) of the Public Health and Municipal, Maximum permitted concentration of certain metals present in specified foods. https://www.cfs.gov.hk/english/food_leg/food_leg_mc.html

24. Akcay H., Oguz A. and Karapire, C., 2003, *Water Research*, **37**, 813-822.

25. Yan-wu Zhou, Bo Zhao, Yi-sheng Peng and Gui-zhu Chen., 2010, *Marine Pollution Bulletin*, **60(8)**, 1319-1324.

26. Shou Zhao, Chenghong Feng, Yiru Yang, Junfeng Niu and Zhenyao Shen, 2012, *Journal of Hazardous Materials*, **241-242**, 164-172.

27. Vo Van Minh, Nguyen Van Khanh, Kieu Thi Kinh and Vu Thi Phuong Anh., 2014, *Journal of Biology*, **36(3)**, 378-384.

RNI No. MAHENG/2017/74063
ISSN No. (Print) 2581-5911
ISI Impact Factor 1.022 (2019-2020)

Synthesis and Spectral Characterization of Zn(II) and Cd(II) Complexes of α-Benzilmonoximethiocarbohydrazide-p-dimethylaminobenzaldehyde

Priya Belavale [1], Raj Badekar[2*] Ganga Gore[3] and Rama Lokhande[1].
[1]School of Basic Sciences, Jaipur National University, Jaipur, India.
[2]Riva Industries, Ambernath MIDC, Dist. Thane, Maharashtra, India,
[3]Dapoli Urban Bank College, Dapoli, Dist. Ratnagiri, Maharashtra, India
Email: badekarrr@gmail.com

Abstract
Novel complexes of Zn(II) and Cd(II) metal ions with the title ligand were synthesized and characterized. Zn(II) and Cd(II) metal complexes of p-dimethylaminobenzaldehyde derivative of Benzilmonoximethiocarbohydrazide were prepared with ML_2 composition (where M=Metal and L=Ligand). The synthesized metal complexes were characterized by elemental analysis, molar conductivity measurements, IR, electronic spectra and magnetic susceptibility. The physico-chemical and spectral analysis data suggests that both complexes are non-electrolyte in nature and they have tetrahedral geometry.

Keywords: *Benzilmonoxime, Thiocarbohydrazide, p-dimethylaminobenzaldehyde, Zn(II), Cd(II), Tetrahedral geometry, spectral analysis.*

Introduction

Metal complexes of Schiff bases play an important role in agriculture, pharmaceutical industry and chemical sector. Schiff base and their transition metal complexes continue to be interest due to their antibacterial[2-3] antioxidant[4], antimalarial[5], antiviral[6], anticancer[7-8], antifungal[9-10], antinflamnatry[11-15] applications. Schiff bases derived from benzilmonoxime and its derivatives have been reported by many researchers[11-12]. Benzilmonoxi-mehydrazone[13-16] and benzilmonoximethiocarbohydrazide and its various metal complexes have also been reported earlier. The present study deals with the preparation of Schiff base of substituted dimethylamino-benzaldehyde and benzilmonoximethiocarbohydrazide and its Zn(II) and Cd(II) metal complexes. The solid complexes have been synthesized and studied by elemental analyses and various spectroscopic techniques.

Materials and Method

The elemental analyses were carried out by standard methods[17]. All chemicals and solvents used were Analytical grade. The molar conductance measurement of these complexes in nitrobenzene was obtained using an Eg-660 conductivitimeter. FTIR spectra were recorded on FTIR-1615 of Perkin-Elmer Spectrometer using KBr pellets. The effective magnetic moments were calculated

after diamagnetic correction for ligand component using Pascal's constant[21]. The UV-visible spectrum was recorded on Shimadzu UV-190 spectrophotometer and magnetic susceptibility measurements were carried out by by Gouy's balance.

Synthesis of Ligand

The title ligand was prepared by reported method[18].

Preparation of metal complexes of HBMTDAB liagnd

Zn (BMTDAB)

Zn (II) metal complexes of HBMTDAB were prepared by dissolving 4.450 g of HBMTDAB in minimum quantity of ethanol and adding 1.473g of zinc Sulphate. The final mixture was neutralized with 0.1N sodium hydroxide. On cooling, the precipitate formed was filtered using hot water and dried at 110°C.

Cd(BMTDAB)

The Cd(II) metal complex of HBMTDAB were prepared by dissolving 4.450g of HBMTDAB in minimum quantity of ethanol and adding required amount of $CdCl_2$. The mixture was neutralized using 0.1N Sodium hydroxide. The precipitate obtained was washed with hot water and dried at 110°C.

Results and Discussion

Table 1: Analytical and physical data for HBMTDAB and its divalent metal complexes

Compound	Color	Yield	DP in °C	% yield expected (observed)						Conductance in Ω^{-1}
				M	C	H	N	O	S	
HBMTDAB	Yellow	86.94	204	-	64.84 (64.01)	5.44 (5.29)	18.90 (18.78)	3.60 (3.30)	7.21 (7.01)	-
Zn(BMTDAB)	Red	86.30	281	6.87 (6.66)	60.47 (60.00)	4.83 (4.79)	17.64 (17.73)	3.36 (3.20)	6.72 (6.68)	0.36
Cd(BMTDAB)	Red	85.60	296	11.25 (11.03)	57.63 (57.09)	4.60 (4..44)	16.81 (16.13)	3.20 (3.1)	6.4 (6.38)	0.35

Magnetic moment

The Zn(II) and Cd(II) complexes are diamagnetic and tetrahedral in nature[21]

Electronic Absorption Spectra

The electronic spectral absorption of the complexes of Zn(II) and Cd(II) are shown in **Table 2**. The band observed at 265nm in the Zn(II) complex is assigned to a charge transfer transition and confirms that Zn(II) complex is diamagnetic.

The electronic absorption spectra of Cd(II) complex in methanol solution shows absorption bands at 417 nm and 262 nm with high molar extinction coefficient (Table 2) and can be assigned as ligand to metal charge transfer transition.

Table 2. Electronic spectral data for divalent metal complex of HBMTDAB in MeOH

Sr. No.	Compound	Band position in nm	Intensity €	Assignment
1	Cd(BMTDAB)	417 262	5723.04 6859.23	Charge Transfer M-L
2	Zn(BMTDAB)	265	5467.20	Charge Transfer M-L

Infrared Spectra

FTIR spectral data for divalent metal complexes of HBMTDAB is shown in Table 3. In the title ligand, medium absorption band observed at 3385 cm^{-1} is due to oximino proton but in its metal complexes, this band is absent, suggesting that the coordination of the metal ion to ligand is through the oximino proton and this proton is deprotonated during complex formation.

The broad and medium band observed at 1508cm^{-1} is assigned to stretching vibration of >C=N-N (Azomethine group) and band observed at 1504cm^{-1} is assigned to > C=N-O (oximino group) in the title ligand. Both bands are shifted to higher frequencies in its metal complexes (Table 3), indicating coordination of metal ion to oximino and azomethine nitrogen atom. n(C-S-H) band of the title ligand reported at 2329cm^{-1}, which was also shifted to higher side 2360-2362 cm^{-1} suggests that the thiophene group also participates in the complex formation.

Table 3. FT(IR) spectral data for divalent metal complexes of HBMTDAB

Compound	-OH $\bar{\upsilon}$ cm^{-1}	Ar(c-c) $\bar{\upsilon}$ cm^{-1}	-CH = $\bar{\upsilon}$ cm^{-1}	C-S-H $\bar{\upsilon}$ cm^{-1}	N-M $\bar{\upsilon}$ cm^{-1}	>C=N-N $\bar{\upsilon}$ cm^{-1}	>C=N-O $\bar{\upsilon}$ cm^{-1}	Phenyl Ring $\bar{\upsilon}$ cm^{-1}	M-N, M→N $\bar{\upsilon}$ cm^{-1}
HBMDAB	3385	3155	2926	2359	1606	1508	1504	722	
$Zn(BMTDAB)_2$		3241	2910	2362	1593	1550	1516	742	589,518
$Cd(BMTDAB)_2$		3181	2916	2360	1601	1550	1519	743	591,533

Conclusions

Zn(II) and Cd(II) complex have high decomposition points, suggesting high thermal stability and they are non-electrolyte in nature The spectral and magnetic data obtained suggest that Zn(II) and Cd(II) complexes are tetrahedral in nature. On the basis of physical and spectral data, the structure assigned to Zn(II) and Cd(II) complexes is shown in Figure 1.

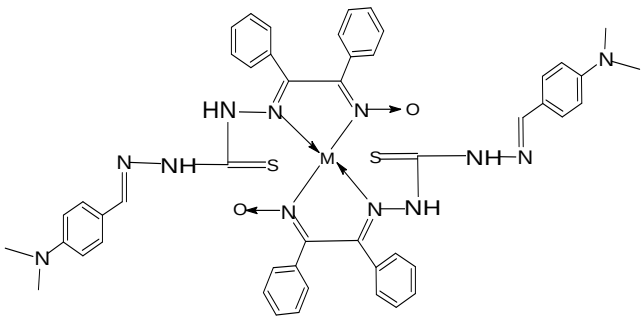

where M = Zn(II) and Cd(II)

Fig. 1: Tetrahedral geometry of Zn(II) and Cd(II) metal complexes

References

1. Mayers, D.L., 2009, Antimicrobial Drug Resistance C; Springer Dordrecht Heidelberg, London, p.681-1347.

2. Guschin, A., 2015, *BMC Infect. Dis*., **15**, 1-7.

3. Cacic, M., Molnar, M., Sarkani, B., Hutschon, E. and Rajkovic, V., 2007, *Molecules*, **13**, 6793-680.

4. Dave, S. and Bansal, S., 2003, *Internationl Journal of Pharmaceutical Research*, **51**, 6-7.

5. Thangudurai, T. and Ihm, S., 2003, *J. Ind. Eng. Chem.,* **9**, 563.

6. Mladenova, R., Ignatova, M., Manolova, N., Petrova, T. and Rashkov, I., 2002, *Eur- Polym. J.,* **38**, 989.

7. Walsh. O.M., Meejan, M.J., Prendergast, R.M. and Makib, T.A., 1996, *Eur. J. Med. Chem.,* **31**, 989.

8. Singh, K., Barwa, M.S. and Tyagi, P., 2006, *Eur. J. Med. Chem.,* **41**, 1,

9. Pannerselvam, P., Nair, R.R., Vijayalakshmi, G., Subramanion, E.H. and Sridhar, S.K., 2005, *Eur. J. Med. Chem.,* **40**, 225.

10. Bawa, S. and Kumar, S., 2009, *Indian Journal of Chemistry,* **48B**, 142.

11. Lavecchia, G., Berteina-Robin, S. and Guillaumet, G., 2005, *Tetrahedron Lett;* **46,** 5851-5855.

12. Cottam, H.B., Petrie, C.R., McKernan, P.A., Goebel, R.J., Dalley, N.K., Davidson, R.B., Robins, R.K. and Revankar, G.R., *J. Med. Chem*., 1984, **27**, 1119-1227.

13. Griengl, H. and Günzl, F., 1984, *J. Heterocycl. Chem.,* **21**, 505-508.

14. Petrie, I, C.R., Cottam, H.B., McKernan, P.A., Robins, R.K. and Revankar, G.R., 1985, *J. Med. Chem.,* **28**, 1010-1016.

15. Ugarkar, B.G., Cottam, H.B., McKernan, P.A., Robins, R.K. and Revankar, G.R., 1984, *J. Med. Chem.,* **27**, 1026-1030.

16. Hussen, A.I., 2006, *J. Coord. Chem*., **59**, 157.

17. Karthikeyan, S., Prasad, M.J., Poojary, D. and Bhat, B.S., 2006, *Bioorg Med. Chem*., **14**, 7482.

18. Belavale, P., Badekar, R., Kulkarni, S. and Lokhande, R., 2019, *International Journal of Advance and Innovative Research*, **6(2) (IX)**.

19. Dave, S. and Bansal., 2013, *Internationl Journal of Pharmaceutical Research,* **5C1**, 6-7.

20. Jeffery, G.H. and Bassett, J., 1996, Vogel's Textbook of Quantititive Chemical Analyses; 5th edition, Longman Publication.

21. Datta, R.L. and Syamal, A., 1982, Elements of Magnetochemistry, S. Chand and Company Ltd. Ramnagar, New Delhi.

22. Geary, W.J., 1971, *Coord. Chem. Rev., 7*, 81.

23. Low, W., 1960, Paramanetic Resonance in Solids, Acad Press, N.Y. p.76.

24. Lever, ABP., 1968, Inorganic Electronic Spestroscopy, Elserier, Amsterdam, p.168.

25. Drago, R.S., 1965, Physical Methods in Inorg. Chem., EWP, New Delhi, p.135-181.

26. Koing, E., 1971, Structure and Bonding, **9**, R175.

27. Wulfsberg, G., 2000, "Inorganic Chemistry", University Science Books, p.890.

RNI No. MAHENG/2017/74063
ISSN No. (Print) 2581-5911
ISI Impact Factor 1.022 (2019-2020)

Let Us Have a Sip of Green Tea — A Mini Review from a Chemist's Point of View

Amrit Krishna Mitra
Department of Chemistry, Government General Degree College,
Singur, Hooghly, West Bengal 712 409, India
Email: amritsepistles@gmail.com

Abstract
Tea is one of the most extensively consumed beverages across the world. Tea is composed of caffeine, minerals, polyphenols, trace amounts of vitamins, amino acids and carbohydrates. Tea is available in various forms. Depending on the fermentation process, the composition of the tea varies. However, Green tea is more enriched in antioxidants compared to other forms of tea. The phytochemicals present in green tea have the ability to stimulate the central nervous system along with the prevention of chronic diseases such as heart disease, various types of cancer and neurodegenerative diseases. It has always been a challenge to find authentic molecular mechanisms for the mode of action of their in vivo effectiveness. This mini review discusses the historical background, different forms of tea and the chemistry within it along with a special mention of Green Tea with respect to its usefulness, anti-oxidant properties and different side effects.

Keywords: *Green tea, Camellia sinensis, Antioxidant, EGCG, Polyphenols, Caffeine*

Tea and those times

"I say let the world go to hell, but I should always have my tea."

.....Fyodor Dostoyevsky, Notes from Underground

As some Chinese legends go, tea was a serendipitous finding made by Chinese Emperor Shen Nong when leaves of the *Camellia Sinensis* plant floated into an open pot of boiling water. In 59 B.C., Wang Bao penned the first known book giving details on how to buy and make tea. It was in 22 C.E., that tea was considered to be possessing abilities to enhance the functioning of the brain. This was brought to light by eminent physician and surgeon Hua Tuo[1]. Another Buddhist legend talks about Bodhidharma, an Indian priest from the 6th century who was responsible for bringing Buddhism to China, had cut off his eyelids in sheer anger when he failed to remain awake during meditation. The spot at which his eyelids fell sprouted a plant that was later recognised to be tea. This legend indicates that the stimulating qualities of tea were also recognised by monks during meditation. Tea gained popularity among the masses when farmers began to develop ways to cultivate tea as an alternative method to harvesting of leaves from wild trees. The Tang Dynasty comprised the pioneers of producing powered tea. Caravans carried tea on the Silk Road thus opening opportunities to trade with India, Turkey and

Russia. Apart from Wang Bao, Lu Yu also wrote a book on the methods of cultivation and preparation of tea in 780 C.E.[1,2].

Basic forms of Tea

The beneficial effects of using various types of tea leaves have often caught the fancy of the common man, thereby making it an oft discussed subject. It was much before the development of pharmaceutical industry that people used herbal products for curing various conditions. Interestingly, after water, tea stands as the most widely consumed beverage worldwide. Though it is grown in only about 30 countries, its demand spans across the globe. The varieties of tea with respect to the level of oxidation are three in number. They are black (fermented), oolong (partially fermented) and green (unfermented)[3]. Several factors determine the origin and chemical composition of green tea. The most decisive ones are climatic conditions, properties of soil, genetic strain, plucking season, processing and storage. For example, with respect to the factor of plucking season, the best quality green tea leaves are plucked during the first flush or the season of best produce in late April and early May[4-6]. There is a gradual abatement in the quality of the leaves in later harvests. At the time of processing, absolute care is taken to ensure that only the buds and the first two leaves are plucked by hand or by a machine designed for plucking. The technique of preparing green tea revolves around the idea of excluding the oxidation of green leaf polyphenols. However, when black tea is produced, it is oxidation that becomes imperative so that most of polyphenols are oxidized. However, oolong tea is a partially oxidized product. It is surprising to note that less than 2% of 2.5 million metric tons of the annual produce of dried tea. The share of green tea in this produce stands at 20%[3-5].

The flavour of Chemistry in Tea

Polyphenols, amino acids, methylxanthines and many volatile organic compounds are chiefly responsible for the production of flavour, taste and aroma of tea. The interesting feature is that the fresh tea leaves do not contain most of these aromatic compounds. It is during the steps of processing like leaf withering, fermentation and drying that the aroma is made to develop from other substances. Polyphenols and flavonoids amount to almost 39% of the dry weight of fresh tea leaves[7]. These are important metabolites produced by the plant to defend itself from predators. A common claim is that tea contains more caffeine than coffee. However, this information is based on percentage weight since tea generally requires greater dilution in comparison to coffee[8]. It must also not be forgotten that tea is often diluted much more than coffee. The percentage of caffeine actually extracted into the final drink depends to a large extent on the variety of tea used and the brewing methodology[9].

Since ancient times, tea has been considered to possess medicinal properties. It was early in the 19th century that western chemists started synthesising the compounds of tea after having confirmed their chemical constituents. Vitamin E, Vitamin C, fluoride and potassium are some of the nutritional components of tea. Xanthine derivatives such as caffeine, theophylline, theobromine and the glutamide derivative, theanine are the fundamental constituents of tea[10]. Such compounds are extremely precious because they act as powerful stimulants alongside enhancing memory and strengthening the immune system. Catechins, the phenolic constituents of tea, account for its astringency[11]. Catechins come from a group of compounds that are closely related to tannins owing to the presence of phenolic hydroxyl groups. The phenolic hydroxyl groups on the gallic acid moiety cause tannins to display acidic characteristics. Tannins can be considered to be good antioxidants and on reacting with metals, they produce chelates[12]. Catechins or hydroxylated flavanols and their gallic acid esters make up tannins in tea. It is estimated that approximately 50% of the substance in tea that dissolves in hot water constitutes these compounds. Phenolic oxidative coupling

reactions of these catechins produce red catechin dimers such as thearubigins or proanthocyanidins (structure of these compounds are not properly known till date) during the process of fermentation[13]. The dark colour of the oolong and black tea is created by the presence of these compounds that also have antibiotic and immuno-modulatory effects. However, catechin dimers do not make up the major chunk of the components of green tea[14]. Figure 1 shows the chemical structures of the most important constituents and their building blocks. It is believed that catechins have a wide array of beneficial health effects such as anti-inflammatory, neuroprotective, antiviral, antiulcer, antibacterial and antiparasitic effects. Out of many such catechins, the most widely studied catechin in relation to health affairs is epigallocatechin 3-gallate (EGCG). EGCG constitutes more than half of the total flavonoid content in green tea and is an extremely effective antioxidant[10, 15]. Some findings suggest that it might have beneficial effects in the treatment of some types of cancer, neurodegeneration, periapical lesions, chronic fatigue syndrome, endometriosis, spinal muscular atrophy, Sjögren's syndrome and regulating the HIV viral load amongst others.

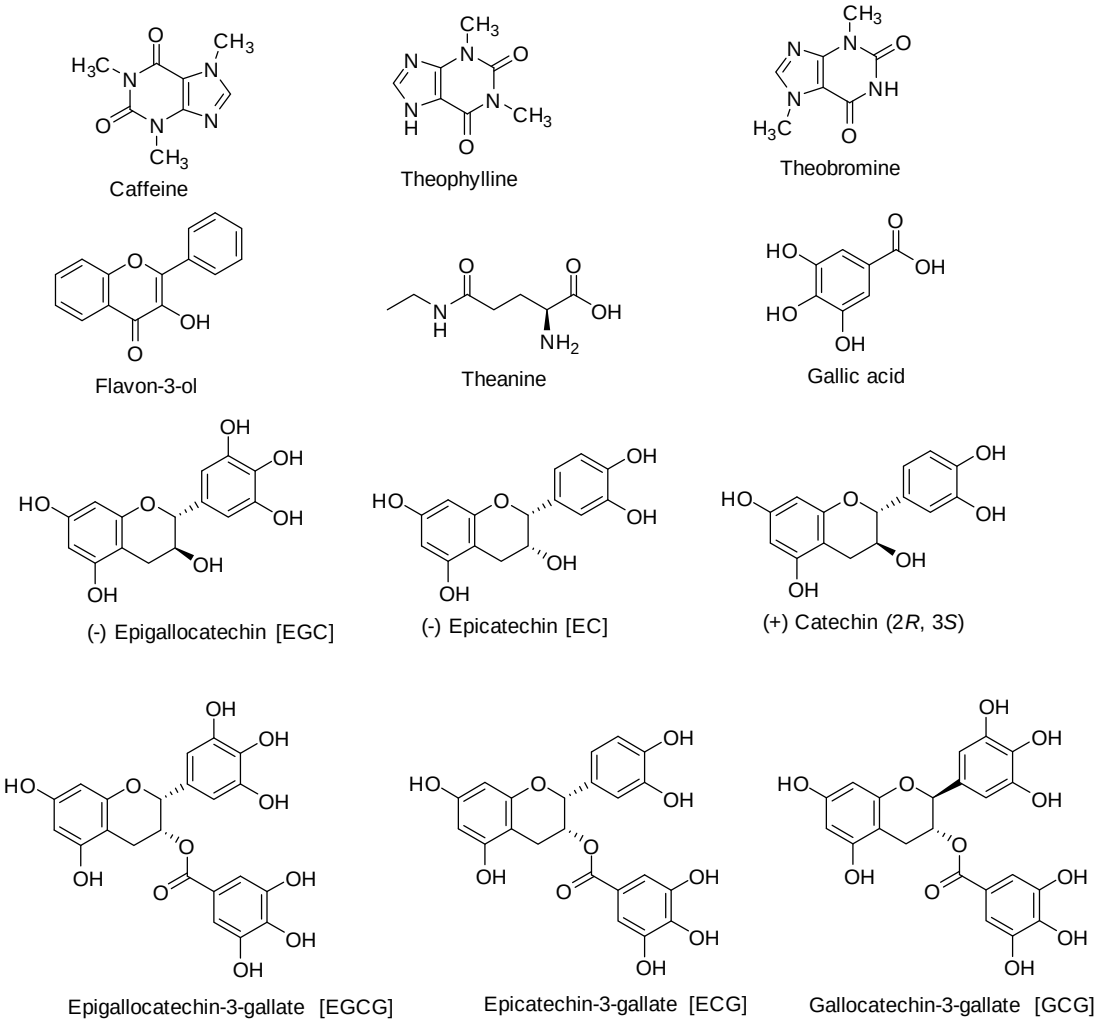

Fig. 1: Some of the representative compounds in tea

All varieties of tea are obtained from the dried leaves of the *Camellia sinensis* plant. The type of tea is determined by the level of oxidation of the leaves. Green tea is one of the less processed types of tea and it contains the most antioxidants and beneficial polyphenols since it is obtained from unoxidized leaves[16]. Caffeine, the component of tea that is responsible for giving the beverage its invigorating quality, is present at an average level of 3% along with miniscule amounts of the other common methylxanthines, theobromine and theophylline[10, 13, 16]. The amino acid theanine (5-N-ethylglutamine) is also unique to tea (discussed in the later part of the manuscript). Aluminum and manganese is accumulated by tea. During black tea manufacture, active polyphenol oxidase present in green tea catalyzes the aerobic oxidation of the catechins when the leaf cell structure is disrupted. Condensation reactions on quinones produced by the enzymatic oxidations yield a series of compounds, including bisflavanols, theaflavins, epitheaflavic acids and thearubigens which impart the characteristic taste and colour properties of black tea (structures are given in Fig. 2)[17]. Caffeine reacts with these compounds to form several complexes[18]. Tannic acid is absent in tea. Amongst the extractable matter in black tea, thearubigens form the largest percentage. The complex also includes proanthocyanidins in a small fraction. Their generation may require the usage of peroxidase. The formation of many of the hundreds of volatile compounds found in the black tea aroma fraction is initiated by the catechin quinones. Apart for a few enzymatically catalyzed changes, green tea is closely similar in composition to the fresh leaf. The drying stage witnesses the formation of new volatile substances. The composition of oolong tea is somewhere intermediate between that of green and black teas[19].

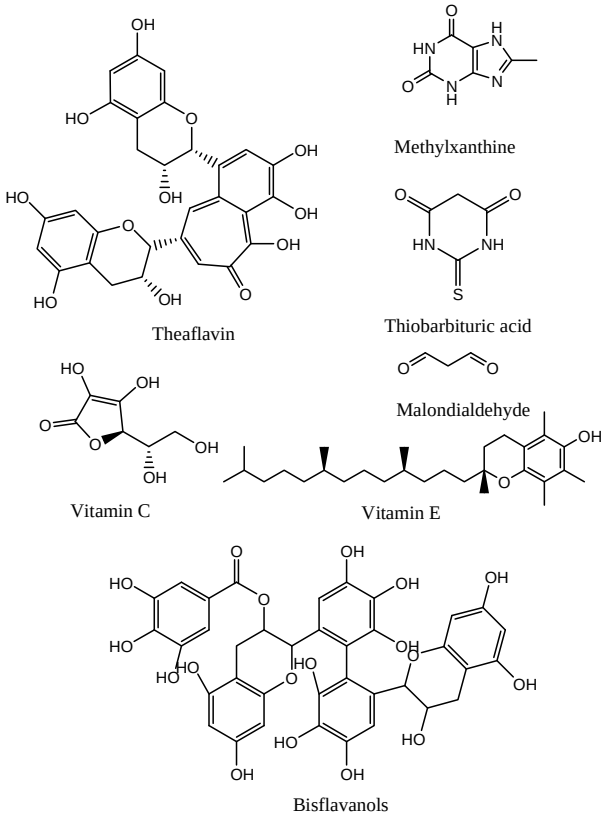

Fig. 2: Some of the representative compounds in black tea

Here comes our cup of green tea with many positive effects

Reports from the history of Indian and Chinese medicine claim that green tea was used in the healing of wounds, regulation of body temperature and control of bleeding. It was believed that green tea also played a significant role to improve heart condition[10, 13]. Apart from aiding in digestion, green tea is known to improve mental health. Encouraging effects of green tea have been observed from losing weight to liver disorders[20]. It is also very effective against type 2 diabetes and Alzheimer's disease. *L*-theanine (often referred to as *theanine*) present in green tea affects alpha brain wave activity and supports relaxation. Theanine is an amino acid that has a relaxing, but not sedating, effect[21]. Theanine is responsible for umami of tea, a flavour which is considered the fifth taste sensed by humans. Theanine readily crosses the blood-brain barrier, making it an effective brain supplement ingredient. Methylxanthine present in green tea gives a bitter taste and methylxanthine is responsible for its stimulant effect by blocking the action of adenosines. People who usually consume green tea have been found to have lowered risk of cancer. It is believed that polyphenols in tea are responsible for decreasing tumour growth[22]. Studies have shown that green tea has positive effects on several cancers like: breast, bladder, ovarian, colorectal (bowel), oesophageal (throat), lung, prostate, skin and stomach. However, in 2005, the Food and Drug Administration (FDA) has clearly mentioned that there is no reliable proof for the relation between green tea consumption and reduced risk of cancers. Green tea contains Catechins and Epigallocatechin gallate, important antioxidants. Catechins help to reduce the amount of malondialdehyde and thiobarbituric acid-reactive substances in the blood. These acids in the blood aid in creating a repository of fat within the body[23]. The use of Catechins is to cut down the amounts of the acid and help us so that body does not gain more weight. On the other hand, Epigallocatechin gallate improves the cognitive function of our brain, helping in faster circulation of the blood to the brain. It is believed that casein proteins in milk could bind with the polyphenols present in green tea and, as a result, prevent their antioxidant effect[24].

There are two ways in which EGCG exhibits antioxidant activity— either by the quenching of ROS or by the interruption of free radicals. The mechanism, in all probability, proceeds via a hydrogen-atom transfer. It must be noted that the resultant phenoxy radical is stabilized by intramolecular hydrogen bonding as shown in Scheme 1.

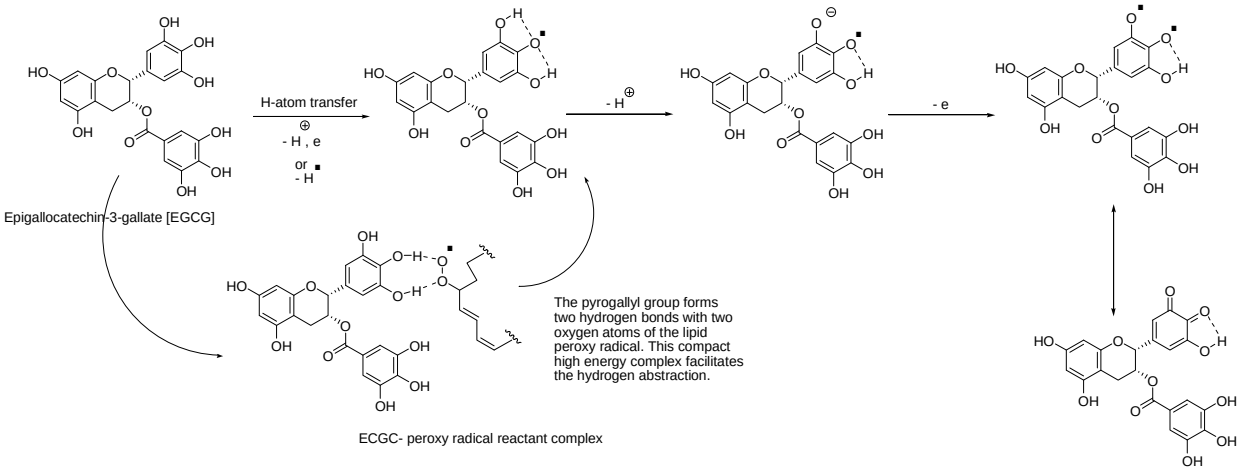

Scheme 1: EGCG antioxidant mechanism[10].

At high pH, *in vitro* pro-oxidant effects can be enhanced by green tea polyphenols. During autoxidation in alkaline (pH 13) conditions, EGCG readily forms free radicals by radical oxidation according to findings from EPR analysis (outlined in Scheme **2)**. EGCG pro-oxidant reactions have been shown in Scheme 3.

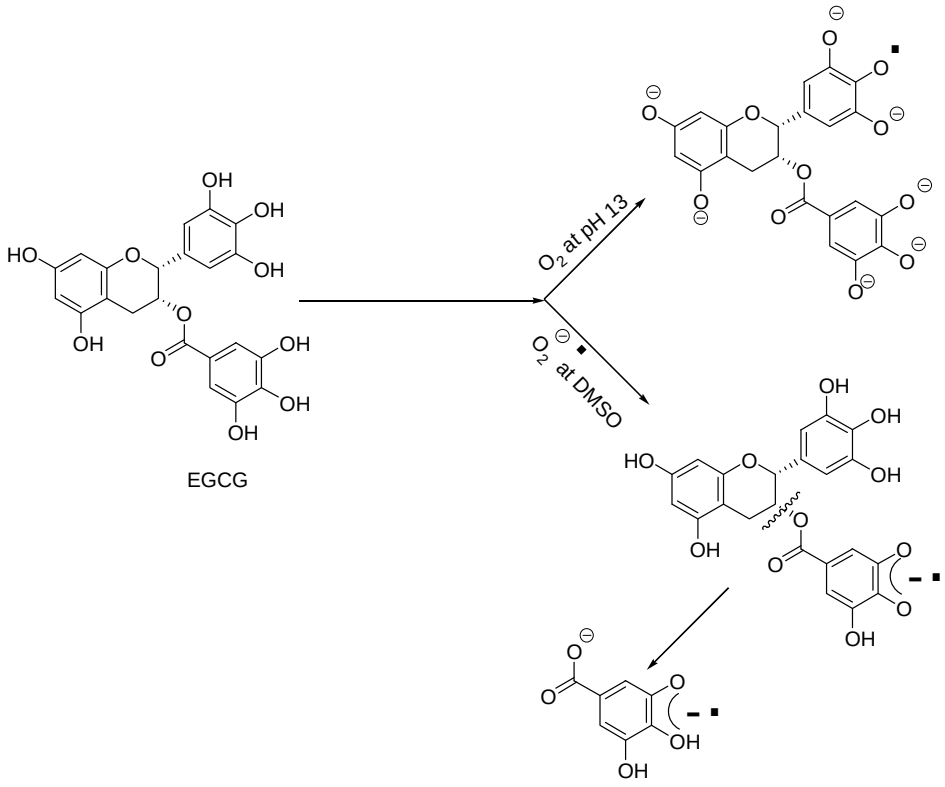

Scheme 2: EGCG autooxidation and superoxide reactions[10].

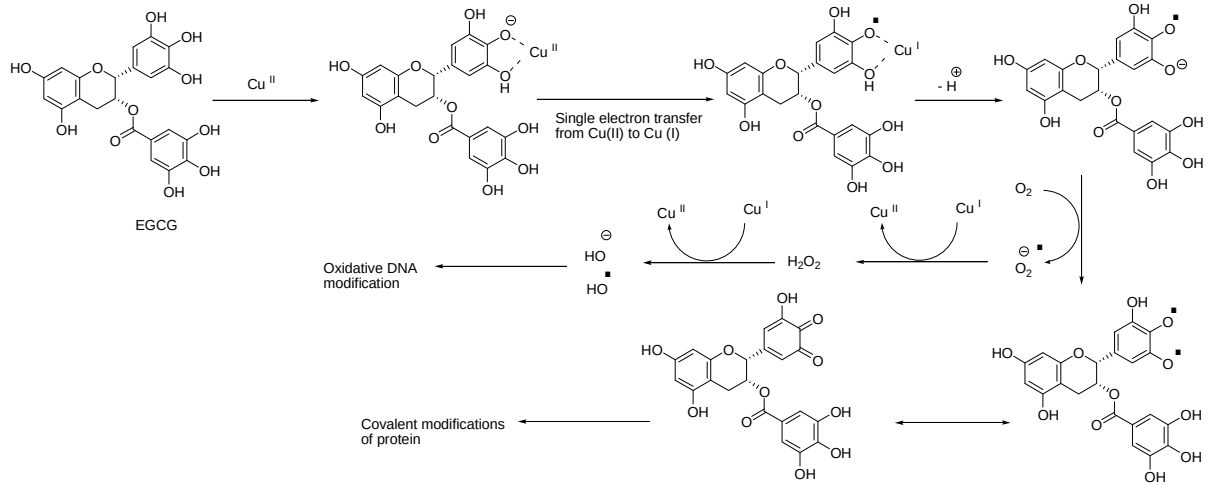

Scheme 3: EGCG pro-oxidant reactions[10].

Just recalled that famous line... "Every action has an equal and opposite reaction."

Going green is the key, they said. That is what I believed too when I started writing this article with a cup of green tea in my hand. Everything was going smoothly (both my writing and having green tea) till I was interrupted by a new research finding about green tea that was not-so-appealing. The new finding claims that green tea consumption has side effects. Initially, I shall throw light on caffeine as I have already mentioned that green tea contains caffeine. Caffeine, if consumed in high amounts, can increase the levels of anxiety, cause insomnia (problem with sleeping), upset stomach, generate tremors, restlessness and related problems[25]. Those who suffer from caffeine intolerance tend to be affected by insomnia as well. Caffeine increases the amount of acid produced in the digestive procedure causing pain or nausea. Caffeine also acts as a potent stimulant for the heart. It can accelerate the pulse thus making it irregularly high. This disorder is known as tachycardia. Pregnant women should be discouraged from consuming caffeine because of its diuretic nature. Any diuretic substance can drastically drop the water content of the body thus leading to dehydration that can be fatal during pregnancy[26-28]. There may be an unhealthy lopsidedness in the body's electrolytes if loss of water is too much. It must be mentioned that uncontrolled consumption of green tea reduces the ability of the body to absorb iron. During the process of digestion, the iron in the intestinal cells are bound by polyphenols and are thus prevented from entering the bloodstream. This polyphenol-iron complex is eventually excreted from the body paving the way for deficiency of iron and serious health problems. Tannins, which have been discussed earlier, can also block the absorption of iron from food and food supplements[30-37].

As already discussed, EGCG is the main constituent of green tea. Myeloperoxidase is an enzyme whose formation may be inhibited by EGCG resulting in inflammation. Studies suggest that drinking of green tea with lemon juice or in between meals can ward off this issue. Besides these, side effects of green tea include diarrhoea, heartburn, dizziness, kidney issues, convulsions, muscle tremors and contractions, liver disease, tinnitus, bleeding disorders, glaucoma, high blood pressure, osteoporosis, skin allergies, frequent urination and fertility problems. Majority of these disorders are caused by caffeine present in green tea[38-45].

Last but not the least

Before I leave you, I would want to lay all your doubts to rest by saying that there are no cases of green tea causing health disorders when consumed in moderation. The quality of green tea matters too. It would therefore be a good idea to have at least one cup of green tea in your daily diet if you want to adopt a healthier lifestyle.

Acknowledgement

The author is extremely thankful to Mrs. Sayantani Mitra, Teacher, Department of English, Sushila Birla Girls' School, Kolkata for her constant support in writing the manuscript.

References

1. Weisburger, J. H., 1997, Tea and health: a historical perspective, *Cancer Lett.* **114**, 315.

2. Vuong, Q.V., 2014, Epidemiological evidence linking tea consumption to human health: A review, *Crit. Rev. Food Sci. Nutr.*, **54**, 523.

3. Graham, H.N., 1992, Green tea composition, consumption, and polyphenol chemistry, *Prev. Med.*, **21**, 334.

4. Gardner, E.J., Ruxton, C.H. and Leeds, A.R., 2007, Black tea—Helpful or harmful? A review of the evidence, *Eur. J. Clin. Nutr.*, **61**, 3.

5. Wierzejska, R., 2014, Tea and health—A review of the current state of knowledge, *Przegl. Epidemiol.*, **68**, 595.

6. Sakanaka, S., Kim, M., Taniguchi, M. and Yamamoto, T., 1989, Antibacterial substances in Japanese green tea extract against Streptococcus mutans, a cariogenic bacterium, *Agric Biol Chem.*, **53**, 2307.

7. Ho, C.T. and Zhu, N., The Chemistry of Tea. In: Caffeinated Beverages, ACS Symposium Series 754, Chapter 32, p.316–326.

8. Jhoo, J.W., Antioxidant and Anti-Cancer Activities of Green and Black Tea Polyphenols. In: Antioxidant Measurement and Applications, ACS Symposium Series 956, Chapter 15, p.215–225.

9. Khan, N., Afaq, F. and Mukhtar, H., 2008, Cancer chemoprevention through dietary antioxidants: progress and promise, *Antioxid Redox Signal.*, **10**, 475.

10. Hügel, H.M. and Jackson, N., 2012, Redox Chemistry of Green Tea Polyphenols: Therapeutic Benefits in Neurodegenerative Diseases, *Med. Chem*., **12**, 380.

11. Imai, K., Suga, K. and Nakachi, K., 1997, Cancer-preventive effects of drinking green tea among a Japanese population, *Prev. Med*., **6**, 769.

12. Jakob-Rotetne R. and Jacobsen H., 2009, Alzheimer's Disease: From Pathology to Therapeutic Approaches, *Angew. Chem*., **48**, 3030.

13. Cabrera C., Artacho R. and Gimenez R., 2006, Beneficial effects of green tea – a review, *J. Am. Coll. Nutr*., 25, 79.

14. Liao S., Kao Y.H. and Hiipakka R.A., 2001, Green tea: biochemical and biological basis for health benefits, *Vitam Horm*., **62**, 1.

15. Kawai, K., Tsuno, N.H., Kitayama, J., Okaji, Y., Yazawa, K., Asakage, M., Hori, N., Watanabe, T., Takahashi, K. and Nagawa, H., 2003, Epigallocatechin gallate, the main component of tea polyphenol, binds to CD4 and interferes with gp120 binding, *J. Allergy Clin. Immunol.*, **112**, 951.

16. Ahmad, N., Feyes, D.K. and Nieminen A.L., 1997, Green tea constituent epigallacatechin-3-gallate and induction of apoptosis and cell cycle arrest in human carcinoma cells, *Journal of Cancer Research*., **89**, 1881.

17. Sadzuka, Y., Sugiyama, T. and Hirota, S., 1998, Modulation of cancer chemotherapy by green tea, *Clin Cancer Research*., **4**, 153.

18. Nehlig, A., 2018, Interindividual Differences in Caffeine Metabolism and Factors Driving Caffeine Consumption, *Pharmacol Rev.*, **70**, 384.

19. Hong, J., Lu, H., Meng, X., Ryu, J.H., Hara, Y. and Yang, C.S., 2002, Stability, cellular uptake, biotransformation, and efflux of tea polyphenol (")-epigallocatechin-3-gallate in ht-29 human colon adenocarcinoma cells, *Cancer Res*., **62**, 7241.

20. Béliveau, R. and Gingras, D., 2004, Green tea. Prevention and treatment of cancer by nutraceuticals, *Lancet.*, **364**, 1021.

21. Banerjee, S. and Chatterjee, J., 2014, Efficient extraction strategies of tea (Camellia sinensis) biomolecules, *J. Food Sci. Technol*., 1.

22. Mahmood, T., Akhtar, N. and Khan, B.A., 2010, The morphology, characteristics, and medicinal properties of Camellia sinensis' tea, *J. Med. Plants Res*., **4**, 2028.

23. Ernst, E. and Cassileth, B.R., 1999, How useful are unconventional cancer treatments, *Eur. J. Cancer*, **35**, 1608.

24. Ye, J., Fan, F., Xu, X. and Liang, Y., 2013, Interac-

tions of black and green tea polyphenols with whole milk, *Food Res. Int*., **53**, 449.

25. Hodgson, J.M., Puddey, I.B., Croft, K.D., Burke, V., Mori, T.A., Caccetta, RA. and Beilin, L.J., 2000, Acute effects of ingestion of black and green tea on lipoprotein oxidation, *Am. J. Clin. Nutr*., **71**, 1103.

26. Yilmazer-Musa M., Griffith A.M., Michels A.J., Schneider E. and Frei B., 2012, Grape seed and tea extracts and catechin 3-gallates are potent inhibitors of -amylase and -glucosidase activity, *J. Agric. Food Chem*., **60**, 8924.

27. Mandel, S.A., Amit, T., Weinreb, O.and Youdim, M.B.H., 2011, Understanding the Broad-Spectrum Neuroprotective Action Profile of Green Tea Polyphenols in Aging and Neurodegenerative Diseases, *J. Alz. Dis*., **25**, 187.

28. Green, R.J., Murphy, A.S., Schulz, B., Watkins, B.A. and Ferruzi, M.G., 2007, Common tea formulations modulate in vitro digestive recovery of green tea catechins, *Mol. Nutr. Food Res*., **51**, 1152.

29. Smith, A., Giunta, B., Bickford, P.C., Fountain, M., Tan, J. and Shytle, R.D., 2010, Nanolipidic particles improve the bioavailability and á-secretase inducing ability of epigallocatechin-3-gallate (EGCG) for the treatment of Alzheimer's disease, *International Journal of Pharmaceutics*, **389**, 207.

30. Storey, E. and Cappai, R., 1999, The amyloid precursor protein of Alzheimer's disease and the Abeta peptide, *Neuropathol. Appl. Neurobiol*. **25**, 81.

31. Vaidyanathan, J.B. and Walle, T., 2002, Glucuronidation and sulfation of the tea flavonoid (")-epicatechin by the human and rat enzymes, *Drug Metab Dispos*., **30**, 897.

32. Khan, N. and Mukhtar, H., 2013, Tea and Health: Studies in Humans, *Curr Pharm Des*., **19**, 6141.

33. Naldi, L., Gallus, S., Tavani, A., Imberti, G.L. and La Vecchia C., 2004, Risk of melanoma and vitamin A, coffee and alcohol: a case-control study from Italy, *Eur. J. Cancer Prev*., **13**, 503.

34. Sun, C.L., Yuan, J.M., Koh, W.P. and Yu, M.C., 2006, Green tea, black tea and breast cancer risk: a meta-analysis of epidemiological studies, *Carcinogenesis*. **27**, 1310.

35. Yang, C.S., Maliakal, P. and Meng, X., 2002, Inhibition of carcinogenesis by tea, *Annu. Rev. Pharmacol. Toxicol*., **42**, 25.

36. Negishi, H., Xu, J.W., Ikeda, K., Njelekela, M., Nara, Y. and Yamori, Y., 2004, Black and green tea polyphenols attenuate blood pressure increases in stroke-prone spontaneously hypertensive rats, *J. Nutr*., **134**, 38.

37. Hu, G., Bidel, S., Jousilahti, P., Antikainen, R. and Tuomilehto, J., 2007, Coffee and tea consumption and the risk of Parkinson's disease, *Movement Disorders*, **22**, 2242.

38. Alic, M., 1999, Green tea for remission maintenance in Crohn's disease, *Am. J. Gastroenterol*., **94**, 1710.

39. McKenna, D.J., Huges, K. and Jones, K., 2000, Green tea monograph, *Alt Ther*., **6**, 61.

40. Nakachi, K., Suemasu, K., Suga, K., Takeo, T., Imai, K. and Higashi, Y., 1998, Influence of drinking green tea on breast cancer malignancy among Japanese patients, *Journal of Cancer Research*., **89**, 254.

41. Sofrata, A., Lingström, P., Baljoon, M. and Gustafsson, A., 2007, The effect of miswak extract on plaque pH. An in vivo study, *Caries Res*., **41**, 451.

42. Hegarty, V.M., May, H.M. and Khaw, K.T., 2000, Tea drinking and bone mineral density in older women, *Am. J. Clin. Nutr*., **71**, 1003.

43. Zhang, B., Rusciano, D. and Osborne N.N., 2008, Orally administered epigallocatechin gallate attenuates retinal neuronal death in vivo and light-induced apoptosis in vitro, *Brain Res.*, **1198**, 141.

44. Okello, E.J., Savelev, S.U. and Perry, E.K., 2004, In vitro anti-beta-secretase and dual anti-cholinesterase activities of Camellia sinensis L. (tea) relevant to treatment of dementia, *Phytother. Res.*, **18**, 624.

45. Feng, W.Y., 2006, Metabolism of green tea catechins: An overview, *Curr. Drug Metab.*, **7**, 755–809.

Conference Alerts

1) Gordan Research Seminar on Inorganic Reaction Mechanisms
March 6-7, 2021, Galveston, TX, USA
Website: https://www.grc.org/find-a-conference/

2) 5th International Conference on Green Energy and its applications (ICGEA2021)
March 6-8, 2021, Singapore
Website: http://www.icgea.org

3) PITTCON 2021-Conference on Analytical Chemistry and Applied Spectroscopy
March 7-11, 2021, New Orleans, LA, USA
Website://pittcon.org

4) 10th International Conference on Clean and Green Energy (ICCGE2021)
March 10-12, 2021, Prague, Czech
Website: http://www.iccge.org/

5) The Environment-A Global Interdisciplinary Conference
April 18-19, 2021, Vienna, Austria
Website:https://www.progressiveconnexions.net/interdisciplinary-projects/global-transformations/the-environment/conferences/

6) Polymers 2021: New Trends in Polymer Science
May 17-19, 2021, Turin, Italy
Website: https://polymers2021.sciforum.net/

7) Gordon Research Seminar on Nuclear Chemistry
June 12-13, 2021, New London, NH, USA
Website: https://www.grc.org/nuclear-chemistry-grs-conference/2021/

8) Gordon Research Seminar on Bioinorganic Chemistry
June 12-13, 2021, Andover, NH, USA
Website: https://www.grc.org/find-a-conference/

9) 25th Annual Green Chemistry and Engineering Conference
June 14-16, 2021, Reston, Virginia, USA
Website: http://www.gcande.org/about/future-conferences/

10) 4th International Conference on Nanomaterials, Materials and Manufacturing Engineering (ICNMM2021)
June 17-20, 2021, Singapore
Website: //http://www.icnmm.org

11) HPLC 2021, 50th International Symposium on High Performance Liquid Phase Separation and related techniques
June 20-24, 2021, Dusseldorf, Germany,
Organized by German Chemical Society
Website: https://www.hplc2021-dusseldorf.com/

12) Gordon Research Conference on Physical Organic Chemistry
June 26-27, 2021, Holderness, NH, USA
Website: https://www.grc.org/find-a-conference/

13) 44th International Conference on Coordination Chemistry
June 28-July 2, 2021, Rimini, Italy
Website: http://www.iccc2020.com/

RNI No. MAHENG / 2017 / 74063

ISSN No. 2581-5911

BI-ANNUAL SUBSCRIPTION : Rs. 2000/-

G P GLOBALIZE RESEARCH JOURNAL OF CHEMISTRY

VOLUME 4 (Issue 2) January - June 2021

BI-ANNUAL 2021

GAURANG PUBLISHING

GAURANG PUBLISHING GLOBALIZE PRIVATE LIMITED

1, Plot-72, P.M.M.M. Marg, Tardeo, Mumbai-400034. **Tel.:** 022 23522068 **(M) :** +91 9969392245

Email : gpglobalize@gmail.com | **Web :** www.gpglobalize.in

CIN No. U22130MH2016PTC287238 | UAN - MH19D0008178